

MN DEPT OF NATURAL RESOURCES#

Sulfate and Mercury Cycling in Five Wetlands and a Lake Receiving Sulfate from Taconite Mines in Northeastern Minnesota

Michael Berndt and Travis Bavin

12/15/2011

Final Report

Minnesota Department of Natural Resources
Division of Lands and Minerals
500 Lafayette Rd.
St. Paul MN 55155

Table of Contents

Summary	3
Introduction	3
Site Selections and Descriptions	4
Methods	6
Chemical Analysis.....	6
Sulfur and Oxygen Isotopes in Dissolved Sulfate	7
Results	10
Discussion: Site Specific	10
Long Lake Creek Watershed	10
Sand River Watershed: ArcelorMittal Tailings Basin Seepage	11
Second Creek Watershed.....	15
SC-1 to SC-2.....	15
SC-2 to SC-3 and Pit 1 Input	17
SC-3 to SC-4 and Pit 6 Input	18
ETR-1 to 3: Lake Manganika, East Two River Watershed	19
Range Wide Implications	23
Sulfate Reduction in Wetlands.....	23
MeHg Production and Transport	24
Conclusion	25
Acknowledgements.....	25
References	26
Tables	30
Figures.....	42
Appendices.....	65

Summary

Inlets and outlets for five wetlands and a lake that receive water containing elevated sulfate (SO_4^-) on Minnesota's Iron Range were sampled nine times between May and October in 2010. The goal was to provide insights on potential links between SO_4^- released from mining operations and the production and transport of methyl mercury (MeHg) in nearby streams. This report details the observed SO_4^- , mercury (Hg), MeHg, and dissolved organic carbon (DOC) concentrations and relationships between these variables at each site. Additionally, sulfur isotopes were used as a tool to help quantify the extent of SO_4^- removal by reduction at each locality.

The wetland areas received water with SO_4^- concentrations ranging from less than 100 up to just over 1000 mg L^{-1} SO_4^- . Sulfur isotope data suggest that up to 180 mg L^{-1} of the SO_4^- in the source fluid was reduced to sulfide and removed within the wetlands. More SO_4^- was removed during the summer and fall than in spring. Despite high biologic activity, very little net SO_4^- reduction occurred within the lake. Production and transport of MeHg out of the wetlands and lake exhibited considerable intra- and inter-site variability but there was little, if any, correlation to the net mass of SO_4^- reduced. MeHg concentrations ranged from below detection to levels as high as 2.2 ng L^{-1} , with the highest levels being found in the stream leading from the lake during the mid-summer months.

Dissolved organic carbon (DOC) is a well established carrier of MeHg in lakes and rivers. However, MeHg often became elevated in the absence of DOC increases in this study, most notably at the lake outlet and at the toe of a tailings basin. Geochemical calculations suggested that these occurrences were related to enhanced transport of MeHg-bisulfide (MeHgHS^0), a species predicted to form in reducing pore fluid environments when Fe^{++} availability is insufficient to trap HS^- and H_2S as Fe-sulfide minerals. MeHgHS^0 is highly mobile owing to its neutral charge, but is likely to be short-lived under the oxidizing conditions found in most surface waters. This notion is supported by the observation that MeHg concentrations commonly exceeded those measured previously at downstream sites under similar hydrologic conditions and at comparable DOC levels.

Introduction

Mercury (Hg) is a pervasive global pollutant that is released to the atmosphere from many natural and anthropogenic sources, with coal-fired power plants being the largest source of atmospheric Hg in the United States. Ultimately, the Hg that is released to the atmosphere is deposited back to the surface via wet and dry deposition. The deposition increases the concentration of Hg in terrestrial and aquatic ecosystems. Most of the effort to decrease human exposure to Hg in Minnesota has focused on decreasing Hg deposition by curbing anthropogenic discharges and emissions. However, potential also

exists to reduce Hg exposure by preventing the conversion of inorganic Hg to CH_3Hg^+ (Methylmercury or MeHg). Unlike inorganic Hg, MeHg is considered bioaccumulative in aquatic environments (Watras et al., 1998) and so its formation and transport provide key steps in the pathway from atmospheric emission to human exposure. Therefore, limiting MeHg formation and transport could also limit the amount of Hg that is available to accumulate in aquatic organisms and ultimately in humans.

Most MeHg in the environment is formed as a byproduct of bacterial sulfate (SO_4^-) reduction to sulfide (Choi and Bartha, 1994; Gilmour et al., 1992). Indeed, SO_4^- loading in some instances has been shown to cause an increase in local MeHg levels (Jeremiason et al., 2006). This has led to concern in northeast Minnesota that the release of SO_4^- -bearing waters into reducing environments, such as in the anoxic sediments of wetlands and lakes, might increase MeHg formation. However, the sampling of non-mining and mining rivers within the St. Louis River watershed after spring snow melt and during base-flow periods between 2007 and 2009 revealed little difference in MeHg concentrations among the high and low- SO_4^- streams (Berndt and Bavin, 2009, 2011a). Berndt and Bavin (2011a) found that MeHg concentrations in the streams and rivers feeding the St. Louis River appeared to be controlled by transport-related process involving dissolved organic carbon (DOC) sourced from wetlands within the watersheds. This process was believed to be similar to what Brigham et al. (2009) found for streams across the United States. However, in the case of tributaries to the St. Louis River, colloidal processes relating to high ionic strength add to the complexity of the MeHg and DOC relationships. Berndt and Bavin (2011a) inferred that preferential flocculation of a low-MeHg but high-molecular weight DOC-component caused MeHg concentrations in mining streams to be elevated compared to non-mining streams when compared on a DOC-normalized basis.

To further investigate how SO_4^- loading impacts Hg methylation in mining impacted watersheds, five wetland areas and one lake were sampled for Hg, SO_4^- , DOC, and other chemical and physical parameters on nine separate occasions between May and October in 2010. This study also adds to a growing database on sulfur and oxygen isotope measurements for dissolved SO_4^- ($\delta^{18}\text{O}_{\text{SO}_4}$ and $\delta^{34}\text{S}_{\text{SO}_4}$, respectively) in the St. Louis River watershed. Isotopic changes are used in this instance to assess the amount of SO_4^- reduction that occurred in each wetland and lake, while the chemical changes were used to assess the mechanisms of MeHg production and transport associated with the SO_4^- reduction process.

Site Selections and Descriptions

Five wetland areas and one lake were chosen for monitoring in this study (Fig. 1). Previous water quality surveys conducted by the DNR and for the PolyMet and Mesabi Nugget mine projects indicated these areas had a diverse range of SO_4^- concentrations and MeHg levels. From west to east, the wetland sample sites included:

(1) One wetland on Long Lake Creek (**LLC**) –located south of the City of Eveleth in the Long Lake Creek watershed (Fig. 2). The wetland was sampled at its inlet (LLC-1), located near United Taconite’s South Pit area, and at its outlet (LLC-2), approximately 0.7 miles to the south of site LLC-1.

(2) One wetland area on an unnamed creek that flows into the Sand River (**SR**). This wetland is located northwest of the City of Virginia in the Sand River watershed (Fig. 3). The wetland was sampled near the toe of Arcelormittal’s tailings basin (SR-1), which was inactive during the study period. The wetland’s outlet was located about 1 mile to the north (SR-2).

(3) Three wetland areas on Second Creek (**SC**). These wetlands are located in the Second Creek watershed near Hoyt Lakes (Figs. 4a – 4d). The creek was sampled at a seepage point at the toe of the former LTV-tailings basin (SC-1) and at three sites downstream (SC-2 to SC-4) at sites selected to assess effects of successive major SO_4^- inputs from two abandoned mine pits to the stream.

In addition to the wetlands, Lake Manganika, located to the south of the City of Virginia in the East Two River (**ETR**) watershed (Fig. 5), was sampled at its two major inflows (ETR-1 and ETR-2) and on the East Two River about 0.5 miles downstream from the lake’s outlet (ETR-3).

The Long Lake Creek wetland (Fig. 2) is bounded to the north by United Taconite’s South Pit. Water from this area flows south towards the studied wetland. Water was not being pumped from the mine site into the wetland during this study. Thus, the water flow rate was relatively limited (estimated to be approximately 10 gpm or less) during the study period, meaning that water’s residence time within the wetland was relatively high. After passing through the wetland, the water exits the complex through a road culvert on the southwest side of the wetland and flows south to the St. Louis River. The location was disturbed in late May when the road culvert was replaced. Aerial photos show standing water in the wetland. Large stands of cattails near the road culvert indicate part of the wetland consists of an emergent type wetland. Reconnaissance conducted in 2009 revealed that SO_4^- concentrations in the stream were several hundred mg L^{-1} .

The Sand River wetland is located immediately downstream of a tailings basin that is owned and operated by ArcelorMittal (Fig. 3). The basin was not used for tailings deposition during the study, but water was routinely exchanged between the basin and the taconite processing plant. The company estimates that water seeps from the tailings basin at approximately 1000 gpm and reported average SO_4^- and Cl^- concentrations in the basin from 2001 to 2009 to be approximately 57 and 53 mg L^{-1} , respectively (Table 12). Three culverts drain water from near the toe of the basin into the northern part of the wetland. It also appears that some water from the tailings basin daylighted within the wetland because the observed flow through the three culverts was much less than 1000 gpm. The water exits the wetland via a small stream located about a mile north of the basin. After passing under Highway 169, the water enters another wetland area before entering the Sand River; just upstream of its confluence with the Pike River. It was observed that the area nearest to the tailings basin had large stands of cattails in it and remained permanently flooded throughout the season. In contrast, much of the flow on the north side of the wetland at the outlet was confined to the stream channel.

The wetlands located in the Second Creek watershed (Fig. 4a - 4d) span the former LTV mine site. Much of the area is currently owned by Mesabi Nugget, PolyMet, and Cliffs Natural Resources. Because of the long history of mining in this area, mine features have a significant influence on Second Creek's chemistry and hydrology. Seepage at an inactive tailings basin served as the stream's headwaters (Site SC-1) during the study period. The creek then flows through a series of wetland areas consisting of emergent type wetlands, wet meadows, shrub/scrub type wetlands, and other wetland types. Eventually, the water from the creek drains into the Partridge River just downstream of Colby Lake near its confluence with the St. Louis River.

Along the way, the flow in the creek can be supplemented by water discharged from Pit 1 (between SC-2 and SC-3; Fig. 4c) and water seeping out of Pit 6 (between SC-3 and SC-4, Fig. 4d). Both of these pits are currently owned by Mesabi Nugget. Mesabi Nugget has previously reported Pits 1 and 6 to have SO_4^- concentrations of approximately 380 and 1150 mg L^{-1} , respectively. Samples were not collected from Pits 1 and 6 during this study, but averaged surface water compositions for them are provided in the appendix. Mesabi Nugget was dewatering Pit 1 at nearly 4000 gpm during the first part of the study; however, pumping was stopped on July 1, 2010, during the middle of this study. Discharge from Pit 1 appeared to completely dominate the flow at SC-3 prior to the cessation of pumping, because flow at SC-3 all but dried up once pumping was stopped.

The hydrology of Second Creek is also heavily influenced by beaver activity. Mesabi Nugget reports have noted several instances where beaver dams in the creek were removed and then were promptly rebuilt by the area's very active beaver population. A large beaver dam with approximately three feet of head behind it was located just upstream of sampling location SC-4, however flow in the creek had overtopped it.

Lake Manganika was selected because Berndt and Bavin (2009, 2011a) identified occasionally elevated MeHg in the East Two River, well downstream from this site, near where the river enters the St. Louis River. This lake, located just south of the City of Virginia (Fig. 5), receives two major water inputs: one from the Virginia wastewater treatment plant (ETR-1) and the other from United Taconite (ETR-2). The lake has only one outlet stream (ETR-3) that is a major source of water for East Two River. The lake is highly productive and has historically low Secchi depths (<1 m). The lake also is relatively shallow and has previously been found to remain relatively well mixed during the summer months in 2004 to 2006 (See Appendices). No thermocline developed during any of those previous studies but O_2 levels decreased in the deepest parts of the lake during the summer months.

Methods

Chemical Analysis

Surface water samples were collected from the different sampling locations on nine separate occasions between May 5th, 2010 and October 20th, 2010.

The temperature and pH of each sample were measured in the field using a portable temperature and pH meter (Beckman Model 255). Conductivity was determined using a conductivity meter (Myron L Conductivity Meter, Model EP-10).

For cation and anion analysis, 60 mL samples for each were filtered in the field. A portable vacuum pump was used to pull the sample through acid-washed, 0.45 μm Nalgene filters. The cation samples were preserved with nitric acid and shipped along with the anion samples for analyses by the University of Minnesota – Geochemistry Laboratory (Minneapolis, MN) by ICP –AES and ion-chromatography respectively. Both cation and anion samples were kept cold with ice during shipment.

An additional 50 mL sample was filtered in the field for DOC analysis. The DOC samples were preserved with sulfuric acid and were shipped to the Minnesota Department of Health (St. Paul, MN) where they were analyzed using a non dispersive-infrared analyzer (reference method SM 5310c). 500 mL of unfiltered water was also collected at each site and shipped to the Minnesota Department of Agriculture (St. Paul, MN) for nutrient analysis where EPA method 353.2 was used to analyze for nitrate-nitrite, and standard methods 4500N, 4500PE, and 4500F were used to analyze total nitrogen, phosphorus, and ammonia, respectively. A 60 mL sample was also filtered in the field, and taken to the Minnesota Department of Natural Resources Hibbing Lab where alkalinity was measured by titration with 0.02 N sulfuric acid.

Mercury samples were collected using a Teflon sampling cup and were processed using clean hands/dirty hands techniques. All Hg samples were filtered in the field by pulling ~500 ml of water through a pre-packaged, 0.45 μm , sterile Nalgene filter and were stored in square Nalgene sterile media bottles. The bottles are free of low-level Hg contamination direct from the manufacturer and undergo no cleaning prior to sampling. Bottle blanks are analyzed whenever a new lot is received and three method blanks are processed for each analytical batch (consisting of up to 20 samples). The bottles have been consistently found to be free of mercury contamination. In addition, a quality control sample was created for each batch, and recoveries are consistently well within the quality control criteria of the method, demonstrating no loss in mercury due to either wall effects or volatilization. Sample blanks and a sample duplicate were also included with each round of samples to ensure the sampling method was not introducing any appreciable Hg to the samples. The samples were preserved in the field using pre-measured aliquots of Hg free hydrochloric acid stored in glass cuvettes and were shipped cold to the Minnesota Department of Health Laboratory (St. Paul, MN) within a few days of their collection. The samples were analyzed at the lab using US EPA Method 1631, Revision E for total mercury (THg), which is the sum of Hg and MeHg, and US EPA Method 1630 was used to analyze for MeHg.

Sulfur and Oxygen Isotopes in Dissolved Sulfate

Dissolved SO_4^- is composed of sulfur and oxygen atoms. The isotope composition of sulfur and oxygen in dissolved SO_4^- ($\delta^{34}\text{S}_{\text{SO}_4}$ and $\delta^{18}\text{O}_{\text{SO}_4}$) is potentially affected by a number of processes, including sulfide oxidation and bacterial SO_4^- reduction (Taylor et al, 1984; Toran and Harris, 1989; Detmers et al., 2001; Johnston et al., 2007). The present study relies on the changes in isotopic composition to assess the amounts of SO_4^- reduction occurring in the wetland and to evaluate other processes affecting SO_4^- cycling.

The oxygen added to sulfur to create SO_4^- molecules can come from ambient water or atmospheric O_2 and this affects the oxygen isotope composition of the dissolved SO_4^- molecule. Thus, $\delta^{18}\text{O}_{\text{SO}_4}$ potentially provides insight on the environment where the SO_4 molecules were formed. Meanwhile, the bacteria that convert SO_4^- to sulfide in reducing environments such as in wetlands and lake sediments preferentially use SO_4^- molecules containing the lighter sulfur and oxygen isotopes, ^{32}S and ^{16}O , respectively. Thus, once SO_4^- reduction occurs, the residual dissolved SO_4^- becomes enriched in the heavier isotopes, ^{34}S and ^{18}O , respectively. The amount of this heavy isotope enrichment depends, to a large degree, on the amount of SO_4^- reduction that occurs relative to the amount of dissolved SO_4^- that remains in solution.

One liter samples were collected and shipped to University of Waterloo Environmental Isotope Laboratory (Waterloo, CA) where they were analyzed for $\delta^{34}\text{S}_{\text{SO}_4}$ and $\delta^{18}\text{O}_{\text{SO}_4}$. The samples collected at the beginning of the season were filtered at the isotope laboratory while the samples collected on September 15th and October 20th were filtered at the DNR lab in Hibbing, MN using 0.7 μm filter paper. This change in the processing at the lab was made at the request of the analytical facility which had difficulty filtering the large volume of samples that were being sent to them.

SO_4^- was precipitated out of the samples at the analytical facility using excess $\text{BaCl}_2 \cdot 2\text{H}_2\text{O}$. Low- SO_4^- samples were concentrated before this step either by evaporation on a hot plate or by passage through an anion exchange column (BIO-Rad AG-1-X8 anion exchange resin). The relative amounts of ^{34}S and ^{32}S in the SO_4^- precipitate were determined using an Isochrom Continuous Flow Stable Isotope Ratio Mass Spectrometer (GV Instruments, Micromass, UK) coupled to a Costech Elemental Analyzer (CNSO 2010, UK). Relative ^{18}O and ^{16}O amounts were determined using a GVI Isoprime Mass Spectrometer coupled to a Hekatech High Temperature Furnace and a Euro Vector Elemental Analyzer.

Isotopic ratios ($\delta^{34}\text{S}_{\text{SO}_4}$ and $\delta^{18}\text{O}_{\text{SO}_4}$) are represented in this report using per mil notation (‰) which is a convenient means for reporting small ratios that vary by small amounts. For $\delta^{34}\text{S}_{\text{SO}_4}$, the reported value represents the difference between the $^{34}\text{S}/^{32}\text{S}$ ratio measured in the sample and an accepted standard value (FeS in Canyon Diablo meteorite) multiplied by a factor of 1000 and divided by $^{34}\text{S}/^{32}\text{S}$ ratio in the standard. A $\delta^{34}\text{S}_{\text{SO}_4}$ value of 1‰ means, for example, that the $^{34}\text{S}/^{32}\text{S}$ ratio in the sample is 0.1% higher than the measured standard value. For $\delta^{18}\text{O}_{\text{SO}_4}$, the reported values represent the difference between $^{18}\text{O}/^{16}\text{O}$ ratio measured in the sample and the $^{18}\text{O}/^{16}\text{O}$ ratio for H_2O in Standard Mean Ocean Water (SMOW), also multiplied by a factor of 1000 but divided by the $^{18}\text{O}/^{16}\text{O}$ ratio in the standard.

In this study, we assume that a Rayleigh distillation process applies for both $\delta^{34}\text{S}_{\text{SO}_4}$ and $\delta^{18}\text{O}_{\text{SO}_4}$ during SO_4^- reduction. The key assumptions are that the sulfide atoms formed by SO_4^- reduction are considered to be in isotopic equilibrium with the SO_4^- at the time of formation, but they are then instantaneously removed from the system as Fe-sulfide or H_2S gas. The sulfide is isotopically enriched in ^{32}S compared to ^{34}S , while the residual dissolved SO_4^- becomes progressively enriched in ^{34}S compared to ^{32}S in a process referred to as isotopic fractionation.

Isotopic fractionation is most conveniently represented using, Δ -notation, which in this case has the following formulation:

$$\Delta_{(\text{SO}_4^- \text{ sulfide})} = \delta^{34}\text{S}_{\text{SO}_4^-} - \delta^{34}\text{S}_{\text{sulfide}}. \quad (1)$$

In detail, fractionation is represented by a fractionation factor, α , whereby:

$$\alpha = \left(\frac{^{34}\text{S}/^{32}\text{S}}{\text{sulfide}} \right) / \left(\frac{^{34}\text{S}/^{32}\text{S}}{\text{sulfate}} \right), \quad (2)$$

but because α is usually close to unity and the primary interest is in the amount by which α varies from unity, we can represent α with an approximation that has ‰ units:

$$\Delta_{(\text{SO}_4^- \text{ sulfide})} = (\alpha - 1) \times (1000) \text{ (‰)} \quad (3)$$

where $\Delta_{(\text{SO}_4^- \text{ sulfide})}$ is usually a value between 0 and about 40 ‰. If it is assumed that SO_4^- reduction is uni-directional and instantaneous, then the dissolved SO_4^- that remains in solution can be represented by a Rayleigh Distillation process:

$$\delta^{34}\text{S}_{\text{SO}_4^-} = (\delta^{34}\text{S}_{\text{SO}_4^-, \text{init}} + 1000) F^{(\alpha-1)} - 1000. \quad (4)$$

Where $\delta^{34}\text{S}_{\text{SO}_4^-, \text{init}}$ is the initial isotopic ratio (in ‰ notation) and F is the fraction of SO_4^- remaining in solution.

F is the key variable of interest in the present study because, for example, for water entering a wetland having a known value for $\delta^{34}\text{S}_{\text{SO}_4^-, \text{init}}$, we can use the measured $\delta^{34}\text{S}_{\text{SO}_4^-}$ value at the outlet to determine the fraction of SO_4^- removed within the wetland. To obtain the mass of SO_4^- removed within the wetland, one needs only to multiply F by measured SO_4^- concentration in the inlet water.

In principle, a similar relationship can be written for $\delta^{18}\text{O}_{\text{SO}_4^-}$, whereby:

$$\delta^{18}\text{O}_{\text{SO}_4^-} = (\delta^{18}\text{O}_{\text{SO}_4^-, \text{init}} + 1000) F^{(\alpha-1)} - 1000. \quad (5)$$

However, as discussed later, by Berndt and Bavin (2011b) and Berndt (2011), included in appendix for this report), $\delta^{18}\text{O}_{\text{SO}_4^-}$ tends to re-equilibrate with O_2 and H_2O in the watersheds and so is less useful for calculating F. It still has some use, however, in detailing the environment where the S was last oxidized and so those values are included in the tables and plots in this report.

For calculations in this study, we assumed a numeric value for $\Delta_{(\text{SO}_4^- \text{ sulfide})}$ of +17. This number was chosen because it correctly estimated the amount of SO_4^- reduction at two sites (SR-1 and SC-4) where alternative methods existed to estimate SO_4^- loss. This value is also consistent with $\Delta_{(\text{SO}_4^- \text{ sulfide})}$ values measured in laboratory experiments involving freshwater SO_4^- reducing bacteria (Detmers et al., 2001). However, it is possible that the actual $\Delta_{(\text{SO}_4^- \text{ sulfide})}$ values could vary among sites or could vary at the same sites during different seasons as bacteria populations and availability of food sources change. Rather than attempt to vary this parameter using an arbitrary method, we elected to hold it constant until better studies can be conducted to quantify and verify $\Delta_{(\text{SO}_4^- \text{ sulfide})}$ the range of site-specific values that should be used in the environments studied here.

Results

Results for each of the study areas are summarized in Tables 1 through 11 and Figures 6 to 18. Considerable variability was present among the sites requiring site-specific interpretation. Thus, the data for each site are discussed in detail in the following sections, followed by a general discussion on the overall implications of the results with respect to our understanding of $\text{SO}_4^{=}$ reduction in wetlands and lakes and the affect they have on MeHg production and transport process on Minnesota's Iron Range.

Discussion: Site Specific

Long Lake Creek Watershed

$\text{SO}_4^{=}$ concentrations at the wetland outlet at Long Lake Creek (LLC-2) (Table 1, Fig. 6) were only about half those measured at the inlet (LLC-1). Although analyzing the change in Cl^- level could normally help to determine if this change in concentration was due to dilution or to reduction in the wetland, Cl^- levels at LLC-2 were always higher than at LLC-1 indicating that there is a source for this element to the wetland in this case. It is thought that this Cl^- source may be related to runoff from winter addition of salt to the road that runs along the west side of the basin.

$\delta^{34}\text{S}_{\text{SO}_4}$ and $\delta^{18}\text{O}_{\text{SO}_4}$ values for the dissolved $\text{SO}_4^{=}$, on the other hand, were consistently higher at LLC-2 (Table 1, Fig. 7) than at LLC-1, indicating that either another $\text{SO}_4^{=}$ source exists in the wetland or that considerable $\text{SO}_4^{=}$ reduction occurs in the wetland. While an alternative source exists for Cl^- in the wetland, the high $\text{SO}_4^{=}/\text{Cl}^-$ ratio in the water at LLC-2 make it much less likely that a comparably sized alternative source for $\text{SO}_4^{=}$ exists in the wetland. Thus, the isotopic changes are interpreted to result from $\text{SO}_4^{=}$ reduction processes within the wetland.

The arrow in Figure 7 illustrates a potential pathway for $\text{SO}_4^{=}$ isotopic composition of dissolved $\text{SO}_4^{=}$ that enters the wetland at LLC-1 (start of arrow) and is partially reduced within the wetland before exiting at LLC-2 (end of arrow). Using Equation 4 and substituting the average inlet $\delta^{34}\text{S}_{\text{SO}_4}$ value (8.6 ‰) for $\delta^{34}\text{S}_{\text{SO}_4,\text{init}}$, the fraction of $\text{SO}_4^{=}$ remaining in the wetland for an assumed outlet $\delta^{34}\text{S}_{\text{SO}_4}$ of 13.4 ‰, is 0.754. The average $\text{SO}_4^{=}$ concentration at LLC-2 was 136 mg L^{-1} while that at LLC-1 was 252 mg L^{-1} . Using these inputs and knowing that $F=0.754$, it can be calculated that the water entering the wetland at LLC-1 was diluted by an average of about 40% within the wetland and that approximately $62 \text{ mg L}^{-1} \text{ SO}_4^{=}$ was lost due to reduction.

Generally, $\text{SO}_4^{=}$ concentrations at both LLC-1 and LLC-2 were lower in May and June than they were from July through October. In early August a large rain event dumped two to four inches of water across the region and caused $\text{SO}_4^{=}$ levels at LLC-2 to decline to levels lower than observed at other times at the site. A permanent decrease in $\delta^{18}\text{O}_{\text{SO}_4}$ at LLC-1 and temporary decreases in $\delta^{34}\text{S}_{\text{SO}_4}$ and $\delta^{18}\text{O}_{\text{SO}_4}$ at LLC-2 suggest that this rain event replaced much of the old $\text{SO}_4^{=}$ in the wetland with new $\text{SO}_4^{=}$ from the source region. Using individual $\delta^{34}\text{S}_{\text{SO}_4}$ values (Table 12) measured at LLC-2 and an averaged value for LLC-1 of

8.6 (averaged because the residence time in the wetland is long in this case), it can be calculated that F varies from 0.69 to 0.85 and dilution in the wetland varied from almost none up to 269 % (after the major rainfall event). This suggests that in-wetland reduction accounted for a loss of between 36 and 77 mg SO_4^- from water entering the wetland at site LLC-1 compared to that leaving through LLC-2.

DOC levels were elevated at LLC-2 compared to at LLC-1, indicating that the wetland is a primary source for this component. MeHg and THg concentrations at both LLC-1 and LLC-2 varied considerably throughout the sampling season, but there were pronounced MeHg and THg increases (and DOC) at the latter site following the large rain event in August.

Berndt and Bavin (2009, 2011a) have found that both the quantity and quality of DOC concentrations play an important role in controlling MeHg levels in watersheds. This is also suggested here, where we find that MeHg levels at both LLC-1 and LLC-2 are positively correlated to DOC concentrations but at different DOC levels (Fig. 8). The slopes for the MeHg versus DOC regressions at the two sampling sites are very similar, however, the trends intersect the DOC axis at different points. Similar to Berndt and Bavin's interpretation for MeHg and DOC relationships in the St. Louis River, MeHg and DOC systematics at this site are attributed to differences in the quantity and quality of DOC carried in the streams.

The water at LLC-1 was always clear in appearance, whereas that at LLC-2 was always amber in color, suggesting that the water from the mine site picked up colored organic carbon as it passed through the wetland. This high molecular weight hydrocarbons shifted the DOC level, but not the MeHg concentration, indicating it had relatively low levels of adsorbed MeHg.

The one clear exception was the rain event, when DOC, MeHg, and THg all increased at the outlet compared to the inlet to this wetland. Similar to observations from Balogh (2006) for MeHg in streams following a large rain event, the MeHg concentration at LLC-2 became elevated compared to the existing MeHg/DOC trend during this period. The flooding associated with the greater rainfall potentially provides a greater source of oxidized Hg(II) for methylation in the wetland and can also expand the areas where SO_4^- reduction can occur. Finally, by increasing the flow rates, it significantly decreases the residence time of water within the wetland so that there is a greater chance that MeHg produced within the wetland can be transported out before demethylation occurs.

MeHg concentrations at both sites are somewhat elevated compared to values measured by Berndt and Bavin (2011) in mining and non-mining tributaries at their confluence with the St. Louis River, but as will be discussed in the final section of this paper, this may be attributed to demethylation in waters as they move downstream.

Sand River Watershed: ArcellorMittal Tailings Basin Seepage

Several important geochemical processes are suggested by the trends shown in Figures 9 and 10. First, SO_4^- concentrations decreased at SR-1 during mid-summer compared to fall and spring and these decreases coincided with increases in MeHg concentrations, but with little or no increase in DOC. SR-1 $\delta^{34}\text{S}_{\text{SO}_4}$ and $\delta^{18}\text{O}_{\text{SO}_4}$ values, meanwhile, were the highest measured among all sites included in the present study, suggesting that SO_4^- reduction was actively occurring. Most of the SO_4^- in the wetland at SR-1 is sourced from the tailings basin's clear water pool, which seeps beneath the perimeter dike into a

surrounding ditch and wetland at estimated rates of approximately 1000 gpm. Cl^- concentrations at SR-1 ranged between 40 and 50 mg L^{-1} throughout the sampling period, which are comparable to but only slightly lower than values reported by the company for the clear water pool (average 53.1, Appendix 1). SO_4^{2-} concentrations at SR-1 ranged from 3.5 to 16.4 mg L^{-1} during the study period, much lower than the SO_4^{2-} concentrations in the clear water pool (historical average of about 56.7 mg L^{-1} as calculated from company reports). The large decrease in SO_4^{2-} relative to Cl^- demonstrates that SO_4^{2-} reduction strongly regulates SO_4^{2-} loading into the wetland at this site.

In this basin, the percentage of SO_4^{2-} that is lost due to SO_4 reduction can be estimated without relying on $\delta^{34}\text{S}_{\text{SO}_4}$ and $\delta^{18}\text{O}_{\text{SO}_4}$ data. This is because the change in Cl^- concentration can be used to constrain dilution and all remaining decrease in the SO_4^{2-} concentration can be attributed to SO_4^{2-} reduction. If we assumed that the average SO_4^{2-} and Cl^- concentrations for water entering the basin are 56.7 and 53.1 mg L^{-1} , respectively, then we can calculate that approximately 77% of the SO_4^{2-} in water seeping under the dike from the clear water pool is reduced even before entering the wetland (SR-1). The percentage reduced increases during the summer months up to as high as 86%.

The consistently high $\delta^{34}\text{S}_{\text{SO}_4}$ and $\delta^{18}\text{O}_{\text{SO}_4}$ values measured at SR-1 are also indicative of a large amount of SO_4^{2-} reduction occurring at this site (Table 3, Figure 10). However, water in the clear water pool has not been analyzed for $\delta^{34}\text{S}_{\text{SO}_4}$ and $\delta^{18}\text{O}_{\text{SO}_4}$ at this point. If it is assumed that the $\delta^{34}\text{S}_{\text{SO}_4}$ and $\delta^{18}\text{O}_{\text{SO}_4}$ in the tailings basin is similar to that for mining related SO_4^{2-} observed elsewhere on the Iron Range (about 7.0 and -10, respectively, Berndt and Bavin, 2011b), then a potential SO_4^{2-} reduction pathway for water seeping beneath the dike from the tailings basin is represented by the arrow in Figure 10. This arrow represents a case where $F=0.19$ and an 81% SO_4^{2-} loss. This amount is consistent with the SO_4^{2-} losses that can be calculated independently using changes in $\text{SO}_4^{2-}/\text{Cl}^-$ ratios. A similar approach used for the samples collected at SR-1 suggest that F ranged from 0.15 to 0.25 throughout the sampling period (Table 12). The results suggest that about 43 to 48 mg of SO_4^{2-} was lost by SO_4^{2-} reduction before the water seeped into the wetland. More reduction occurred during the summer months than in the spring and fall (Table 12).

$\delta^{18}\text{O}_{\text{SO}_4}$ values depart significantly from those expected for a simple SO_4^{2-} reduction pathway (e.g., the modeled arrow in Figure 10). This is especially true for mid-summer samples, when $\delta^{34}\text{S}_{\text{SO}_4}$ increases, but $\delta^{18}\text{O}_{\text{SO}_4}$ decreases slightly. Berndt and Bavin (2011b) have found, in practice, that once water emerges into the open river system in this area, $\delta^{18}\text{O}_{\text{SO}_4}$ values are often reset, many times approaching values between about 1 and 8 ‰. This suggests biologic processes cause an exchange of oxygen atoms on the SO_4^{2-} molecules without changing $\delta^{34}\text{S}_{\text{SO}_4}$. For this reason, $\delta^{18}\text{O}_{\text{SO}_4}$ is less useful than $\delta^{34}\text{S}_{\text{SO}_4}$ for quantifying the amount of SO_4^{2-} reduction in wetland settings. But it does suggest that SO_4^{2-} assimilation, reductions, and reoxidation process may be important in the area where the water daylights in this wetland.

Once the water that emerged from the tailings basin at SR-1 enters the wetland, it appears that processes other than simple reduction must be affecting SO_4^{2-} concentrations before the water emerges from at SR-2. $\delta^{34}\text{S}_{\text{SO}_4}$ and $\delta^{18}\text{O}_{\text{SO}_4}$ values at SR-2, for example, are both lower than at SR-1, the opposite of what would be expected for simple reduction of SO_4^{2-} from SR-1 (Fig. 10). Our interpretation is that

the SO_4^- concentrations in water entering the wetland are sufficiently low that atmospheric sources begin to become comparable to those from the tailings basin on a quantitative basis. The SR-2 data can, in fact, be interpreted as the result of mixing between normal, atmospherically derived SO_4^- that has been processed in wetlands with SO_4^- derived from the SR-1 site. Berndt and Bavin (2009, 2011b), for example, reported that isotopic data for non-mining watersheds having $\delta^{34}\text{S}_{\text{SO}_4}$ range from about 6.8 to 10.7 ‰ and $\delta^{18}\text{O}_{\text{SO}_4}$ ranges from 5.4 to 6.7 ‰. This may represent a reasonable value for atmospherically derived SO_4^- that has been biologically processed in wetlands in this area. The SR-2 isotopic data appear to fall on a mixing line between these values and those measured at SR-1.

While SO_4^- decreased at SR-1 owing to increased SO_4^- reduction during the summer months, MeHg concentration increased gradually beginning in June before decreasing again towards the end of the summer. Thus, an obvious question that must be asked is whether this is a case where increased SO_4^- reduction led to accelerated MeHg production. The answer to this, however, is not obvious when analyzed in detail. For example, the degree to which SO_4^- reduction occurs in the spring and fall (77%) when MeHg levels were less than 0.1 ng L^{-1} is not greatly different from that occurring at the same site in the mid-summer months (86%) when MeHg levels increased to 0.32 ng L^{-1} . Furthermore, DOC, which is thought to be the primary transporting agent for MeHg, barely increased during the time period when MeHg concentrations increased the most. Finally, it was found that MeHg concentrations actually decreased in August following a major rain event that caused MeHg increases in the other areas during the present study. The MeHg concentrations at this site, therefore, appear not to be influenced strongly by the amount of SO_4^- reduction taking place at the site or by the occurrence of a major rainfall in the wetland. The summer MeHg increases, in this case, appears to occur across a backdrop of relatively continuous amounts of SO_4^- reduction and DOC-release.

Modeling with Geochemist's Workbench (Bethke, 2002) was performed to better characterize geochemical processes potentially leading to MeHg release in this setting. The program's default database was updated to include specific values for equilibrium constants for MeHg species provided by Jonnson et al. (2010) and references therein. This was done to permit modeling of the relative tendency for MeHg to form complexes with organic carbon and reduced sulfur species (S^- and HS^-) in a pore fluid environment controlled by local mineral and water-flow processes. The pore fluid was assumed to hold 10 mg/l of DOC containing 0.015% thiol sites (RS-) and total dissolved MeHg at a concentration of 10 ng/l (see Skyllberg (2008)) but the speciation for reduced sulfur species, pH, Fe, and Mn concentrations were all calculated by the program. MeHg speciation was also calculated.

The model also needed to account for an increase in Mn concentration without a similar increase in Fe concentration, and provide for an increase in MeHg concentration (Figure 11) precisely when Mn increases were found to occur, via a process that occurred during the summer months. While initially it was thought that the increase in Mn was due to a transition from oxidizing to reducing conditions, an alternative model was developed involving a pH decrease to account for the Mn increase. This alternative model was preferred, owing to the fact that it allowed SO_4^- reduction processes to continue to take place throughout the season, even when Mn concentrations were low. SO_4^- reduction processes are inconsistent with Mn-oxidation.

The alternative model began by assuming that P_{CO_2} increased during the summer months owing to an increase in biologic activity. All other parameters remained fixed (cation and anion concentrations, organic carbon, total dissolved sulfide, total MeHg), with the exception that Fe and Mn concentrations were controlled by mineralogic processes. Mn^{++} concentrations were assumed to be controlled by saturation with respect to rhodochrosite (MnCO_3), consistent with interpretations based on water chemistry sampled previously from nearby wells at the toe of the tailings basin dike (Berndt et al., 1999). Fe concentrations were fixed by the concentration of sulfur species; becoming suppressed if H_2S supply dominated the supply of Fe into the pore fluid environment.

As expected, increasing P_{CO_2} caused pH in the pore fluid to decrease, with the resulting increase in Mn^{++} concentration and conversion of HS^- to H_2S . This was accompanied simultaneously with the detachment of MeHg from the organic carbon as MeHgHS^0 . In a pore fluid environment, it is typical that most MeHg and Hg is fixed to non-mobile organic carbon species, so this transition from an organic carbon hosted MeHg species to a reduced sulfur MeHg species represents much greater potential for transport of MeHg. Indeed, MeHgHS^0 has long been thought to be an important species in reduced marine settings (Dyrssen and Wedborg, 1991) and has also recently been emphasized as potentially important in promoting MeHg transport in some freshwater settings (Gray and Hines, 2009; Jonnson et al., 2010). The modeled results suggest that this species becomes increasingly important with increasing P_{CO_2} if significant H_2S or HS^- concentrations are present. Moreover, the model “predicts” a correlation between Mn^{++} and MeHg concentration, similar to that seen in the field, owing to the dependence of both on decreasing pH.

Field notes from the site also support this interpretation. In June, for example, the water at SR-1 turned a milky white color, possibly due to oxidation of H_2S to elemental sulfur. The precipitate was not analyzed in our study, but a similar looking elemental sulfur precipitate has been reported previously in a study that used a shallow aeration settling pond to remove excess hydrogen sulfide from a pit lake (Gammons and Franson, 2001). The samples at SR-1, however, were also saturated with calcite and aragonite so it is possible the white precipitate contained a carbonate phase. Future studies should attempt to observe and identify this white precipitate if it forms at SR-1 again in upcoming field seasons.

Because MeHgHS^0 is a neutral species, it would be expected to be less prone than MeHg^+ to adsorb to minerals or organic carbon and may also have a tendency to volatilize and degas from wetland waters. Alternatively, it may react quickly with O_2 and dissipate or convert to other mercury or methylmercury species.

Also consistent with an interpretation of a relatively unstable MeHg species at SR-1 is the lack of correspondence in MeHg at this site compared to those measured at site SR-2. MeHg concentrations at SR-2 appear to be more closely related to DOC concentration, increasing in May and then declining again, until a rain event in mid-July caused the MeHg level to increase again by more than 50%.

During the same period, the THg and DOC levels also increased and the water color at the SR-2 site changed from clear to amber. In August, the water level at the SR-2 rose considerably and the color of the water changed from amber back to clear. However, the MeHg concentration remained elevated

while both the THg and DOC concentration decreased considerably. It has long been known that flooding can induce MeHg generation and transport (Kelly et al., 1997; Hall et al., 2009, Balogh et al., 2006, 2008) and similar processes appear to account for MeHg concentrations measured at SR-2.

Thus, it is proposed that the increased MeHg concentrations at site SR-1 occurred as a result of increased transport of MeHgHS⁰ from the sediments, but those at SR-2 reflected changes in transport mechanisms affecting DOC transport within the wetland.

Second Creek Watershed

SC-1 to SC-2

SO₄⁼ concentration at SC-1 varied little over the sampling season because most of the water is sourced from the old LTV tailings basin (Table 5, Fig. 12). This is a large basin compared to that at the SR-1 site, and seeps are therefore not affected by local rainfall or seasonal changes in air temperature. Also unlike the SR-1 site, the seep at SC-1 emerged as a distinct rapidly flowing surface flow and, thus, were largely unaffected by summertime changes in biologic activity. Both THg and MeHg levels at SC-1 were very low, presumably, because the flow path for the waters is long and the abundant Fe-oxides in taconite tailings are thought to provide excellent adsorption sites for Hg⁺⁺.

It is noteworthy that the Cl concentrations in this seep ranged from about 11.5 to 12.0 mg L⁻¹ which are much less than 33 mg L⁻¹ average value for the clearwater pool sampled before the company (LTV) closed (Berndt et al., 1999). Moreover, SO₄⁼ concentration in the clear water pool in the late 1990s averaged 120 mg L⁻¹ while that measured in the present study at the seep averaged 170 mg L⁻¹. It is clear, therefore, that the original water has been diluted in the long period since mine closure and/or during transit along the flow path from pond to seep, but that this dilution process was accompanied by considerable release of SO₄⁼ from tailings as the water flowed through the basin.

δ³⁴C_{SO4} at SC-1 is close to 7.0‰, consistent with primary sulfides from the Biwabik iron formation as the primary source (Theriault, 2011; Berndt and Bavin, 2011b). However, δ¹⁸O_{SO4} at this site is close to 1.0 ‰, a value consistent with a mixed source of oxygen derived from the atmosphere and meteoric water (Berndt, 2011, included in the appendix). Accordingly, sulfide oxidation in the tailings pile appears to involve atmospheric oxygen to a greater degree than that at many other sites around the region where δ¹⁸O_{SO4} is often close to the meteoric water value of -10 ‰ (Berndt and Bavin, 2011b).

Downstream, at SC-2, Cl⁻ levels were consistently higher than at SC-1 indicating subsurface seepage from the tailings basin is more concentrated in Cl⁻ than the surface seepage. However, unlike Cl⁻, SO₄⁼ concentrations at SC-2 were sometimes elevated and at other times depleted relative to those measured at SC-1. In order to evaluate the degree of SO₄⁼ reduction and dilution in the wetland between SC-1 and SC-2, therefore, the need arose to rely on sulfur isotopes. There is a clear increase in δ³⁴C_{SO4} at SC-2 compared to at SC-1, suggesting considerable SO₄⁼ reduction took place throughout the study period (Table 6 and 7, Fig. 13).

Using Equation 4 to estimate SO₄⁼ loss due to reduction and assuming an isotopic evolution pathway like that shown in Figure 12 (SC2-Mod arrow), it can be calculated that F, the fraction of SO₄⁼ remaining in

solution at SC-2 compared to that released originally from the tailings ($\delta^{34}\text{S}_{\text{SO}_4^-}$ = averaged measured value at SC-1 = 7.2 ‰) is about 0.60. For SO_4^- concentration of 174 mg L^{-1} (average value at SC-2), this implies that the average concentration for all water entering the wetland upstream of site SC-2 was approximately 292 mg L^{-1} , but that 118 mg L^{-1} was removed from solution by SO_4^- reduction. The modeled 292 mg L^{-1} SO_4^- concentration greatly exceeds the 170 mg L^{-1} value measured for the surface seep at site SC-1, but the higher value is needed to account for the elevated SO_4^- concentration and higher $\delta^{34}\text{S}_{\text{SO}_4^-}$. Alternatively, a separate source for SO_4^- in the area between SC-1 and SC-2 with a uniquely elevated $\delta^{34}\text{S}_{\text{SO}_4^-}$, but no such source was identified in the present study. That $\delta^{34}\text{S}_{\text{SO}_4^-}$ increased during the summer months, compared to fall and spring, also suggests that this wetland area is the site of large amounts of SO_4^- reduction.

Using the same approach for individual $\delta^{34}\text{S}_{\text{SO}_4^-}$ values at SC-2 (assuming the same 7.2 ‰ initial value), the fraction of SO_4^- released from tailings that remained in the water at SC-2, ranged from 0.51 to 0.80 (Table 12). The lowest values for $\delta^{34}\text{S}_{\text{SO}_4^-}$ occurred in the summer and highest values in the fall and spring. This seasonal dependence suggests that much of the SO_4^- is reduced within the wetland at this site, rather than during seepage because SO_4^- reduction during deep seepage would not likely be temperature sensitive.

$\delta^{34}\text{S}_{\text{SO}_4^-}$ and $\delta^{18}\text{O}_{\text{SO}_4^-}$ data diverge from a simple SO_4^- reduction path (Compare “ideal” path represented by the arrow in Figure 12 to that of the actual measured data). This suggests that SO_4^- assimilation and re-oxidation processes are important in this wetland. This is not entirely unexpected because, as discussed previously, $\delta^{18}\text{O}_{\text{SO}_4^-}$ values can adjust independently from $\delta^{34}\text{S}_{\text{SO}_4^-}$ when O in SO_4^- re-equilibrates with atmospheric O_2 . Because the SO_4^- entering this wetland already had elevated $\delta^{18}\text{O}_{\text{SO}_4^-}$ values compared to that at other sites, the SO_4^- reduction within the wetland should cause the $\delta^{18}\text{O}_{\text{SO}_4^-}$ to adjust to even higher levels than those measured at SC-2, as shown by the arrow in Figure 12. The re-exchange of O atoms in SO_4^- appeared, in this case, to cause a downward shift in $\delta^{18}\text{O}_{\text{SO}_4^-}$ values to between 1 and 5 ‰. Alternatively, the original SO_4^- source may have had a slightly more negative $\delta^{18}\text{O}_{\text{SO}_4^-}$ value than those measured at SC-1.

THg and MeHg concentrations at SC-2 generally increased through the summer and decreased in the fall (Figure 12). While an increase in SO_4^- reduction might account for these difference, it is important to note that a similar increase in the DOC levels were found during the summer months. This suggests that the MeHg increase may be related simply to increased DOC transport. However, while the summer-related increase in DOC transport can account for some of the elevated MeHg levels at SC-2, MeHg increases unrelated to changing DOC concentration also occurred during two of the sampling periods (June 22nd and July 7th). Based on results from SR-1, we could infer the possibility of an added MeHgHS⁰ component for those time periods.

Fe concentrations at SC-2 remained low throughout the study suggesting that its availability was too low to trap all of the sulfide produced. However, Mn concentrations were also generally low, suggesting that the pH in the waters may have simply been too alkaline for metal transport or that no Mn phases (e.g., rhodochrosite) was available as a source. Mn concentrations did, however, become slightly elevated compared to Fe following the periods of when MeHg concentrations were elevated. The

metals data do, therefore, suggest the possibility that an excess of H_2S or HS^- exists in pore fluids in the basin limits Fe mobility, rather than the reverse situation where abundant Fe limits the mobility of HS^- or H_2S . Low Fe concentrations, considered together with elevated MeHg concentration in the absence of an increase in dissolved DOC, are consistent with (but does not prove) the existence and enhanced mobilization of MeHg as a bisulfide species (MeHgHS^0) in the wetlands between SC-1 and SC-2.

SC-2 to SC-3 and Pit 1 Input

While the tailings basin is almost certainly the primary source of water at SC-1 and SC-2, Pit 1 was clearly the dominant source of water at SC-3, at least while the pit was being pumped (prior to July 1). Not only were SO_4^- and Cl^- levels at SC-3 (about 350 mg L^{-1}) close to values reported for Pit 1 (Fig. 14), but the water flowing at SC-3 virtually dried up when the pumping stopped. Interpretations in this case, are based on an assumption, therefore, that water with Pit 1 chemistry (See Appendices 2 and 3) is the source of water at SC-3. $\delta^{34}\text{S}_{\text{SO}_4}$ and $\delta^{18}\text{O}_{\text{SO}_4}$ values for Pit 1 water were found previously to be 8.8 and -7.3 ‰, respectively. These values are characteristic of oxidation of primary Biwabik Iron Formation sulfides which are known to be present in rocks in this area.

Similar to the wetland between SC-1 and SC-2, the amount of SO_4^- reduction at SC-3 appeared to vary seasonally, as indicated by an increase in $\delta^{34}\text{S}_{\text{SO}_4}$ from Pit 1 values (8.8 ‰) to values of 9.1 ‰ in May and to 11.5 ‰ in June. A proposed “ideal” pathway for isotopic evolution during SO_4^- reduction at this site (prior to $\delta^{18}\text{O}_{\text{SO}_4}$ re-equilibration) is shown in Figure 13 (SC3-Mod arrow). Applying Equation 4 for the SC4-Mod path produces $F = 0.89$. This represents the fraction of the SO_4^- from Pit 1 water remaining in solution at site SC-3, implying that about 11% of the SO_4^- entering the wetland from Pit 1 is removed by SO_4^- reduction within the wetland. Direct input of $\delta^{34}\text{S}_{\text{SO}_4}$ and SO_4^- values for SC-3 produce F values that decrease from 0.98 in the spring to 0.85 by the time pumping ceased in July 1 (See Table 12). These values imply that 6 to 56 mg of SO_4^- was lost in the wetland for each liter of water pumped from Pit 1, with lower amounts removed in the spring compared to the summer.

$\delta^{34}\text{S}_{\text{SO}_4}$ and $\delta^{18}\text{O}_{\text{SO}_4}$ values measured for SC-3 samples collected in July as the creek was drying up (owing to the stoppage of pumping from Pit 1) became similar to those expected for a mixture of water from SC-2 and Pit 1.

While both the $\delta^{34}\text{S}_{\text{SO}_4}$ and $\delta^{18}\text{O}_{\text{SO}_4}$ values for the SO_4^- at SC-3 increased from the assumed starting values in Pit 1, the $\delta^{18}\text{O}_{\text{SO}_4}$ values were much higher than would be expected for simple reduction of SO_4^- from Pit 1 (Fig. 13). As mentioned previously, $\delta^{18}\text{O}_{\text{SO}_4}$ can be affected by other isotope equilibration processes that cause a shift towards values of about 2 to 8 ‰ with no corresponding change in $\delta^{34}\text{S}_{\text{SO}_4}$ (Berndt and Bavin, 2011b). As suggested for the other sites, these isotopic shifts suggest strongly that SO_4^- assimilation and re-oxidation occurs in the wetland between sites SC-2 and SC-3.

THg, MeHg, and DOC levels at SC-3 also increased from early May through the end of June, likely due to the higher productivity and increasing SO_4^- reduction in the wetland combined with transport of Hg and MeHg bound to DOC and possibly to reduced sulfur species such as MeHgHS^0 . However, following the stoppage of pumping, THg and MeHg concentrations at SC-3 dropped without a corresponding decrease in DOC concentration (although DOC dropped the following sample period). The reason for these

decreases is unknown, but could be due to increased residence time and corresponding demethylation of earlier formed MeHg in the water. In effect, this MeHg was lost from pools of water that were largely standing in the wetland following the stoppage of pumping.

It is noted that MeHg levels measured at this site by Barr Engineering on behalf of Mesabi Nugget increased to as high as 1.7 ng L^{-1} in the summer of 2008 (Barr, 2009). The present study did not find values this elevated. The Mesabi Nugget report suggests the elevated MeHg related to the activities of beavers in the watershed. Indeed, this process has been shown to increase MeHg to elevated levels in wetlands containing relatively little SO_4^- (Roy et al., 2009). However, the data collected in the present study do not shed light on the relationship between beaver activity and MeHg in this watershed. It is important to note, however, that water pumped into the wetland in 2008 likely encountered a much larger supply of fresh, labile organic carbon than that encountered by waters pumped along the same flow paths in 2010. That data, considered with the present data, might suggest that the MeHg generating processes in this environment may be limited more by the availability of labile organic carbon than to presence or absence of SO_4^- .

Fe concentrations at this site are slightly more elevated than those at the previous sites, ranging between 0.1 and 0.6 mg L^{-1} indicating, potentially, that at least some of the wetland pore-fluids still have capacity to trap reduced SO_4^- as Fe sulfide, perhaps reducing the potential formation and transport of MeHg as MeHgHS^0 species.

SC-3 to SC-4 and Pit 6 Input

Prior to the cessation of Pit 1 pumping, approximately half of the SO_4^- at SC-4 was sourced from Pit 1 and half was sourced from Pit-6, assuming as at SC-3 that SO_4^- loading from other potential upstream sources was small compared to that from the pits. After pumping from Pit 1 was stopped there was a rapid increase in SO_4 concentration at SC-4 up to values similar to, but slightly less than those measured in Pit 6 (Table 8, Fig. 15, Appendix 2). This implies that virtually all of the SO_4^- at SC-4 was derived from Pit 6 near the end of the study. Mesabi Nugget reports that flow rate at SC-4 also declined by approximately 50% after the cessation of Pit 1 pumping (Appendix 4) and that the flow for the entire creek became similar to the estimated seepage rate at Pit 6 during the same period. This is consistent with our own observation that flow at SC-3 nearly dried up. Thus, water at SC-4 was assumed to originate from both Pit 1 and Pit 6 early in the summer, but almost exclusively from Pit 6 late in the summer.

Unlike at SC-2 and SC-3, neither the $\delta^{34}\text{S}_{\text{SO}_4}$ or $\delta^{18}\text{O}_{\text{SO}_4}$ values exhibited detectable seasonal dependence. However, even after pumping from Pit 1 stopped, the $\delta^{34}\text{S}_{\text{SO}_4}$ and $\delta^{18}\text{O}_{\text{SO}_4}$ values at SC-4 were elevated compared to those measured in Pit 6 (Table 8, Fig. 13). This indicates some of the SO_4^- seeping out of the pit was reduced before flowing past the SC-4 sampling site.

A proposed pathway in $\delta^{34}\text{S}_{\text{SO}_4}$ or $\delta^{18}\text{O}_{\text{SO}_4}$ space for simple reduction of SO_4^- for water migrating from Pit 6 to the sampling site as SC-4 is shown in Figure 13 (SC4-Mod). Although the shift in sulfur isotope composition is small compared to shifts observed at other sites, the amount of SO_4^- reduced suggested

by this path is relatively high. It takes a larger amount of SO_4^- reduction to shift the sulfur isotopic values of dissolved SO_4^- in a high- SO_4 water than in a low- SO_4 water.

Assuming $\delta^{34}\text{S}_{\text{SO}_4, \text{init}}$ is 5.4 ‰ (as measured previously for Pit 6) and applying Equation 4 to the “ideal” path illustrated Figure 13 (SC4-Mod), it can be calculated that F is approximately 0.88. This value means that nearly 12 % of the SO_4 in the water leaving the pit was reduced to sulfide and lost before the water emerged from the wetland at SC-4. Assuming Pit 6 water has 1146 m L^{-1} (See appendices), this represents a loss of about 138 grams of SO_4 from each liter of water escaping the pit. Using the actual concentrations and isotope values measured at site SC-4 (Table 12), F for the last three sample periods (after input from SC-3 dried up) ranged from 86 to 90% and corresponded to 103 to 158 mg SO_4^- reduced per liter of water passing through the wetland.

As at SC-3, the $\delta^{18}\text{O}_{\text{SO}_4}$ values measured at SC-4 were higher than would be expected if the SO_4^- in Pit 6 was reduced and precipitated by a simple reduction process that fractionated sulfur and oxygen equally. As discussed for the other sites, change in the $\delta^{18}\text{O}_{\text{SO}_4}$ without change in $\delta^{34}\text{S}_{\text{SO}_4}$ has been observed elsewhere in the watershed and thus eliminates use of $\delta^{18}\text{O}_{\text{SO}_4}$ as a means to assess the degree of SO_4^- reduction. The elevated $\delta^{18}\text{O}_{\text{SO}_4}$ values do, however, suggest that assimilation and re-oxidation of SO_4^- likely does occur upstream from SC-4.

Despite the large amount of reduction indicated by the sulfur isotopic data, the maximum MeHg values found at SC-4 were lower than at the other sites located upstream. Following the stoppage of pumping, DOC and MeHg values all declined considerably while the SO_4^- concentration increased. The significant drop in MeHg levels after pumping stopped suggests that much of the MeHg at SC-4 early in the summer may have been sourced upstream from SC-3, or possibly that the higher water levels before Pit 1 pumping was stopped contributed to elevated MeHg in the wetland. Interestingly, a MeHg concentration of over 4.0 ng L^{-1} was measured near SC-4 during the summer of 2008 (Barr, 2009) when the beaver dam was removed and subsequently rebuilt (e.g., allowing the area to dry out and then re-flood). As was the case for site SC-3, the data collected in the present study do not shed light on the relationship between beaver activity and MeHg in this watershed. However, the difference in behavior of MeHg in 2010 compared to 2008 suggest that the presence and absence of labile organic carbon may override addition of SO_4^- as a means to generate high MeHg at either site.

Fe^{++} concentrations were low for all samples collected at SC-4, although Mn^{++} levels reached values as high as 0.6 mg L^{-1} (Table 8). Thus, the data suggest that Fe mobility is potentially limited by an excess of HS^- and H_2S in the pore fluids in the wetland. This is potentially significant because it means that MeHg transport as MeHgHS^0 may be enhanced relative to that which might occur associated with DOC alone.

ETR-1 to 3: Lake Manganika, East Two River Watershed

Water from both ETR-1 and ETR-2 were major SO_4^- sources to Lake Manganika and the SO_4^- concentration at the outlet for this lake (ETR-3) was intermediate to those of its two inlet streams (Tables 9 and 10, Fig. 16). $\delta^{34}\text{S}_{\text{SO}_4}$ values for the inlets and the outlets all overlapped (Figure 17), indicating that net SO_4^- reduction in the lake must be relatively small. Using Equation 4 and assuming $\delta^{34}\text{S}_{\text{SO}_4, \text{init}} = 5.65$ (the average value for all measurements from ETR-1 and ETR-2 sites), then the $\delta^{34}\text{S}_{\text{SO}_4}$

values measured at site ETR-3 imply F values through the summer months around 0.96 (Table 12). For the SO_4^- concentrations measured in the outlet, this implies reduction and precipitation of only about 10 mg of SO_4^- per liter of water passing through the lake (ETR-3). However, the two samples with the highest $\delta^{34}\text{S}_{\text{SO}_4}$ values (8.0 ‰ in late May and 7.7 ‰ in late June, respectively) have F values corresponding to 0.87 and 0.88, respectively, implying more net SO_4^- reduction may have occurred in the lake during late spring/ early summer.

The $\delta^{18}\text{O}_{\text{SO}_4}$ values at the lake's outlet (ETR-3) are, on average, higher than at either ETR-1 or ETR-2. This suggests that despite the relatively low net SO_4^- reduction rate within the lake, considerable SO_4^- cycling occurs to water passing through the lake (Table 11, Fig. 17). This cycling strips the SO_4^- molecule of its original oxygen atoms and replaces it with oxygen atoms containing a higher percentage of atmospheric oxygen compared to the water in the source fluid (See Berndt and Bavin, 2011b). For this lake, where much of the SO_4^- may be reduced to H_2S and HS^- , rather than to Fe-sulfides in the sediments, this may represent a case where H_2S escaping from sediments is re-oxidized back to SO_4^- within the water column. On the other hand, the SO_4^- may be assimilated and converted to organic sulfur prior to being re-oxidized. This, too, would create an upward shift in $\delta^{18}\text{O}_{\text{SO}_4}$ with little or no corresponding change in $\delta^{34}\text{S}_{\text{SO}_4}$, provide the bulk of the SO_4^- that was initially assimilated eventually returned to the water column as dissolved SO_4^- .

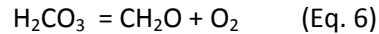
Both the THg and MeHg levels at ETR-3 were very low at the beginning of the season but began to increase in late May (Table 11, Fig. 17). No such increase was measured at either ETR-1 or ETR-2 indicating the MeHg was largely sourced from within Lake Manganika. MeHg concentrations increased at the lake outlet through late spring and early summer, reaching a peak of 2.2 ng L⁻¹ in early July. Values abruptly decreased to less than 1.0 ng L⁻¹ in late July and August. Even lower levels were found in September and October.

Assuming MeHg production is linked to SO_4^- reduction processes (Benoit et al, 1999), then MeHg would be expected to form only in the anoxic portions of the water column where SO_4^- reduction takes place (e.g., Watras et al., 2005; Eckley and Hintelmann, 2006; He et al. 2008; Gray and Hines, 2009) or within anoxic sediments (Ulrich et al., 2001). Clarisse et al. (2009) carefully evaluated speciation in a stratified boreal lake in Ontario and found dissolved MeHg increases at the top of the hypolimnion where it was either newly formed or released by freshly decomposed organic matter. Additional MeHg was found associated with colloid-rich waters at the water/sediment interface.

However, simple hypolimnetic formation of MeHg appears unlikely for Lake Manganika, since this lake has, in the past, retained measurable D.O. throughout the summer in all but the deepest waters (See Appendix). Furthermore, THg in the inlet streams is less than the MeHg concentration in the outlet stream. This means that any model accounting for an increase in MeHg must also provide a means to produce an increase in mercury that was derived internally from within the lake, likely the sediments. Finally, the elevated MeHg levels were found in the outlet waters which, presumably, represent the surface waters of the lake. This is inconsistent with a model involving MeHg formation in a hypolimnion because the lake would need to experience an overturn to allow this MeHg to escape

through the surface water streams. Elevated MeHg in this lake was almost certainly generated in the lake sediments.

To evaluate the source of MeHg in Lake Manganika, it is important to evaluate not just $\text{SO}_4^{=}$ reduction, but also the specific effects of high productivity on the geochemistry of surface waters and sediments. For example, high productivity leads to a large increase in pH and a corresponding decrease in Ca for the outlet compared to either inlet stream (Figure 18). This is because extensive photosynthesis converts carbonic acid in surface waters to O_2 as follows:

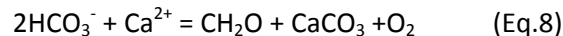


where CH_2O is used to represent organic matter.

This removal of carbonic acid from the water shifts the carbonate speciation towards formation of CO_3^{-2} and drives the water chemistry into distinct supersaturation with respect to calcium and magnesium carbonate minerals. Kinetic limitations on nucleation of magnesium carbonate minerals favor the precipitation of CaCO_3 as high-Mg calcite or aragonite:



Adding equations 1 and 2, and reconstituting the carbonate species as HCO_3^{-} results in:



an equation that reveals that the observed changes in pH and Ca in the lake should be accompanied by high deposition rates for CaCO_3 and organic matter.

These reactions are important because they indicate that there would be a continuous source of organic matter to promote $\text{SO}_4^{=}$ reduction in the sediments of this lake. Furthermore, the pH in the surface waters should remain sufficiently elevated to trap any H_2S diffusing from sediments as HS^{-} within the water column. This HS^{-} would, in turn, be prone to re-oxidation in the water column.

If O_2 and nitrate are generally present in the water column, then reduction of $\text{SO}_4^{=}$ to sulfide species (HS^{-} and H_2S) does not become thermodynamically favored, except in the sediments. It can be inferred, therefore, that $\text{SO}_4^{=}$ reduction and the conversion of Hg to MeHg, takes place in the sediments rather than within the water column.

The increase in MeHg in this case appeared to begin abruptly in May and grow through the summer months during a relatively dry period. This effectively rules out any sort of flood-related transport process to account for elevated MeHg (see Balogh et al., 2006 and 2008). Furthermore, the MeHg increase occurred without an increase in DOC. This lake level has also not risen recently, so flood-related process with its mixing together of organic carbon, Hg^{++} , and unreduced $\text{SO}_4^{=}$ (Porvari and Verta, 1995) cannot account for the MeHg increases here. DOC-related transport of MeHg into the lake is not, therefore, a viable mechanism to account for high MeHg in this case.

Alternatively, one could appeal to a mechanism involving sediments highly polluted with respect to Hg – as is known to occur near chlor-alkali plants. Jonsson et al. (2010) measured considerable gaseous emissions of MeHg from contaminated water-sediment microcosms constructed using sediments collected near a chlor-alkali plant. This unexpected emission of gaseous MeHg was attributed to formation of MeHgHS^0 . If a similar system were to evolve in the sediments of Lake Manganika, it is highly likely that these emissions would be trapped in the water column. No sediments were sampled from this site because it was not known prior to the field season that this lake would produce high MeHg. Water treatment plants have been known to be sources of mercury in the past but this plant does not appear to be contributing high Hg input to the lake in the present. Moreover, a highly contaminated sediment source does not account for the lack of high MeHg in May, followed by the rapid and abrupt increases and decreases later.

A third possibility, considered to be the most likely case here, relates to the formation of MeHgHS^0 in either with, or without, a previously existing source of Hg pollution. MeHgHS^0 formation, if it forms, will promote high MeHg effusion rates from the sediments (Hammerschmidt et al., 2004; Covelli et al., 2008; Gray and Hines, 2009) and solves the ephemeral source problem. This species has high diffusion rates and could also be swept into the water column during CH_4 and CO_2 ebullition, which is, itself, a common process in highly productivity and shallow lakes and ponds (Homibrook et al., 2000; Casper et al., 2002; Kankaala et al., 2003; Joyce and Jewell, 2003; McGinnis et al., 2006).

MeHgHS^0 stability in Lake Manganika sediments was tested using Geochemist's Workbench, using the same database as described in the section on SR-1. The simulation was, in this case, initiated using oxygenated lake water, similar to that sampled at Lake Manganika's outlet. As before, the pore fluid was assumed to hold 10 mg/l of DOC containing 0.015% thiol sites (RS-) to which MeHg was bound (see Skyllberg (2008)). Because MeHg is a trace component, its specific concentration in the output is not as important in this calculation as is the determination of its distribution among the various possible species. Reaction in the system was accomplished by adding 2 mg CH_4 to 1 liter of water as a reactant. This CH_4 promoted reduction of residual O_2 and conversion of SO_4 to reduced sulfur species, including HS^- and H_2S . As was the case at SR-1, a considerable fraction of the MeHg originally bound to organic carbon was converted to MeHgHS^0 in the pore fluid.

The modeling ignored the potential presence of Fe in the sediments even though Fe-oxides are abundant in the materials piled to the side of the lake. Thus, any sulfide that was formed was converted to HS^- and H_2S , rather than being trapped as Fe-sulfide. This approach was used because it is felt that the upper sediments in this highly productive lake should be dominated by decomposition of organic matter formed by photosynthesis within the lake. The inlet waters deliver no Fe^{2+} to the lake and so whatever Fe^{++} source exists in the pore fluids must be transported from below. A study of the sediments from this lake is likely needed to determine whether the sediments are contaminated with respect to Hg and if the lake sediments are conducive for formation of HS^- and H_2S with accompanying volatilization of MeHg as MeHgHS^0 .

Range Wide Implications

Sulfate Reduction in Wetlands

The data collected in this study reveal that $\delta^{34}\text{S}_{\text{SO}_4}$ measurements can be used to estimate the amounts of SO_4^{2-} reduction occurring at a site by using Equations 1 to 4. Calculation of a value for F, indicating the fraction of SO_4^{2-} in the source fluid is independent of SO_4^{2-} concentration but depends only on $\delta^{34}\text{S}_{\text{SO}_4}$ values measured at the outlet site and an appropriate choice of values for $\delta^{34}\text{S}_{\text{SO}_4, \text{init}}$ and $\Delta(\text{SO}_4^{2-}\text{-sulfide})$. Calculations were provided for each of the wetlands and lake studied here and results are summarized in Table 12 and Figure 19.

The estimates provided herein show that significant SO_4^{2-} reduction occurred at all of the sites (Figure 19), more so in the wetlands than in the lake. The estimated total masses of SO_4^{2-} removed at two of the wetlands, SC-2 and SC-4, approached 200 mg of SO_4^{2-} reduced per liter of water passing through them. The amounts removed at LLC and SC sites were greater in the summer and fall than in the early spring, indicating that the SO_4^{2-} reduction process was slowed by low temperatures. However, SO_4^{2-} reduction occurred at most sites even during the early spring period.

At the LLC wetland, where SO_4^{2-} concentrations were elevated and residence times were long (owing to slow flow rate of about 10 gpm or less), about 80 mg of SO_4^{2-} was removed per liter of water input into the basin during the summer months. This amount is less than those estimated for sites SC-2 and SC-4, where initial concentrations are also high, but where residence times are lower owing to rapid flow rates (1000s of gpm through similarly sized wetlands). Thus, residence time alone is not the primary factor controlling the amount of SO_4^{2-} reduction that occurs. The amount of SO_4^{2-} reduction that occurs in a system also relies on the presence of labile organic matter, which owing to relatively recent increases to flow in the SC-2 to SC-4 sites is probably greater than at the LLC site.

Between 40 and 50 mg of SO_4^{2-} was reduced at SR-1, where SO_4^{2-} reduction occurs during seepage from a tailings basin, but this was the majority of the SO_4^{2-} seeping from the basin. During the summertime, only several mg L^{-1} of SO_4^{2-} remained in the water that seeped into the wetland. Thus, although the water in the tailings basin clearwater pool at this site contained 53 mg L^{-1} and was seeping into the wetland at approximately 1000 gpm, this SO_4^{2-} source became vanishingly small during the summer months. Seepage from tailings basin environments involves both long residence times and intimate contact of SO_4^{2-} with organic matter. This accounts for the high degree of SO_4^{2-} removal at this site.

Very little net SO_4^{2-} reduction appeared to occur for water flowing through Lake Manganika and the reasons for this are worth considering. Fe^{++} concentrations in both the inlet and outlet streams for this lake are extremely low, so there may be no external source of Fe in the upper sediments where SO_4^{2-} reduction and MeHg formation most likely occur. It is also thought that the years of intense biologic activity in the upper column have probably contributed to a thick organic-rich layer of sediments at the bottom of this lake, perhaps limiting the upward movement of Fe^{++} from deeper mineralized layers into the upper more organic-rich sediment layers. It can be proposed, therefore, that the gross SO_4^{2-} reduction rates are much greater than the net SO_4^{2-} reduction rates, but the sulfide produced is not trapped and stored, but diffuses back into the lake and becomes re-oxidized. This reaction will result in

little or no net change in $\delta^{34}\text{S}_{\text{SO}_4}$ but would potentially cause an upward shift in $\delta^{18}\text{O}_{\text{SO}_4}$, as was observed at this site. In-lake upward shift in $\delta^{18}\text{O}_{\text{SO}_4}$ can also be attributed to re-oxidation of previously assimilated organic sulfur.

Nevertheless, the fate of SO_4^{2-} as either H_2S or an iron sulfide is an important consideration in terms of potential consequences (van der Welle et al., 2008). If all of the Fe in a system is converted to Fe-sulfide, then an important mechanism for controlling phosphorous mobility will be lost, resulting in undesirable eutrophication in lakes and wetlands (Lamars et al., 1989; Geurts et al., 2009). H_2S can also be toxic to some types of plants (Armstrong and Armstrong, 2005). Finally, the potentially enhanced mobilization of MeHg as MeHgHS^0 can occur in the presence of dissolved sulfide species under near neutral conditions (Dryssen and Wedborg, 1991; Hammerschmidt et al., 2004; Covelli et al., 2008; Gray and Hines, 2009) compared to that that could be transported with organic carbon alone.

MeHg Production and Transport

Data presented in this paper show that MeHg concentrations in wetlands near mining properties are sometimes correlated to changes in DOC concentrations, but at other times they are not. It is proposed that MeHg released from wetlands and lakes is sometimes controlled more by the release of MeHgHS^0 from wetland soils lake sediments than by enhanced mobility of MeHg-bound DOC. The goal of this section is to examine the data from a more regional perspective to evaluate possible implications of this new data set for production and transport of MeHg to the St. Louis River. For this discussion an additional parameter is used: oxidized mercury (Hg(II)). Hg(II) is calculated by subtracting MeHg from THg concentration. Oxidized mercury is not considered to be bioaccumulated without first being converted to MeHg. Likewise, its transport behavior may be governed by mechanisms different from those affecting MeHg.

Berndt and Bavin (2011a) previously reported MeHg and DOC concentrations for tributaries of the St. Louis River that were measured over a two year time period extending from September 2007 to August 2009. Samples were collected from near the tributary's confluence with the St. Louis River. Each tributary was categorized as either a mining or non-mining influenced stream based on the presence or absence, respectively, of mining features in the watershed. Dissolved MeHg (F-MeHg) and dissolved Hg(II) (F-Hg(II)) concentrations for mining and non-mining tributaries are shown in Figure 20 along with the same parameters collected for the five wetlands and one lake in this study. F-MeHg concentrations in the wetlands and lakes are often elevated compared to values found by Berndt and Bavin (2011a) for similar DOC concentrations at sites well downstream. F-Hg(II) concentrations, on the other hand, tend to be higher in the tributary samples for similar DOC levels than were typically found in either the lake or wetlands studied here. If wetlands are considered the primary sources of both MeHg and DOC to rivers (e.g., St. Louis et al., 1994; Selvendiran et al., 2008), then these data imply that MeHg/DOC relationships are clearly not preserved as water migrates from the wetland areas to downstream sites. In particular, MeHg is lost relative to DOC, while Hg(II) is gained.

Inorganic demethylation can occur with exposure of water to sunlight (Sellers et al., 1996) but biogenic demethylation processes are also important in wetland and lake sediment environments (Matilainen and Verta, 1995; Bridou et al., 2011). Particularly pertinent to the present case, however, may be the

recent observations of Drott et al. (2008), who suggested a direct link between the concentration of MeHgHS^0 and demethylation rates in sites uncontaminated with respect to Hg. A process involving MeHgHS^0 -dependent demethylation can account for both the large downstream decrease in MeHg levels implied by our data and, potentially, also for an increase in Hg(II) . The relative importance and degradation properties of MeHg(HS)^0 in mineland wetlands and rivers needs further study owing to its widespread implications relating to MeHg production, transport, and control in wetlands that receive SO_4 from industrial sources.

Conclusion

SO_4 , MeHg, THg, DOC, and other components were examined for inlets and outlets to five wetlands and a lake during the summer of 2010. The data reveal that SO_4 reduction was widespread, but MeHg production and release varied considerably from site to site and during different seasons at the same site. MeHg increases often occurred independent from changing DOC changes. Geochemical modeling results suggest an important role for MeHgHS^0 species in controlling the transport of MeHg in this region, particularly in reducing environments where iron availability is insufficient to limit H_2S and HS^- concentrations. This species appears to be highly unstable and subject to relatively rapid degradation compared to DOC-bound MeHg. Thus, MeHg(HS)^0 and DOC-bound forms probably need to be considered independently when evaluating the potential environmental effects of SO_4^- release on mercury in NE Minnesota wetlands.

Acknowledgements

Thank you to Mesabi Nugget and PolyMet for letting us collect water samples on their properties. Jean Matthew from the MN Dept. of Natural Resources Hibbing office is gratefully acknowledged for all of her hard work organizing the supplies and equipment for the sampling trips and for helping to collect the samples. Stephanie Theirault from the University of Minnesota – Duluth is also acknowledged for all of her help collecting the samples. Lastly, we would like to thank Dave Antonson and Anne Jagunich from the MN Dept. of Natural Resources Hibbing office for their help with ordering supplies and post collection sample preparation and shipment. We are also indebted to Shane Olund (Minnesota Department of Health), Myra Kunas (Waterloo Isotope Lab), and Rick Knurr (University of Minnesota Geochemistry Lab) for their diligent analytical support. Finally, we thank Dr. Nathan Johnson (University of Minnesota), Dr. Edward Swain (Minnesota Pollution Control Agency), and Dr. Bruce Monson for their participation in many discussions relating to this research project.

References

- Armstrong, J., and Armstrong, W. (2005) Rice: sulfide-induced barriers to rro-radial oxygen loss, Fe²⁺ and water uptake, and lateral root emergence. *Annals of Botany* 96, 625-638.
- Balogh S. J., Swain E. B., and Nollet Y. H. (2006) Elevated methylmercury concentrations and loadings during flooding in Minnesota rivers. *Sci. Total Environ.* 368, 138-148.
- Barr Engineering (2009) Sulfate, mercury, and methyl mercury in Second Creek. Mesabi Nugget Phase II Project report. May, 2009. 15 p. plus tables and figures.
- Berndt, M. E. and Bavin, T. K. (2009) Sulfate and mercury chemistry of the St. Louis River in northeastern Minnesota: A report to the minerals coordinating committee. Minnesota Department of Natural Resources, St. Paul, MN, 83 p.
- Berndt, M. E. and Bavin, T. K. (2011a) Methylmercury and dissolved organic carbon relationships in a wetland-rich watershed impacted by elevated sulfate from mining. *Environ. Pollution, in press.*
- Berndt, M. E. and Bavin, T. K., (2011b) A preliminary assessment of sulfate release and sulfate cycling processes in the St. Louis River watershed. An Environmental and Natural Resources Trust Fund Progress Report. Minnesota Department of Natural Resources, Submitted Report.
- Berndt, M. E., Lapakko, K., and Jakel, E. (1999) In-pit disposal of taconite tailings: geochemistry. Final Report to the Minnesota Department of Natural Resources. 77 p. plus appendices.
- Bethke, C. M. (2002) The Geochemist's Workbench. A User's Guide to RXN, Act2, Tact, React, and Gtplot. Release 4.0. University of Illinois. 224 p.
- Bridou R., Monperrus, M., Gonzalez, P. R., Gyuoneaud, R., and Amouroux, D. (2011) Simultaneous determination of mercury methylation and demethylation capacities of various sulfate-reducing bacteria using species-specific isotopic tracers. *Environ. Toxicology Chem.* 30, 337-344.
- Brigham M. E., Wentz D. A., Aiken G. R., and Krabbenhoft D. P. (2009) Mercury cycling in stream ecosystems. 1. Water column chemistry and transport. *Environ. Sci. Technol.* 43, 2720-2725.
- Casper, P. Chan, O. C., Furtado, A. L. S., and Adams, D. D. (2003) Methane in an acidic bog lake: The influence of peat in the catchment on the biogeochemistry of methane. *Aquat. Sci.* 65, 36-46.
- Choi S. C. and Bartha R. (1994) Environmental factors affecting mercury methylation in estuarine sediments. *Bull. Environ. Contam. Toxicology* 53, 805-812.
- Covelli, S., Faganeli, J., Vittor, C. D., Predonzoni, S., Acquavita, A., Horvat, M. (2007) Benthic fluxes of mercury species in a lagoon environment (Grado Lagoon, Northern Adriatic Sea, Italy). *Appl. Geochem.* 23, 529-546.

- Detmers J., Bruchert V., Habicht K. S., and Kuever J. (2001) Diversity of sulfur isotope fractionations by sulfate-reducing prokaryotes. *Environmental Microbiology*. 67, 888-894.
- Drott, A., Lambertsson, L., Bjorn, E., Skjellberg, U (2008) Potential demethylation rate determinations in relation to concentrations of MeHg, Hg, and pore water speciation of MeHg in contaminated sediments. *Marine Chemistry* 112, 93-101.
- Dryssen, D., and Wedburg, M. (1991) The sulphur-mercury(II) system in natural waters. *Water, Air, Soil Pollution* 56, 507-519.
- Eckley, C. S. and Hintelmann, H. (2006) Determination of mercury methylation potentials in the water column of lakes across Canada. *Sci. Tot. Environ.* 368, 111-125.
- Gammons, C.H., and Frandson, AK. (2001) Fate and transport of metals in H₂S-rich waters at a treatment wetland, *Geochem. Transactions* Vol. 1, DOI: 10.1039/b008234I.
- Gilmour, C. C., Henry E. A., and Mitchell R. (1992) Sulfate stimulation of mercury methylation in freshwater sediments. *Environ. Sci. Technol.* 26, 2281-2287.
- Gray, J. E., and Hines, M. E. (2009) Biogeochemical mercury methylation influenced by reservoir eutrophication, Salmon Falls Creek Reservoir, Idaho, USA. *Chem. Geol.* 258,157-167.
- Geurts, J. J. M., Sarneel, J. M., Willers, B. J. C., Roelofs, J. G. M., Verhoeven, J. T. A., and Lamers, L. P. M. (2009) Interacting effects of sulphate pollution, sulphide toxicity, and eutrophication on vegetation development in fens: a mesocosm experiment. *Environ. Pollution*, 157, 2072-2081.
- Hall, B. D., St. Louis, V. L., Rolfhus, K. R., Bodaly, R. A., Beaty, K. G., Paterson, M. J., and Peech-Cherewyk, K. A., (2005) Impacts of reservoir creation on the biogeochemical cycling of methyl mercury and total mercury in boreal upland forests. *Ecosystems* 8, 248-266.
- Hammerschmidt, C. R., Fitzgerald, W. F., Lamborg, C. H., Balcom, P. H., and Visscher, P. T. (2004) Biogeochemistry of methylmercury in sediments of Long Island Sound. *Marine Chemistry* 90, 31-52.
- He, T., Feng, X., Guo, Y., Qiu, G., Li, Z., Liang, L., and Lu, J. (2008) The impact of eutrophication on the biogeochemical cycling of mercury species in a reservoir: A case study from Hongfeng Reservoir, Guizhou, China. *Environ. Pollution* 154, 56-57.
- Homibrook, E. R. C., Longstaffe, F. J., and Fyfe, W. S. (2000) Factors Influencing stable isotope ratios in CH₄ and CO₂ within subenvironments of freshwater wetlands: Implications for d-signatures of emissions. *Isotopes in Environ. and Health Studies* 36, 151-176.
- Jeremiason J. D., Engstrom D. R., Swain E. B., Nater E. A., Johnson B. M., Almendinger J. E., Monson B. A., and Kolka R. K. (2006) Sulfate addition increases methylmercury production in an experimental wetland. *Env. Sci. and Technol.* 40, 3800-3806.

- Jonsson, S., Skjellberg, U., and Bjorn, E. (2010) Substantial emission of gaseous monomethylmercury from contaminated water-sediment microcosms. *Env. Sci. and Technol.* 44, 278-283.
- Johnston, D. T., Farquhar, J., and Canfield, D. E. (2007) Sulfur isotope insights into microbial sulfate reduction: When microbes meet models. *Geochim. Cosmochim. Acta* 71, 3929 – 3947.
- Joyce, J., and Jewell, P. W. (2003) Physical controls on methane ebullition from reservoirs and lakes. *Env. Eng. Geosci.* 9, 167-178.
- Kankaala, P., Kaki, T., and Ojala, A. (2003) Quality of detritus impacts on spatial variation of methane emissions from littoral sediment of a boreal lake. *Arch. Hydrobiol.* 157, 47-66.
- Karlsson, T. and Skjellberg, U. (2003) Bonding of ppb levels of methyl mercury to reduced sulfur groups in soil organic matter. *Environ. Sci. Technol.* 37, 4912-4918.
- Kelly, C. A., Rudd, J. W. M., Bodaly, R. A., Roulet, N. T., St. Louis, V. L., Heyes, A., Moore, T. R., Schiff, S., Aravena, R. Scott, K. J., Dyck, B., Harris, R., Warner, B., and Edwards, G., (1997) Increases in fluxes of greenhouse gas and methyl mercury following flooding of an experimental reservoir. *Environ. Sci. Technol.* 31, 1334-1344.
- Lamars, L. P. M. H., Tomassen, H. B. M., and Roelofs (1998) Sulfate-induced eutrophication and phytotoxicity in freshwater wetlands. *Environ. Sci. Technol.* 32, 199-205.
- Matilainen, T. and Verta, M. (1995) Mercury methylation and demethylation in aerobic surface waters. *Can. J. Fish. Aquatic Sci.* 52, 1597-1608.
- McGinnis, D. F., Greinert, J., Artemov, Y., Beaubin, S. E., and Wuest, A. (2006) Fate of rising methane bubbles in stratified waters: How much methane reaches the atmosphere. *Jour. Geophys. Res.* 111, C09007, 15p.
- Mitchell C. P. J., Branfireun B. A., and Kolka R. K. (2008) Assessing sulfate and carbon controls on net methylmercury production in peatlands: An in situ mesocosm approach. *Appl. Geochem.* 23, 503-518.
- Porvari, P. and Verta, M. (1995) Methylmercury production in flooded soils: A laboratory study. *Water, Air, Soil Pollution* 80, 765-773.
- Roy, V., Amyot, M. and Carignan, R (2009) Beaver ponds increase methylmercury concentrations in Canadian Shield streams along vegetation and pond-age gradients. *Environ. Sci. Technol.* 43 , 5605–5611.
- St. Louis, V. L., Rudd, J. W. M., Kelly, C. A., Beaty, K. G., Blum, N. S., and Flett, R. J. (1994) Importance of wetlands as sources of methyl mercury to boreal forest ecosystems. *Can. J. Fish. Aquat. Sci.* 51, 1065-1076.

- Sellers, P., Kelly, C. A., Rudd, J. D. W., MacHutchon, A. R. (1996) Photodegradation of methylmercury in lakes. *Nature* 380, 694-697.
- Selvendiran, P, Driscoll, C. T., Bushey, J. T., Montesdeoca, M. R. (2008) Wetland influence of mercury fate and transport in a temperate forested watershed. *Environ. Pollution* 154, 46-55.
- Skyllberg, U. (2008) Competition among thiols and inorganic sulfides and polysulfides for Hg and MeHg in wetland soils and sediments under suboxic conditions: Illumination of controversies and implications for MeHg net production. *Jour. Geophys. Res.* 113, C00C03, 14 p.
- Skyllberg, U. and Drott, A. (2010) Competition between disordered iron sulfide and natural organic matter associate thiols for mercury (II) – an EXAFS study. *Environ. Sci. Technol.* 44, 1254-1259.
- Taylor, B. E., Wheeler, M. C., and Nordstron, D. K. (1984) Stable isotope geochemistry of acid mine drainage: Experimental oxidation of pyrite. *Geochim. Cosmochim. Acta* 48, 2669-2678.
- Therriault, S. A. (2011) Mineralogy, spatial distribution, and isotope geochemistry of sulfide minerals in the Biwabik Iron Formation. MS Thesis. Univ. of MN. 165p.
- Therriault, S. A., Miller, J. D., Berndt, M. E., and Ripley, E. M. (2011) The mineralogy, spatial distribution, and isotope geochemistry of sulfide minerals in the Biwabik Iron Formation. *Inst. for Lake Superior Geol., Extended Abstract.* 2 pp.
- Toran, L. and Harris, R. F. (1989) Interpretation of sulfur and oxygen isotopes in biological and abiological sulfide oxidation. *Geochim. Cosmochim. Acta* 53, 2341-2348.
- Ullrich, S. M., Tanton, T. W., Abdrashiitova, S. A. (2001). Mercury in the aquatic environment: a review of factors affecting methylation. *Crit. Rev. Environ. Sci. and Technol.* 31, 241-293.
- van der Welle, M. E. W., Roelofs, J. G. M., and Lamers, L. P. M. (2008) Multi-level effects of sulphur-iron interactions in freshwater wetlands in the Netherlands. *Sci. Tot. Environ.* 406, 426-429.
- Vile M. A., Bridgham S. D., and Wieder R. K. (2003) Response of anaerobic carbon mineralization rates to sulfate amendments in a boreal peatland. *Ecological Applications.* 13, 720-734.
- Watras C. J., Back R. C., Halvorsen S., Hudson R. J. M., Morrison K. A., Wente S. P. (1998) Bioaccumulation of mercury in pelagic freshwater food webs. *Sci. Tot. Environ.* 219, 183-208.
- Watras, C. J., Morrison, K. A., Kent, A. D., Price, N., Renell, O., Eckley, C., Hintelmann, H., and Hubacher, T., 2005. Sources of methylmercury to a wet-land dominated lake in northern Wisconsin., *Environ. Sci. Technol.* 39, 4747-4758.

Tables

Table 1. Values for select chemical and physical parameters at location **LLC-1** during the different sampling dates. All units are in (mg L^{-1}) unless otherwise noted.

	5/4/2010	5/25/2010	6/9/2010	6/22/2010	7/7/2010	7/19/2010	8/11/2010	9/15/2010	10/20/2010
Time	16:15	15:20	9:20	13:54	14:06	14:30	13:05	15:30	16:15
pH	7.9	8.0	7.9	8.0	8.1	8.3	8.0	8.2	8.1
Cond ($\mu\text{S cm}^{-1}$)	800	800	900	900	1225	1150	1090	1200	1250
Temp (C)			10.0	14.5	10.8	10.3	15.9	8.0	6.4
Alk	450	390	365	475	655	615	575		
DOC	7.4	8.0	8.8	9.1	4.5	3.7	5.0	3.8	2.9
THg F (ng L^{-1})	1.2	2.0	1.7	1.7	0.9	0.6	0.9	0.8	0.7
MeHg F (ng L^{-1})	0.19	0.43	0.28	0.46	0.17	0.09	0.15	0.06	<0.05
$\delta^{34}\text{S}_{\text{SO}_4}$ (‰)	8.4	8.9	8.4	8.6	8.4	9.2	9.6	8.3	7.3
$\delta^{18}\text{O}_{\text{SO}_4}$ (‰)	-1.0	-0.6	-0.7	-1.2	-2.5	0.2	-5.1	-4.1	-4.7
Al	0.00	0.01	0.00	0.01	0.01	0.00	0.00	0.01	0.01
Ba	0.01	0.01	0.01	0.01	0.01	0.01	0.01	0.01	0.01
Ca	58	55	58	55	77	84	60	64	78
Fe	0.1	0.1	0.2	0.2	0.1	0.1	0.1	0.1	0.0
K	15.0	14.1	13.2	13.8	17.1	17.3	17.7	18.4	18.7
Mg	110	106	111	107	142	152	142	144	158
Mn	0.0	0.1	0.1	0.1	0.2	0.3	0.0	0.0	0.0
Na	30.2	27.5	28.0	25.6	36.6	40.1	29.2	33.5	42.3
P	0.0	0.02	0.02	0.03	0.01	0.02	0.02	0.01	0.01
Si	4.5	4.8	5.3	5.3	5.7	5.8	5.3	5.4	5.5
Sr	0.20	0.20	0.20	0.20	0.27	0.29	0.21	0.22	0.27
F	0.1	0.1	0.1	0.2	0.2	0.2	0.2	0.2	0.2
Cl	6.4	4.6	2.4	2.4	2.5	2.5	3.3	2.8	2.5
Br	0.01	0.01	0.01	0.01	0.02	0.01	0.01	0.01	0.01
Nitrate-N	1.2	0.5	0.9	1.7	0.8	1.2	1.3	2.5	1.3
SO₄	232	199	207	187	276	317	267	247	334
Phosphate-P	0.00	0.00	0.06	0.00	0.00	0.04	0.00	0.00	0.01
TKN	0.31		0.6	0.5	0.3	0.4	0.3	0.3	<0.2
Ammonia-N	0.03	0.03	<0.02	0.03	<0.02	<0.02	0.02	<0.02	<0.02
Total P	0.02	0.02	0.03	0.04	0.02	0.02	0.02	0.02	0.01
Nitrate/Nitrite	0.41	<0.4	<0.4	0.41	0.77	0.80	0.74	0.89	1.50

Table 2. Values for select chemical and physical parameters at location **LLC-2** during the different sampling dates. All units are in (mg L⁻¹) unless otherwise noted.

	5/4/2010	5/25/2010	6/9/2010	6/22/2010	7/7/2010	7/19/2010	8/11/2010	9/15/2010	10/20/2010
Time	17:00	16:10	9:45	14:23	14:30	14:47	13:30	15:50	16:40
pH	7.4	7.8	7.7	8.1	8.1	8.2	7.8	8.2	8.3
Cond (μS cm⁻¹)	390	500	600	600	900	710	460	700	850
Temp (C)			14.9	24.8	24.9	21.4	26.4	11.6	8.6
Alk	90	205	240	235	285	310	255		
DOC	25.0	25.3	18.2	19.1	19.7	18.9	29.7	18.3	11.8
THg F (ng L⁻¹)	1.9	2.5	1.8	1.5	1.8	1.0	3.8	1.4	0.6
MeHg F (ng L⁻¹)	0.40	0.40	0.20	0.36	0.41	0.26	0.99	0.20	0.07
δ³⁴S_{SO4} (‰)	11.2	13.0	14.6	14.7	13.4	14.8	12.0	13.2	13.4
δ¹⁸O_{SO4} (‰)	4.9	4.3	4.5	4.8	2.2	3.9	0.0	3.5	5.2
Al	0.15	0.01	0.01	0.03	0.02	0.00	0.11	0.02	0.01
Ba	0.01	5.46	0.01	0.01	0.01	0.01	0.01	0.01	0.01
Ca	33.2	39.6	45.8	43.6	48.4	50.3	30.9	42.0	58.0
Fe	0.7	0.5	0.1	0.1	0.1	0.1	1.0	0.1	0.1
K	5.9	6.8	7.4	6.7	7.0	6.7	6.2	8.2	9.2
Mg	44	50	57	55	68	73	50	74	94
Mn	0.1	0.2	0.2	0.2	0.4	0.2	0.4	0.1	0.1
Na	14.1	15.1	16.2	16.2	18.6	20.2	10.8	17.5	27.9
P	0.0	0.02	0.01	0.02	0.02	0.01	0.01	0.00	0.00
Si	0.7	2.4	6.3	5.7	9.0	11.2	5.3	6.4	8.0
Sr	0.12	0.14	0.17	0.17	0.19	0.19	0.11	0.15	0.21
F	0.1	0.1	0.1	0.1	0.1	0.1	0.1	0.1	0.1
Cl	10.2	9.2	9.0	7.7	6.1	5.9	4.0	5.0	7.3
Br	0.00	0.01	0.01	0.01	0.02	0.01	0.01	0.01	0.01
Nitrate-N	0.7	0.1	0.1	0.6	0.8	0.6	1.7	1.7	0.0
SO₄	120	123	140	137	150	157	77	126	195
Phosphate-P	0.00	0.00	0.00	0.00	0.00	0.03	0.00	0.00	0.01
TKN	0.76		0.8	0.9	1.1	1.0	1.3	0.7	0.5
Ammonia-N	0.04	0.05	0.04	0.05	0.05	0.04	0.05	0.04	0.03
Total P	0.03	0.03	0.02	0.02	0.02	0.02	0.03	0.02	<0.01
Nitrate/Nitrite	<0.4	<0.4	<0.4	<0.4	<0.4	<0.4	<0.4	<0.4	<0.4

Table 3. Values for select chemical and physical parameters at location **SR-1** during the different sampling dates. All units are in (mg L⁻¹) unless otherwise noted. No $\delta^{34}\text{S}_{\text{SO}_4}$ and $\delta^{18}\text{O}_{\text{SO}_4}$ values are available from 7/19 to 8/11 due to sulfate concentrations being too low for the analytical method.

	5/4/2010	5/25/2010	6/8/2010	6/22/2010	7/7/2010	7/19/2010	8/11/2010	9/15/2010	10/20/2010
Time	13:25	12:50	11:30	11:47	11:54	11:40	9:40	12:20	12:30
pH	7.6	7.8	7.7	7.6	7.4	7.6	7.7	7.8	7.5
Cond ($\mu\text{S cm}^{-1}$)	460	500	600	600	850	600	650	650	600
Temp (C)			13.9	17.7	21.3	19.5	21.7	9.4	7.6
Alk	340	335	340	325	340	350	380		
DOC	7.0	7.8	8.0	8.3	8.0	8.3	10.1	7.1	5.7
THg F (ng L⁻¹)	<0.4	0.5	0.4	0.6	0.7	1.0	0.9	0.5	<0.4
MeHg F (ng L⁻¹)	0.06	0.09	0.08	0.13	0.25	0.32	0.23	0.10	0.06
$\delta^{34}\text{S}_{\text{SO}_4}$ (‰)	35.3	36.0	38.5	39.6	36.2			33.7	31.1
$\delta^{18}\text{O}_{\text{SO}_4}$ (‰)	13.5	12.0	13.3	12.2	12.3			14.5	15.8
Al	0.00	0.00	0.00	0.01	0.01	0.00	0.01	0.01	0.01
Ba	0.02	0.24	0.03	0.03	0.06	0.11	0.10	0.04	0.04
Ca	38.1	43.7	45.8	45.1	46.2	47.7	50.9	45.0	41.6
Fe	0.1	0.0	0.1	0.1	0.2	2.7	4.6	1.3	2.3
K	7.7	8.1	6.0	4.1	3.8	3.3	5.6	6.8	6.4
Mg	48.0	48.6	51.0	50.3	52.7	53.9	55.4	57.2	58.3
Mn	0.5	0.6	0.9	2.0	3.5	6.0	4.0	1.3	1.5
Na	27.8	27.9	28.2	27.5	28.8	28.6	29.8	29.2	28.9
P	13.1	0.01	0.01	0.00	-0.01	0.00	0.00	0.00	0.00
Si	5.7	6.5	6.7	7.3	7.8	8.4	8.8	7.4	6.8
Sr	0.18	0.22	0.23	0.23	0.24	0.26	0.29	0.22	0.19
F	2.2	2.3	2.3	2.2	2.5	2.3	2.3	2.4	2.3
Cl	47.1	46.0	44.8	39.8	42.4	41.3	46.8	48.5	46.7
Br	0.32	0.33	0.33	0.32	0.34	0.30	0.39	0.35	0.32
Nitrate-N	0.2	0.4	2.4	1.0	0.1	1.6	0.4	0.6	0.2
SO₄	16.4	8.4	7.6	6.0	5.4	3.5	3.9	7.5	14.5
Phosphate-P	0.00	0.00	0.00	0.00	0.00	0.02	0.00	0.00	0.00
TKN	<0.2		0.4	0.6	0.6	0.7	0.7	0.4	0.4
Ammonia-N	0.10	0.03	0.05	0.04	<0.02	0.02	<0.02	<0.02	0.03
Total P	0.02	0.01	0.02	0.02	0.03	0.03	0.03	0.02	0.01
Nitrate/Nitrite	<0.4	<0.4	<0.4	<0.4	<0.4	<0.4	<0.4	<0.4	<0.4

Table 4. Values for select chemical and physical parameters at location **SR-2** during the different sampling dates. All units are in (mg L⁻¹) unless otherwise noted. No $\delta^{34}\text{S}_{\text{SO}_4}$ and $\delta^{18}\text{O}_{\text{SO}_4}$ values are available from 6/22 to 10/20 due to sulfate concentrations being too low for the analytical method.

	5/4/2010	5/25/2010	6/8/2010	6/22/2010	7/7/2010	7/19/2010	8/11/2010	9/15/2010	10/20/2010
Time	13:49	13:15	11:50	12:05	12:14	12:00	10:00	12:35	12:50
pH	7.5	7.5	7.8	8.1	7.5	8.0	7.6	7.7	7.8
Cond ($\mu\text{S cm}^{-1}$)	190	260	390	360	700	270	550	510	500
Temp (C)			14.5	18.5	21.7	18.3	22.3	11.4	7.6
Alk	240	140	215	205	220	165	305		
DOC	15.0	14.8	13.2	17.3	17.6	26.6	11.7	11.7	8.2
THg F (ng L⁻¹)	2.1	2.2	1.7	2.3	2.2	4.5	1.1	1.7	1.0
MeHg F (ng L⁻¹)	0.42	0.54	0.28	0.32	0.23	0.55	0.43	0.35	0.28
$\delta^{34}\text{S}_{\text{SO}_4}$ (‰)	14.9	14.3	12.5						23.4
$\delta^{18}\text{O}_{\text{SO}_4}$ (‰)	6.7	4.6	4.8						9.8
Al	0.01	0.04	0.03	0.05	0.04	0.08	0.02	0.01	0.02
Ba	0.01	0.01	0.02	0.01	0.02	0.02	0.02	0.01	0.02
Ca	15.5	20.0	29.8	25.4	30.6	22.8	39.1	34.1	36.6
Fe	0.4	0.3	0.3	0.4	0.3	0.7	0.3	0.2	0.1
K	3.1	3.8	4.6	3.1	3.2	1.8	3.9	4.3	4.6
Mg	18.5	23.1	33.5	29.1	34.7	23.6	46.7	43.7	46.1
Mn	0.1	0.1	0.3	0.2	0.3	0.3	0.7	0.1	0.1
Na	11.4	14.6	18.8	16.4	18.5	12.0	24.1	22.6	24.4
P	0.0	0.02	0.02	0.02	0.03	0.03	0.01	0.01	0.01
Si	4.4	4.1	5.8	6.3	6.8	6.1	7.9	7.3	7.0
Sr	0.07	0.10	0.14	0.12	0.15	0.11	0.21	0.16	0.18
F	0.7	1.0	1.4	1.2	1.5	0.9	1.9	1.6	1.7
Cl	19.7	23.3	31.6	23.9	26.9	16.0	36.7	37.0	42.6
Br	0.12	0.15	0.22	0.17	0.22	0.12	0.32	0.27	0.29
Nitrate-N	0.2	0.4	0.4	1.3	0.3	1.5	2.4	0.5	0.1
SO₄	10.5	8.8	5.2	2.6	1.5	1.5	0.9	5.8	4.2
Phosphate-P	0.00	0.00	0.00	0.00	0.00	0.01	0.00	0.00	0.00
TKN	0.5		0.6	0.9	0.9	1.3	0.7	0.6	0.4
Ammonia-N	0.04	0.04	0.03	0.04	0.03	0.04	<0.02	<0.02	<0.02
Total P	0.03	0.02	0.04	0.03	0.03	0.04	0.03	0.24	0.02
Nitrate/Nitrite	<0.4	<0.4	<0.4	<0.4	<0.4	<0.4	<0.4	<0.4	<0.4

Table 5. Values for select chemical and physical parameters at location **SC-1** during the different sampling dates. All units are in (mg L^{-1}) unless otherwise noted.

	5/4/2010	5/25/2010	6/8/2010	6/22/2010	7/7/2010	7/19/2010	8/12/2010	9/15/2010	10/20/2010
Time	10:43	10:45	9:30	9:50	9:50	9:30	10:00	9:45	10:30
pH	7.4	7.6	7.5	7.3	7.4	8.0	7.5	7.9	7.5
Cond ($\mu\text{S cm}^{-1}$)	700	800	900	1100	1200	890	1300	1000	900
Temp (C)			11.4	10.9	11.1	12.3	14.5	9.1	9.3
Alk	540	530	520	530	515	540	520		
DOC	2.6	2.4	2.5	2.6	2.4	2.6	3.0	2.5	2.5
THg F (ng L^{-1})	<0.4	<0.4	<0.4	<0.4	<0.4	<0.4	<0.4	<0.4	<0.4
MeHg F (ng L^{-1})	<0.05	<0.05	<0.05	<0.05	<0.05	<0.05	<0.05	<0.05	<0.05
$\delta^{34}\text{S}_{\text{SO}_4}$ (‰)	7.1	7.1	7.4	7.9	6.5	7.4	7.3	7.3	6.9
$\delta^{18}\text{O}_{\text{SO}_4}$ (‰)	0.8	0.9	1.0	0.9	0.5	0.9	0.2	1.5	1.4
Al	0.01	0.00	0.01	0.01	0.01	0.00	0.00	0.01	0.01
Ba	0.03	0.03	0.03	0.03	0.03	0.03	0.03	0.03	0.03
Ca	78	77	77	77	77	77	76	78	77
Fe	1.3	1.3	1.3	1.3	1.3	1.3	1.0	1.3	1.2
K	8.5	8.3	8.2	8.5	8.3	8.4	8.3	8.4	8.4
Mg	97	97	96	96	97	97	96	98	97
Mn	3.4	3.3	3.3	3.3	3.3	3.3	3.2	3.2	3.2
Na	50.2	49.1	48.2	49.3	49.1	49.0	48.0	48.9	47.5
P	0.0	0.01	0.01	0.01	0.05	0.01	0.00	0.00	0.01
Si	10.2	10.3	10.3	10.5	10.4	10.3	10.4	10.7	10.5
Sr	0.31	0.30	0.30	0.30	0.30	0.30	0.30	0.30	0.30
F	2.1	2.2	2.2	2.3	2.3	2.2	2.3	2.3	2.2
Cl	11.9	12.0	11.8	11.9	11.8	11.5	11.6	11.3	11.4
Br	0.07	0.07	0.08	0.07	0.07	0.06	0.07	0.07	0.06
Nitrate-N	0.2	0.2	34.8	0.3	0.2	1.4	0.2	1.0	0.1
SO₄	170	170	172	173	172	168	166	163	161
Phosphate-P	0.00	0.00	0.00	0.00	0.00	0.02	0.00	0.00	0.01
TKN	<0.2		0.2	0.3	0.2	0.2	0.2	<0.2	0.3
Ammonia-N	0.15	0.11	0.11	0.12	0.12	0.12	0.09	0.10	0.11
Total P	0.01	<0.01	0.01	0.01	<0.01	<0.01	0.02	0.01	<0.01
Nitrate/Nitrite	<0.4	<0.4	<0.4	<0.4	<0.4	<0.4	<0.4	<0.4	<0.4

Table 6. Values for select chemical and physical parameters at location **SC-2** during the different sampling dates. All units are in (mg L⁻¹) unless otherwise noted.

	5/4/2010	5/25/2010	6/8/2010	6/22/2010	7/7/2010	7/19/2010	8/12/2010	9/15/2010	10/20/2010
Time	10:05	10:00	9:06	9:23	9:22	9:00	9:36	9:30	9:45
pH	8.0	8.0	7.9	7.8	7.8	8.1	7.3	8.2	8.1
Cond (μS cm⁻¹)	600	700	800	900	1150	825	1000	750	780
Temp (C)			17.2	20.3	22.6	22.3	24.9	12.0	7.7
Alk	320	340	355	375	355	450	405		
DOC	9.4	11.1	13.1	13.1	15.7	14.0	15.4	12.5	10.0
THg F (ng L⁻¹)	0.7	1.2	1.3	1.7	1.2	2.0	1.5	1.0	0.8
MeHg F (ng L⁻¹)	0.24	0.29	0.37	0.93	0.46	0.64	0.41	0.37	0.24
δ³⁴S_{SO4} (‰)	10.8	13.4	16.9	16.7	14.6	17.0	18.7	16.1	13.7
δ¹⁸O_{SO4} (‰)	2.2	4.1	2.2	4.1	1.3	2.7	3.8	5.7	6.2
Al	0.01	0.00	0.00	0.01	0.01	0.01	0.01	0.01	0.01
Ba	0.02	0.02	0.03	0.02	0.03	0.02	0.02	0.02	0.02
Ca	59.3	60.4	62.2	55.4	70.9	66.1	65.5	61.3	62.6
Fe	0.1	0.1	0.1	0.1	0.2	0.1	0.1	0.1	0.1
K	6.6	7.0	7.0	6.4	5.6	6.9	6.2	7.0	6.8
Mg	74	78	82	76	90	90	90	89	88
Mn	0.1	0.1	0.1	0.1	0.8	0.3	0.6	0.1	0.0
Na	29.0	29.5	28.3	29.3	21.7	32.7	24.4	38.0	37.0
P	0.0	0.02	0.02	0.02	0.01	0.02	0.02	0.01	0.02
Si	2.8	1.7	2.6	1.8	4.7	7.0	7.5	8.1	5.9
Sr	0.21	0.23	0.23	0.22	0.24	0.27	0.24	0.26	0.25
F	1.2	1.2	1.2	1.4	1.1	1.5	1.2	1.6	1.5
Cl	14.9	14.9	15.6	13.1	15.2	12.4	14.4	12.4	13.7
Br	0.03	0.03	0.03	0.03	0.04	0.05	0.05	0.05	0.03
Nitrate-N	0.4	4.0	1.0	1.0	0.9	1.3	0.2	0.9	0.2
SO₄	192	193	180	148	236	147	186	133	149
Phosphate-P	0.00	0.00	0.00	0.00	0.00	0.03	0.00	0.00	0.01
TKN	0.23		0.6	0.9	1.0	1.0	1.2	0.7	0.5
Ammonia-N	0.02	0.05	<0.02	0.04	0.07	0.02	<0.02	<0.02	<0.02
Total P	0.02	0.02	0.03	0.03	0.04	0.04	0.07	0.03	0.02
Nitrate/Nitrite	<0.4	<0.4	<0.4	<0.4	<0.4	<0.4	<0.4	<0.4	<0.4

Table 7. Values for select chemical and physical parameters at location SC-3 during the different sampling dates. All units are in (mg L^{-1}) unless otherwise noted. No samples were collected in August, September, or October due to a lack of flow in Second Creek at that location.

	5/4/2010	5/25/2010	6/8/2010	6/22/2010	7/7/2010	7/19/2010	8/11/2010	9/15/2010	10/20/2010
Time	12:14	11:30	10:30	10:45	10:47	10:15			
pH	8.3	8.1	7.9	7.7	7.9	7.9			
Cond ($\mu\text{S cm}^{-1}$)	800	850	1000	1050	1100	550			
Temp (°C)			16.5	20.8	22.7	18.8			
Alk	275	325	340	325	355	275			
DOC	5.7	8.8	14.1	13.2	14.5	5.6			
THg F (ng L^{-1})	0.6	1.7	2.3	3.0	1.2	0.9			
MeHg F (ng L^{-1})	0.12	0.42	0.51	0.52	0.34	0.31			
$\delta^{34}\text{S}_{\text{SO}_4}$ (‰)	9.1	10.1	10.9	11.5	15.0	11.5			
$\delta^{18}\text{O}_{\text{SO}_4}$ (‰)	-2.1	0.4	-0.5	0.4	4.7	4.9			
Al	0.01	0.01	0.00	0.01	0.01	0.00			
Ba	0.01	0.01	0.02	0.02	0.02	0.02			
Ca	38.9	37.6	41.8	35.3	39.2	43.5			
Fe	0.1	0.3	0.6	0.6	0.2	0.3			
K	11.3	10.2	10.6	9.5	7.9	5.4			
Mg	132	127	135	124	86	59			
Mn	0.1	0.3	0.3	0.2	0.9	2.2			
Na	15.9	14.7	15.7	15.2	15.2	12.4			
P	0.0	0.02	0.03	0.02	0.01	0.01			
Si	1.1	1.7	3.3	3.2	5.2	7.0			
Sr	0.11	0.12	0.13	0.11	0.13	0.14			
F	0.1	0.2	0.2	0.2	0.4	0.2			
Cl	10.4	10.6	11.0	9.8	8.0	5.2			
Br	0.01	0.01	0.01	0.01	0.02	0.02			
Nitrate-N	0.5	0.7	1.0	1.0	0.2	1.5			
SO₄	352	338	341	319	153	123			
Phosphate-P	0.00	0.00	0.00	0.00	0.00	0.04			
TKN	<0.2		1.0	0.9	1.2	0.6			
Ammonia-N	0.02	0.03	0.03	0.04	0.08	0.04			
Total P	0.02	0.03	0.04	0.04	0.04	0.04			
Nitrate/Nitrite	<0.4	<0.4	<0.4	<0.4	<0.4	0.63			

Table 8. Values for select chemical and physical parameters at location SC-4 during the different sampling dates. All units are in (mg L^{-1}) unless otherwise noted.

	5/4/2010	5/25/2010	6/8/2010	6/22/2010	7/7/2010	7/19/2010	8/12/2010	9/15/2010	10/20/2010
Time	9:11	9:15	8:29	8:45	8:36	8:20	8:30	8:45	9:00
pH	7.7	7.9	8.1	7.9	8.2	7.9	7.4	7.7	8.2
Cond ($\mu\text{S cm}^{-1}$)	950	1000	1400	1200	1700	1650	2050	1725	1700
Temp (C)			17.7	21.3	23.4	21.4	24.4	12.0	7.4
Alk	100	325	370	355	405	410	445		
DOC	7.4	9.4	10.7	11.7	13.2	9.9	9.2	8.7	8.1
THg F (ng L^{-1})	0.7	1.1	1.3	1.7	1.4	1.0	1.3	0.9	0.9
MeHg F (ng L^{-1})	0.19	0.28	0.19	0.32	0.32	0.11	0.11	0.11	0.20
$\delta^{34}\text{S}_{\text{SO}_4}$ (‰)	6.9	7.6	7.4	7.8	7.4	7.2	7.2	8.0	7.5
$\delta^{18}\text{O}_{\text{SO}_4}$ (‰)	-5.2	-3.9	-5.0	-3.9	-4.1	-5.6	-5.7	-4.5	-4.9
Al	0.01	0.00	0.01	0.01	0.01	0.00	0.01	0.01	0.01
Ba	0.02	0.02	0.02	0.02	0.02	0.02	0.03	0.03	0.02
Ca	51	48	55	47	56	62	62	66	67
Fe	0.0	0.0	0.1	0.1	0.1	0.1	0.0	0.1	0.1
K	12.3	11.0	13.0	11.4	13.1	15.4	17.2	15.0	14.2
Mg	175	164	200	168	201	248	266	254	278
Mn	0.5	0.6	0.3	0.4	0.6	0.3	0.3	0.2	0.2
Na	28.4	25.1	31.7	27.1	35.5	43.9	50.3	46.8	48.1
P	0.0	0.01	0.01	0.01	0.01	0.02	0.01	0.01	0.01
Si	2.9	6.5	3.3	3.3	4.1	3.3	4.7	4.7	4.8
Sr	0.18	0.22	0.20	0.17	0.21	0.24	0.27	0.26	0.25
F	0.1	0.2	0.2	0.2	0.3	0.2	0.3	0.2	0.2
Cl	8.7	8.0	8.4	8.1	8.5	8.3	9.1	8.5	8.8
Br	0.02	0.01	0.01	0.01	0.00	0.02	0.03	0.02	0.02
Nitrate-N	0.1	4.3	0.2	1.3	0.3	1.7	0.1	0.4	0.1
SO₄	598	549	652	554	689	903	1004	951	1043
Phosphate-P	0.01	0.00	0.01	0.00	0.00	0.03	0.00	0.00	0.00
TKN	0.21		0.7	0.8	0.8	0.8	0.6	0.6	0.4
Ammonia-N	0.04	0.05	<0.02	0.05	0.04	0.03	<0.02	<0.02	<0.02
Total P	0.02	0.03	0.04	0.03	0.03	0.03	0.03	0.02	0.02
Nitrate/Nitrite	<0.4	<0.4	<0.4	<0.4	<0.4	<0.4	<0.4	<0.4	<0.4

Table 9. Values for select chemical and physical parameters at location *ETR-1* during the different sampling dates. All units are in (mg L^{-1}) unless otherwise noted.

	5/4/2010	5/25/2010	6/9/2010	6/22/2010	7/7/2010	7/19/2010	8/11/2010	9/15/2010	10/20/2010
Time	14:45	13:50	7:43	12:44	14:52	13:05	11:00	13:15	15:30
pH	8.0	7.9	7.9	7.9	8.2	8.0	8.1	8.1	8.2
Cond ($\mu\text{S cm}^{-1}$)	950	900	875	900	1250	1100	1150	1600	1500
Temp (C)		20.8	15.0	21.4	19.4	19.3	21.6	15.1	13.5
Alk	375	335	300	320	450	430	395		
DOC	6.2	7.2	6.5	6.9	5.2	2.9	5.4	5.2	3.8
THg F (ng L^{-1})	0.9	1.2	1.1	1.2	1.1	1.3	1.6	1.1	0.8
MeHg F (ng L^{-1})	0.16	0.13	0.08	0.18	0.18	<0.05	0.33	0.10	0.06
$\delta^{34}\text{S}_{\text{SO}_4}$ (‰)	6.4	6.4	7.3	7.1	1.9	5.0	4.2	4.9	5.1
$\delta^{18}\text{O}_{\text{SO}_4}$ (‰)	-6.1	-4.2	-5.1	-2.3	-6.1	-9.3	-8.6	-6.9	-8.2
Al	0.00	0.06	0.03	0.07	0.06	0.08	0.06	0.08	0.04
Ba	0.01	0.02	0.01	0.01	0.02	0.02	0.01	0.02	0.01
Ca	56.2	54.1	43.9	51.6	52.4	61.7	41.3	56.4	51.8
Fe	0.0	0.1	0.1	0.1	0.0	0.0	0.0	0.1	0.0
K	13.5	11.7	10.0	9.7	16.4	14.8	14.6	15.7	18.1
Mg	98	84	75	59	115	97	99	112	143
Mn	0.2	0.3	0.1	0.2	0.2	0.2	0.2	0.2	0.1
Na	90	78	68	80	94	92	74	188	114
P	0.2	0.14	0.40	0.19	0.24	0.10	0.30	0.16	0.33
Si	5.6	5.7	4.8	5.6	6.1	6.3	5.3	6.4	6.3
Sr	0.18	0.18	0.15	0.16	0.17	0.19	0.13	0.17	0.16
F	0.5	0.4	0.3	0.5	0.5	0.4	0.4	0.4	0.5
Cl	117	99	73	110	97	118	69	235	128
Br	0.08	0.07	0.05	0.08	0.09	0.07	0.08	0.08	0.07
Nitrate-N	2.2	3.3	22.4	2.6	5.4	6.3	6.7	7.0	8.0
SO₄	222	184	169	107	256	196	215	223	331
Phosphate-P	0.13	0.08	0.32	0.20	0.18	0.09	0.16	0.10	0.24
TKN	6.7		3.8	6.0	5.4	3.3	7.3	8.9	4.1
Ammonia-N	6.0	2.3	2.7	5.1	4.9	2.5	6.2	8.2	3.0
Total P	0.23	0.18	0.42	0.26	0.31	0.14	0.32	0.25	0.30
Nitrate/Nitrite	2.2	2.9	3.7	2.1	5.4	5.3	4.3	5.2	9.7

Table 10. Values for select chemical and physical parameters at location *ETR-2* during the different sampling dates. All units are in (mg L^{-1}) unless otherwise noted.

Date	5/4/2010	5/25/2010	6/9/2010	6/22/2010	7/7/2010	7/19/2010	8/11/2010	9/15/2010	10/20/2010
Time	15:52	14:56	8:45	13:30	13:37	13:30	12:10	14:45	14:20
pH	8.4	8.3	8.3	8.4	8.6	8.6	8.5	8.7	8.5
Cond ($\mu\text{S cm}^{-1}$)	1200	1200	1350	1400	1750	1525	1600	1600	1600
Temp (C)		24.7	15.0	21.6	22.7	20.0	22.6	12.8	8.5
Alk	485	445	515	510	565	590	625		
DOC	3.8	5.6	3.8	4.7	3.5	5.0	2.0	3.2	2.0
THg F (ng L^{-1})	0.60	1.2	0.7	1.3	0.9	0.9	0.8	0.8	0.49
MeHg F (ng L^{-1})	<0.05	0.10	<0.05	0.11	0.08	0.10	<0.05	0.08	<0.05
$\delta^{34}\text{S}_{\text{SO}_4}$ (‰)	7.2	7.2	7.4	6.6	4.8	6.2	4.3	4.4	5.3
$\delta^{18}\text{O}_{\text{SO}_4}$ (‰)	-7.5	-6.7	-6.8	-7.3	-8.5	-6.2	-10.7	-9.2	-9.8
Al	0.01	0.01	0.01	0.01	0.02	0.00	0.01	0.01	0.01
Ba	0.01	0.01	0.01	0.01	0.01	0.01	0.01	0.00	0.00
Ca	44.1	37.0	38.4	38.0	32.7	30.4	23.1	23.2	29.0
Fe	0.0	0.0	0.0	0.0	0.0	0.0	0.0	0.0	0.0
K	18.8	17.2	19.2	20.1	22.3	26.5	25.7	25.8	25.3
Mg	187	152	164	163	184	196	209	205	247
Mn	0.0	0.1	0.0	0.0	0.0	0.0	0.0	0.0	0.0
Na	81	77	86	84	95	98	104	103	104
P	0.0	0.02	0.01	0.01	0.01	0.01	0.00	0.01	0.01
Si	3.8	3.7	4.4	4.3	4.8	4.8	5.2	5.0	5.3
Sr	0.15	0.14	0.14	0.15	0.13	0.12	0.09	0.09	0.10
F	0.1	0.1	0.1	0.1	0.1	0.1	0.1	0.1	0.1
Cl	49.9	49.8	40.4	36.5	36.5	33.2	27.4	27.3	30.7
Br	0.04	0.04	0.04	0.04	0.05	0.04	0.04	0.04	0.04
Nitrate-N	2.1	2.2	7.8	5.0	7.8	9.7	15.1	13.2	9.8
SO ₄	496	404	432	430	490	511	533	494	655
Phosphate-P	0.00	0.00	0.00	0.00	0.00	0.04	0.01	0.01	0.02
TKN	<0.2		0.5	0.7	0.6	0.5	0.4	0.5	0.5
Ammonia-N	0.04	0.07	0.03	0.05	0.03	<0.02	0.04	<0.02	0.05
Total P	0.02	0.04	0.03	0.03	0.02	0.02	0.02	0.02	0.05
Nitrate/Nitrite	2.0	1.9	7.3	4.0	6.7	8.5	12.0	12.9	9.7

Table 11. Values for select chemical and physical parameters at location *ETR-3* during the different sampling dates. All units are in (mg L^{-1}) unless otherwise noted.

	5/4/2010	5/25/2010	6/9/2010	6/22/2010	7/7/2010	7/19/2010	8/11/2010	9/15/2010	10/20/2010
Time	15:15	14:30	8:20	13:05	13:14	14:05	12:00	14:32	15:15
pH	9.1	8.9	9.1	9.1	9.7	9.5	9.1	9.3	9.0
Cond ($\mu\text{S cm}^{-1}$)	900	1000	1000	1050	1275	1100	1000	1100	1200
Temp (C)		27.3	15.0	23.7	24.4	22.8	26.4	13.5	9.7
Alk	360	320	345	360	360	345	340		
DOC	7.7	6.7	6.4	6.5	6.2	5.9	5.9	5.2	4.5
THg F (ng L^{-1})	1.0	2.2	2.2	2.2	3.3	1.8	2.1	0.8	<0.4
MeHg F (ng L^{-1})	0.14	0.97	0.93	1.47	2.22	0.72	0.91	0.13	<0.05
$\delta^{34}\text{S}_{\text{SO}_4}$ (‰)	5.8	8.0	6.2	7.7	6.2	6.2	6.3	6.4	5.6
$\delta^{18}\text{O}_{\text{SO}_4}$ (‰)	-1.4	-2.3	-2.4	-2.3	-2.1	-3.5	-4.7	-4.0	-2.7
Al	0.01	0.01	0.01	0.01	0.01	0.01	0.01	0.02	0.02
Ba	0.01	0.01	0.01	0.01	0.01	0.01	0.01	0.01	0.01
Ca	21.5	12.8	17.6	20.9	16.4	19.7	14.6	25.6	30.1
Fe	0.0	0.0	0.0	0.0	0.0	0.0	0.0	0.0	0.0
K	15.7	14.7	14.1	14.4	15.1	14.8	15.0	15.9	16.2
Mg	125	118	118	116	118	116	114	126	136
Mn	0.0	0.1	0.1	0.1	0.0	0.0	0.1	0.0	0.1
Na	88.8	84.1	82.9	80.9	85.4	82.5	79.4	82.7	85.2
P	0.0	0.11	0.04	0.04	0.03	0.03	0.02	0.02	0.02
Si	0.6	2.1	2.5	3.6	4.0	4.3	5.2	5.6	6.1
Sr	0.05	0.03	0.04	0.06	0.04	0.05	0.04	0.08	0.09
F	0.3	0.3	0.3	0.3	0.3	0.3	0.3	0.2	0.3
Cl	85.2	88.5	84.3	83.8	85.9	79.9	73.2	66.3	67.6
Br	0.06	0.07	0.07	0.07	0.07	0.06	0.07	0.06	0.05
Nitrate-N	2.2	10.1	0.1	1.2	0.5	0.6	3.1	1.5	1.3
SO₄	296	596	276	273	281	269	267	282	328
Phosphate-P	0.01	0.05	0.01	0.00	0.00	0.04	0.00	0.00	0.02
TKN	2.0		2.4	2.9	4.0	4.7	4.9	5.4	4.1
Ammonia-N	0.11	0.33	0.10	0.40	0.07	0.03	0.22	0.33	0.28
Total P	0.17	0.16	0.24	0.23	0.28	0.21	0.23	0.31	0.05
Nitrate/Nitrite	<0.4	<0.4	<0.4	<0.4	<0.4	<0.4	<0.4	1.11	1.30

***The precision level for the replicate sulfate and nitrate analyses for the May 25th sample were very low therefore these samples should be disregarded.*

Table 12: Input values and results for estimating $\text{SO}_4^{=}$ loss (mg lost per liter of water) due to $\text{SO}_4^{=}$ reduction processes in the wetlands and lake studied in this report. Calculations refer to reduction directly upstream from the listed sample site. DF = dilution factor which, when calculated, represents the mass of water exiting the wetland divided by the mass of water entering the wetland at the $\text{SO}_4^{=}$ source. See text for explanation of other model components.

Parameter	5/4	5/25	6/9	6/22	7/7	7/19	8/11	9/15	10/20
LLC-2									
$\delta^{34}\text{S}_{\text{SO}_4,\text{init}}$ (‰)	8.6	8.6	8.6	8.6	8.6	8.6	8.6	8.6	8.6
$\delta^{34}\text{S}_{\text{SO}_4}$ (‰)	11.2	13.0	14.6	14.7	13.4	14.8	12.0	13.2	13.4
$\text{SO}_4^{=}$ (mg L ⁻¹)	120	123	140	137	150	157	77	126	195
F	0.86	0.77	0.70	0.70	0.75	0.69	0.82	0.76	0.75
$\text{SO}_4^{=}$ initial (mg L ⁻¹)	140	160	199	196	199	227	94	165	259
DF	1.80	1.58	1.27	1.29	1.27	1.11	2.69	1.53	0.97
$\text{SO}_4^{=}$ lost (mg L ⁻¹)	36	58	75	76	62	77	45	60	62
SR-1									
$\delta^{34}\text{S}_{\text{SO}_4,\text{init}}$ (‰)	7.0	7.0	7.0	7.0	7.0			7.0	7.0
$\delta^{34}\text{S}_{\text{SO}_4}$ (‰)	35.3	36.0	38.5	39.6	36.2			33.7	31.1
$\text{SO}_4^{=}$ (mg L ⁻¹)	16.4	8.4	7.6	6.0	5.4	3.5	3.9	7.5	14.5
F	0.19	0.18	0.16	0.15	0.18			0.21	0.24
$\text{SO}_4^{=}$ initial (mg L ⁻¹)	86	46	48	41	30			36	60
DF	0.66	1.22	1.17	1.39	1.89			1.58	0.95
$\text{SO}_4^{=}$ lost (mg L ⁻¹)	46	46	48	48	46			45	43
SC-2									
$\delta^{34}\text{S}_{\text{SO}_4,\text{init}}$ (‰)	7.2	7.2	7.2	7.2	7.2	7.2	7.2	7.2	7.2
$\delta^{34}\text{S}_{\text{SO}_4}$ (‰)	10.8	13.4	16.9	16.7	14.6	17.0	18.7	16.1	13.7
$\text{SO}_4^{=}$ (mg L ⁻¹)	192	193	180	148	236	147	186	133	149
F	0.81	0.69	0.57	0.57	0.65	0.56	0.51	0.59	0.68
$\text{SO}_4^{=}$ initial (mg L ⁻¹)	238	279	317	259	364	262	366	225	219
$\text{SO}_4^{=}$ lost (mg L ⁻¹)	46	86	137	111	128	115	180	92	70
SC-3									
$\delta^{34}\text{S}_{\text{SO}_4,\text{init}}$ (‰) (Pit 1)	8.8	8.8	8.8	8.8	8.8	8.8	8.8	8.8	8.8
$\delta^{34}\text{S}_{\text{SO}_4}$ (‰)	9.1	10.1	10.9	11.5	15.0	11.5			
$\text{SO}_4^{=}$ (mg L ⁻¹)	352	338	341	319	153	123			
F	0.98	0.92	0.89	0.85	0.69	0.85			
$\text{SO}_4^{=}$ initial (mg L ⁻¹)	358	366	385	373	221	144			
DF	1.07	1.05	1.00	1.03	1.74	2.67			
$\text{SO}_4^{=}$ lost (mg L ⁻¹)	6	29	44	56	118	56			
SC-4									
$\delta^{34}\text{S}_{\text{SO}_4,\text{init}}$ (‰) (Pit 6)						5.4	5.4	5.4	5.4
$\delta^{34}\text{S}_{\text{SO}_4}$ (‰)	6.9	7.6	7.4	7.8	7.4	7.2	7.2	8.0	7.5
$\text{SO}_4^{=}$ (mg L ⁻¹)	598	549	652	554	689	903	1004	951	1043
F						0.90	0.90	0.86	0.88
$\text{SO}_4^{=}$ initial (mg L ⁻¹)						1005	1115	1110	1182
$\text{SO}_4^{=}$ lost (mg L ⁻¹)						103	111	158	139
ETR-3									
$\delta^{34}\text{S}_{\text{SO}_4,\text{init}}$ (‰)	5.65	5.65	5.65	5.65	5.65	5.65	5.65	5.65	5.65
$\delta^{34}\text{S}_{\text{SO}_4}$ (‰)	5.8	8.0	6.2	7.7	6.2	6.2	6.3	6.4	5.6
$\text{SO}_4^{=}$ (mg L ⁻¹)	296		276	273	281	269	267	282	328
F	0.99	0.87	0.97	0.88	0.97	0.97	0.96	0.96	1.00
$\text{SO}_4^{=}$ initial (mg L ⁻¹)	299		285	309	290	277	277	294	327
$\text{SO}_4^{=}$ lost (mg L ⁻¹)	3		9	36	9	8	11	12	0

Figures

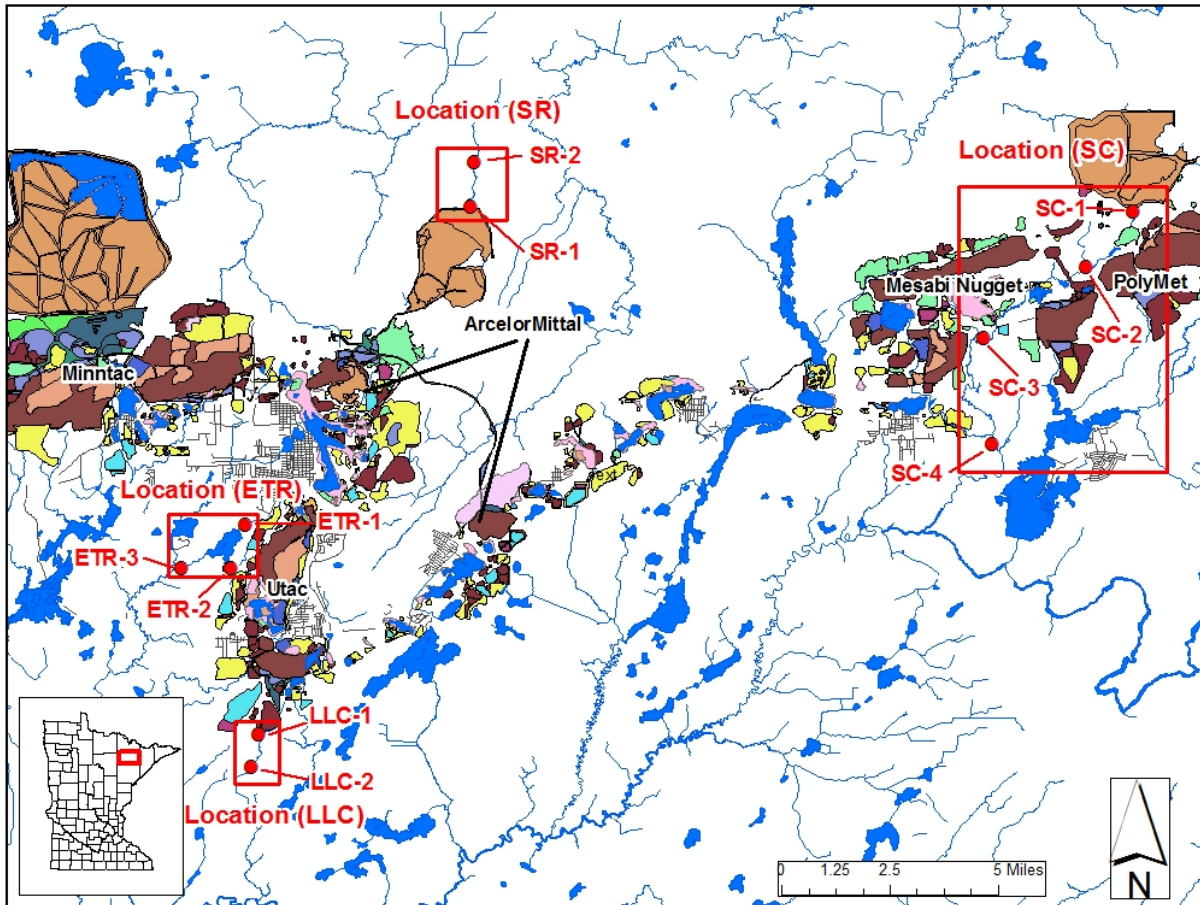


Fig. 1. Location map for the wetlands and lake investigated in this study.



Fig. 2. 2010 aerial photo of the Long Lake Creek Watershed wetland and the location of sample sites LLC-1 and LLC-2.



Fig. 3. 2010 aerial photo of the Sand River Watershed wetland and the location of sample sites SR-1 and SR-2. The reservoir area located to the south of SR-1 is ArcelorMittal's currently inactive tailings basin.

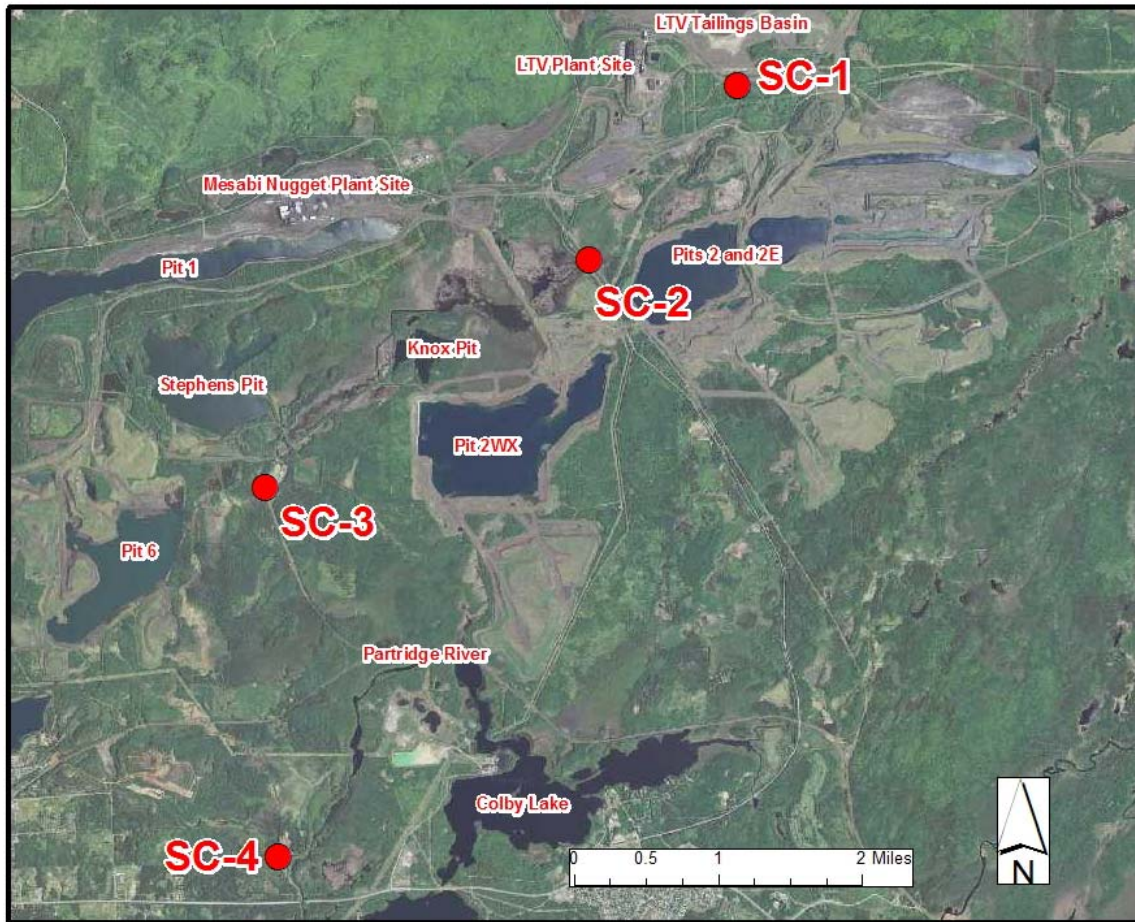


Fig. 4a. 2010 aerial photo of the Second Creek Watershed and the location sample sites SC-1, SC-2, SC-3, and SC-4.

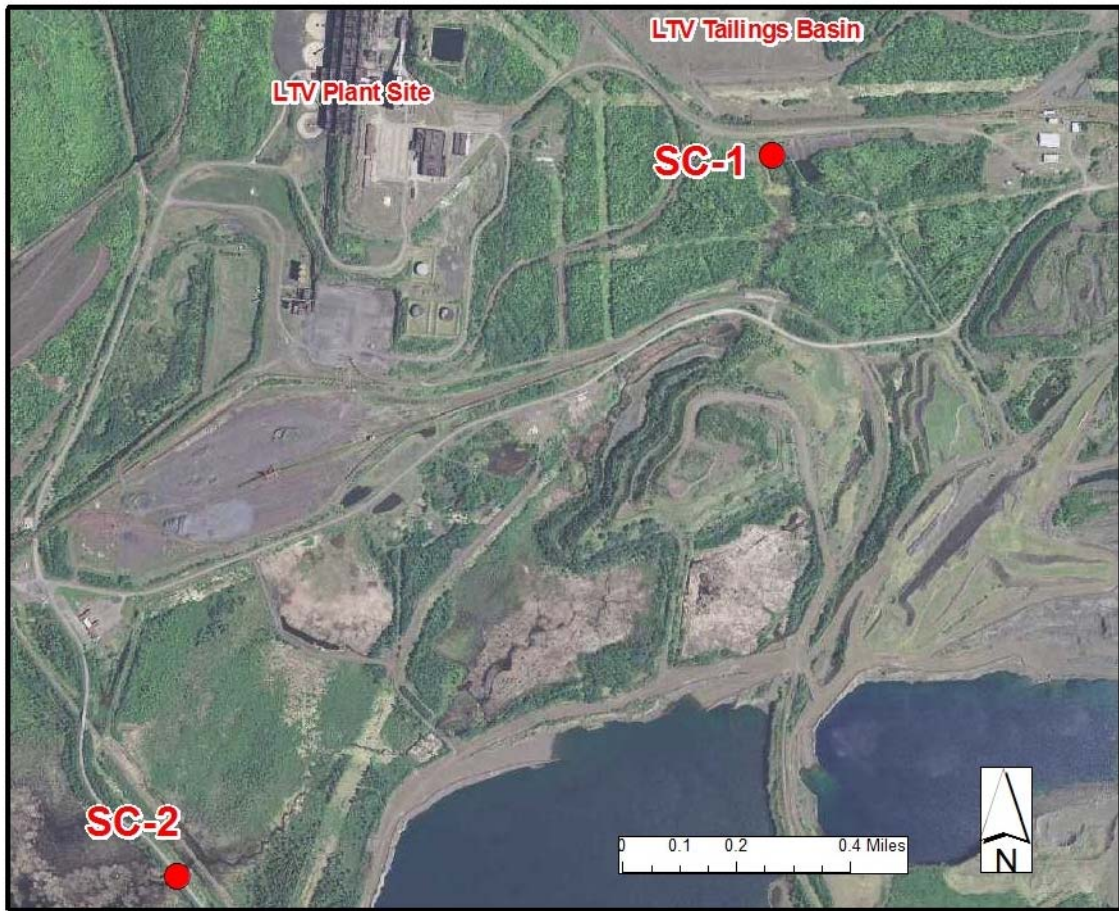


Fig. 4b. 2010 aerial photo of Second Creek between sampling points SC-1 and SC-2.

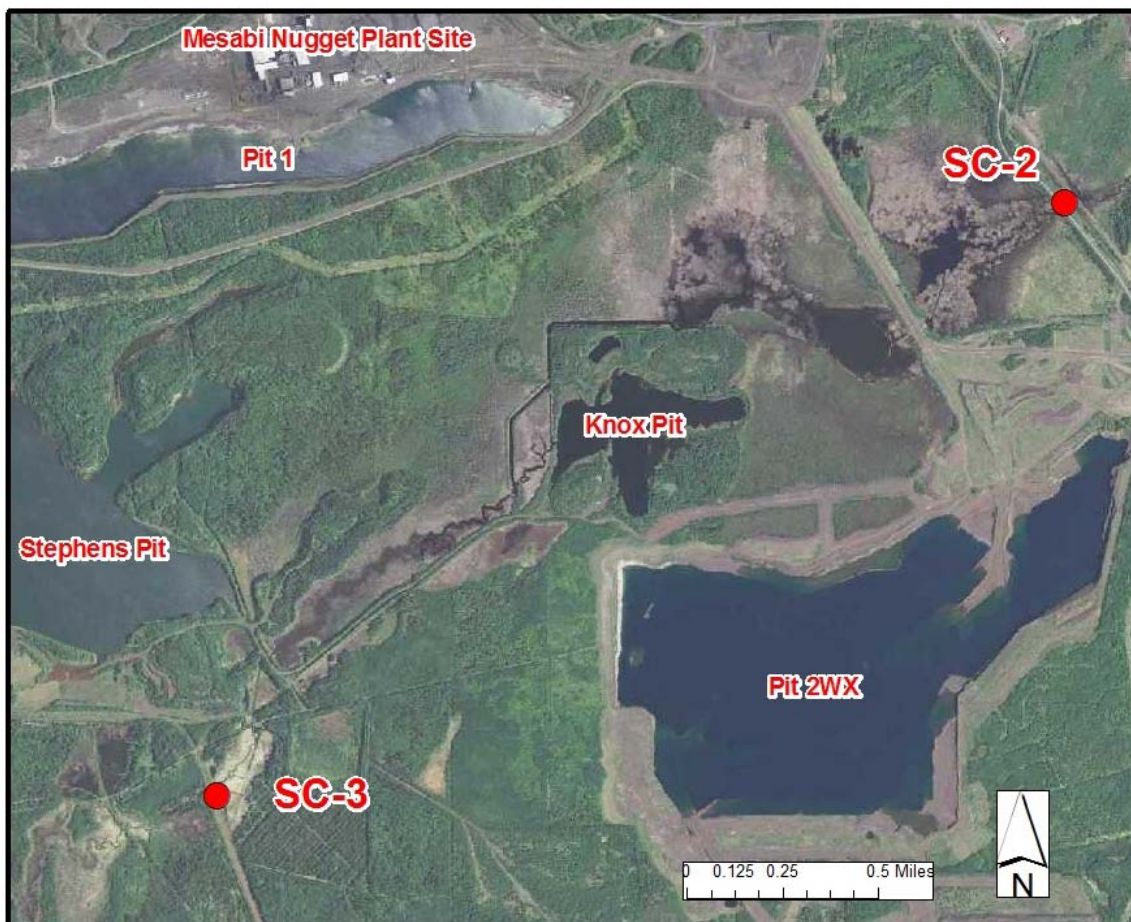


Fig. 4c. 2010 aerial photo of Second Creek between sampling points SC-2 and SC-3

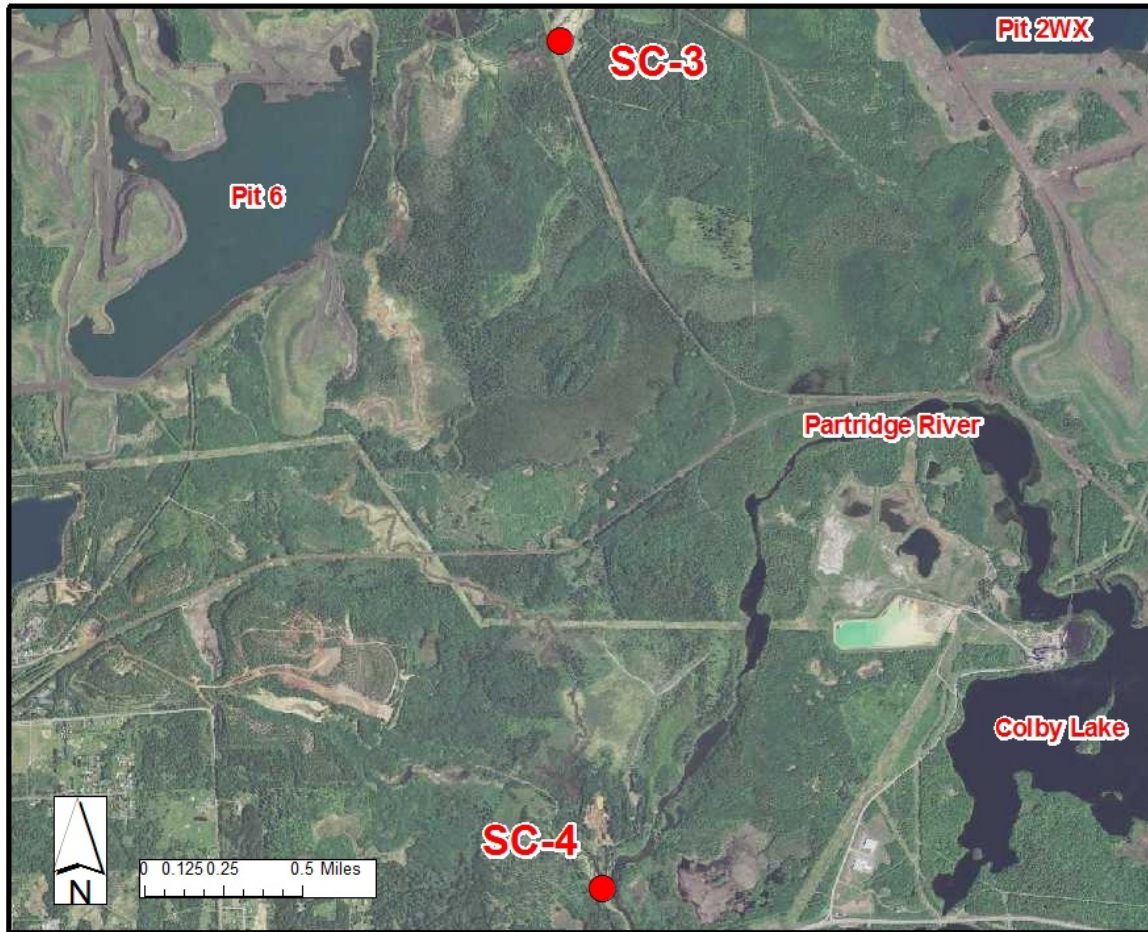


Fig. 4d. 2010 aerial photo of Second Creek between sampling points SC-3 and SC-4.



Fig. 5. 2010 aerial photo of Lake Manganika in the East Two River Watershed and the location of sample sites ETR-1, ETR-2, and ETR-3. The City of Virginia is located northeast of the lake and United Taconite's Thunderbird Pit is located to the east and southeast.

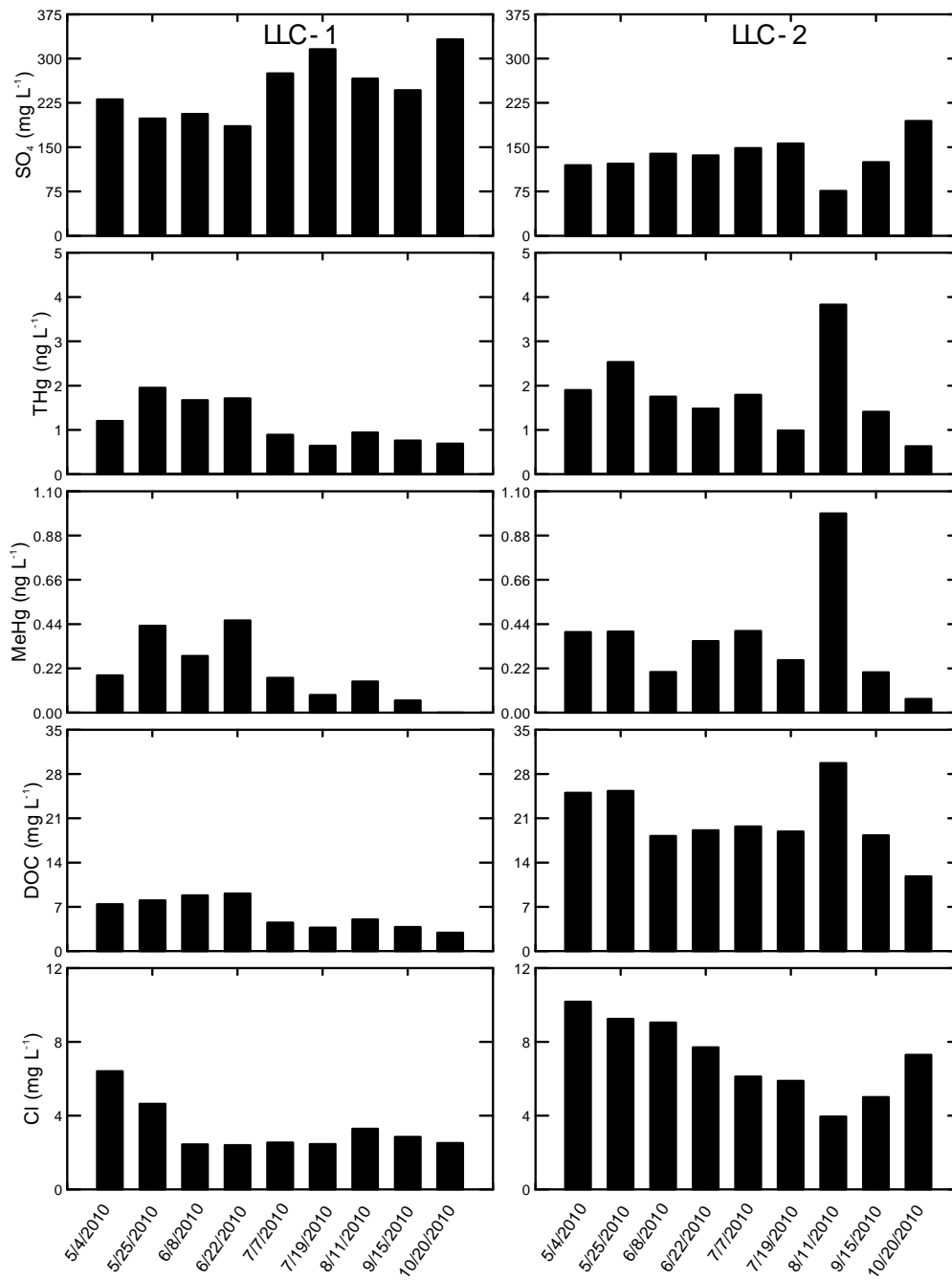


Fig. 6. Sulfate, THg, MeHg, DOC, and chloride levels at study locations **LLC-1** and **LLC-2**.

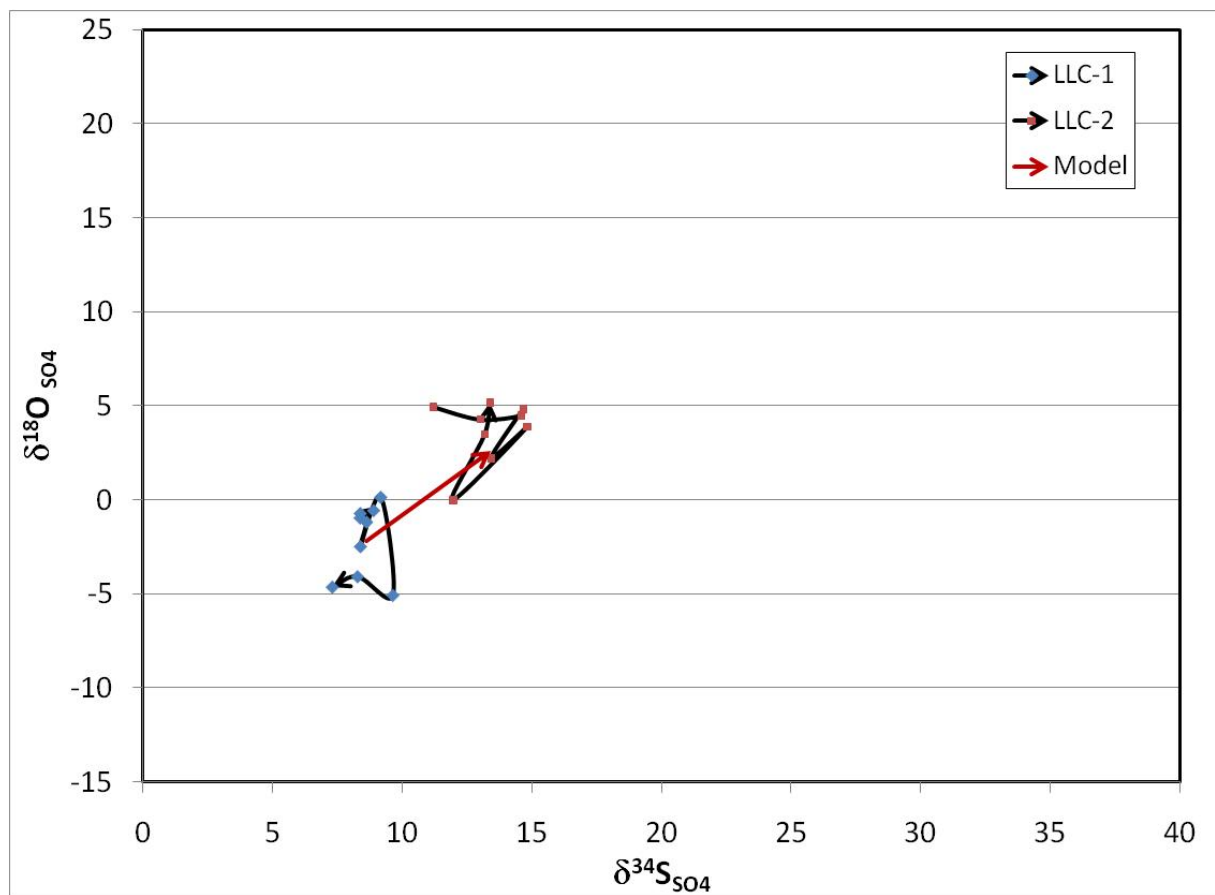


Fig. 7. $\delta^{34}\text{S}_{\text{SO}_4}$ and $\delta^{18}\text{O}_{\text{SO}_4}$ values for the dissolved sulfate at **LLC-1** and **LLC-2**. The arrows connecting the individual data points indicate the temporal progression of the samples. The large arrow represents the relative isotopic shift expected for equal fractionation of oxygen and sulfur isotopes during SO_4^{2-} reduction. See text for explanation.

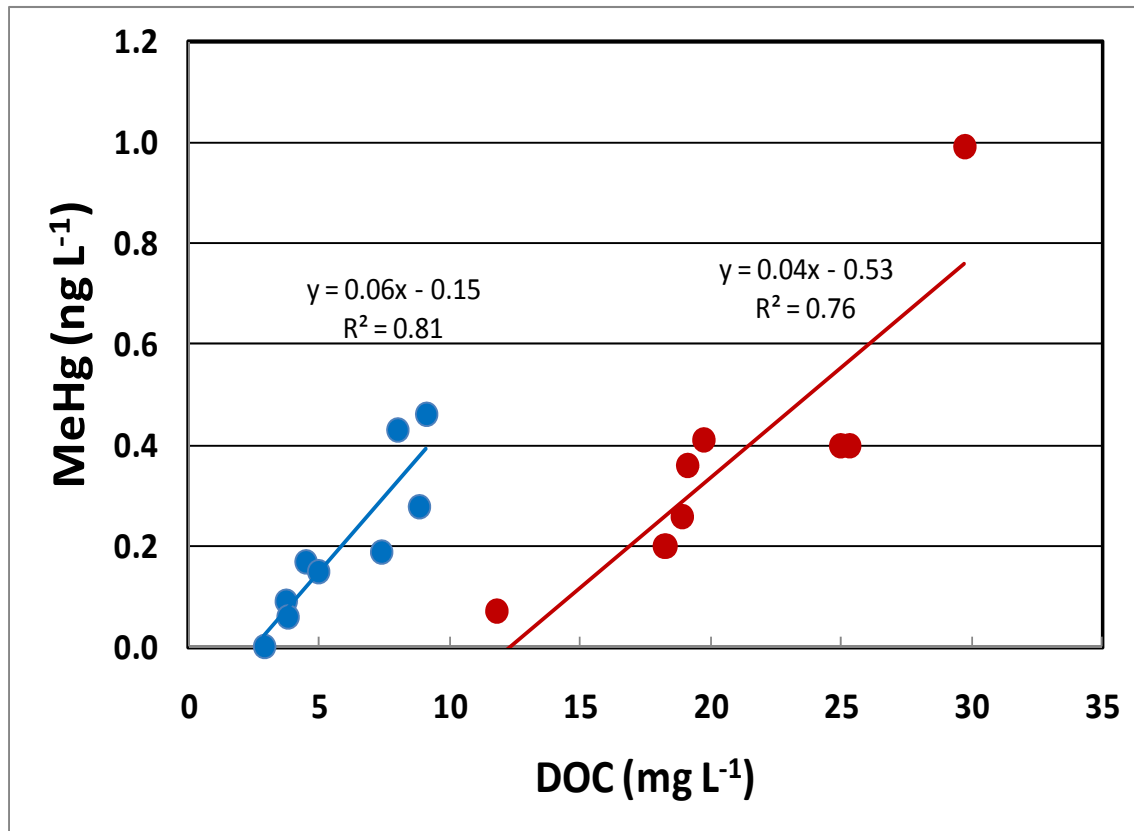


Fig. 8. MeHg vs. DOC concentrations for sampling locations *LLC-1* (blue circles) and *LLC-2* (red circles). Samples from LLC-2 were deeply colored compared to samples at LLC-1, and appeared to contain an extra DOC component that did not carry MeHg with it.

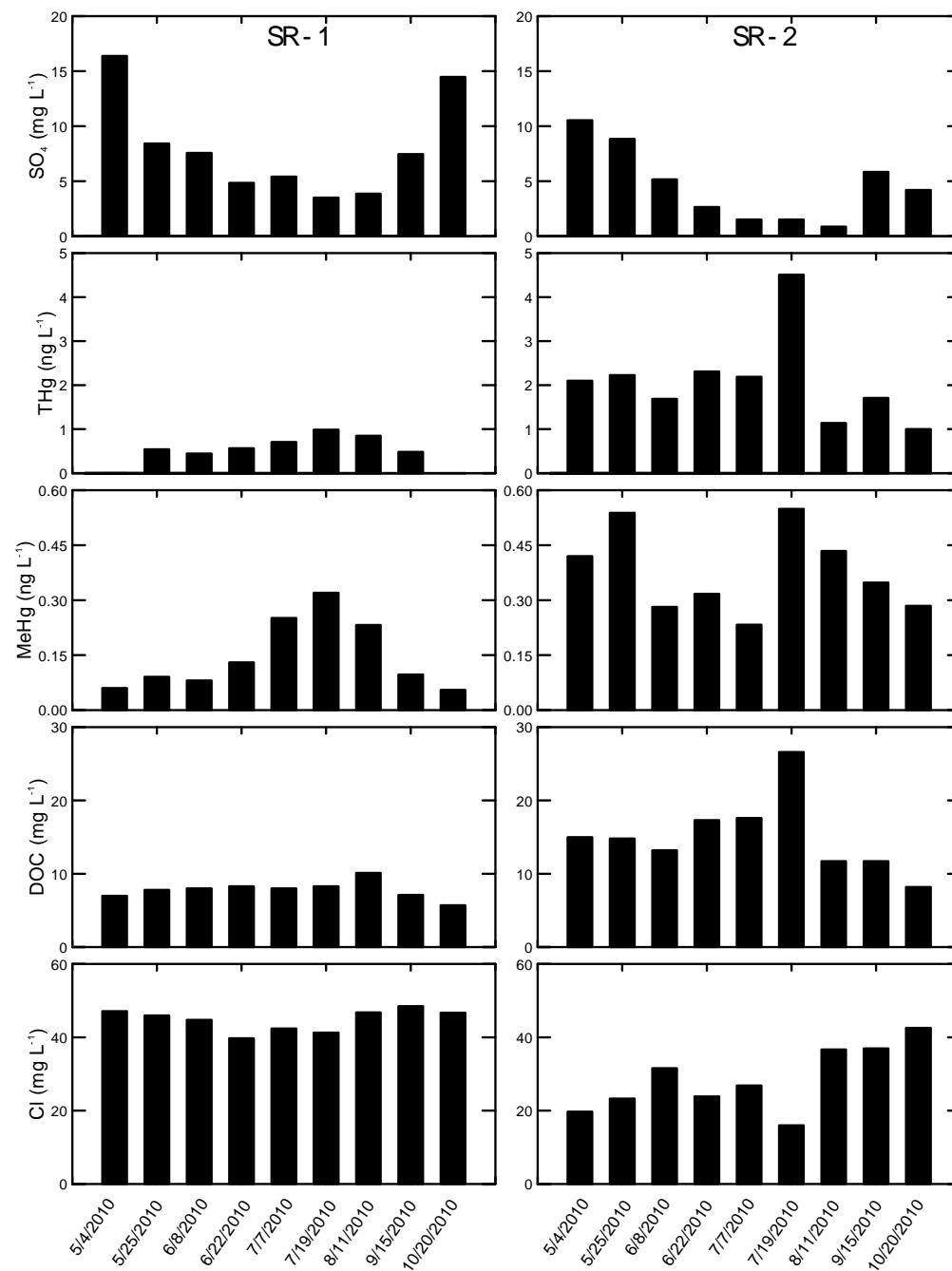


Fig. 9. A comparison of SO_4^{2-} , THg, MeHg, DOC, and Cl levels in samples collected from sites SR-1 and SR-2. SR-1 water is near the toe of a tailings basin that holds water containing an average of 56.7 mg L^{-1} SO_4^{2-} and 53.1 mg L^{-1} dissolved Cl^- . SR-2 is a site located downstream from this past a small wetland.

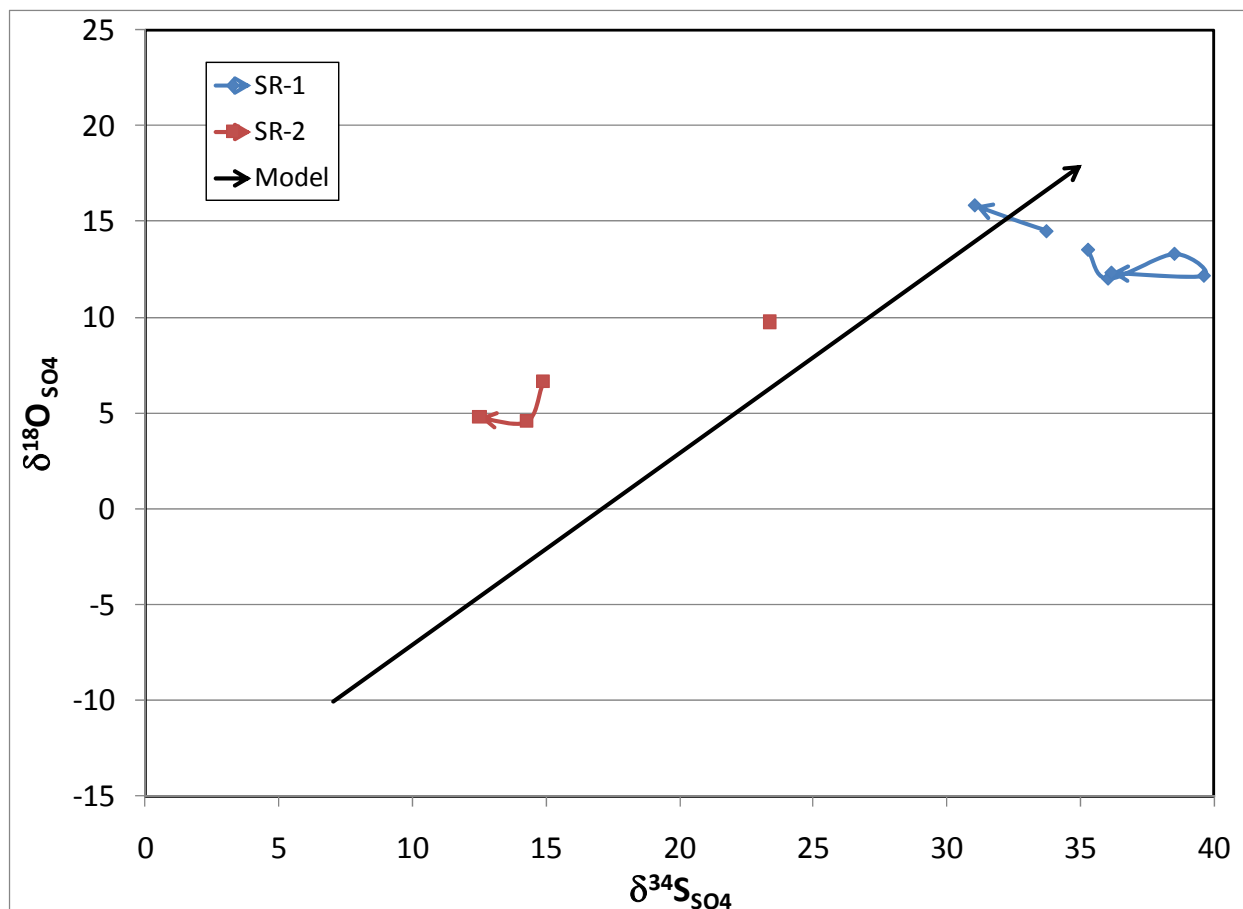


Fig. 10. $\delta^{34}\text{S}_{\text{SO}_4}$ and $\delta^{18}\text{O}_{\text{SO}_4}$ values for the dissolved sulfate at SR-1 and SR-2. The arrows connecting the individual data points indicate the temporal progression of the samples. The black arrow represents the relative oxygen and sulfur isotopic changes predicted for the reduction and precipitation (as sulfide) of about 80% of SO_4^- in basin water that occurs before the water seeps into the basin. $\delta^{34}\text{S}_{\text{SO}_4}$ and $\delta^{18}\text{O}_{\text{SO}_4}$ values in the tailings basin's clear water pool still need to be measured, but they were assumed here to be similar to those in other mining sources. The $\delta^{34}\text{S}_{\text{SO}_4}$ and $\delta^{18}\text{O}_{\text{SO}_4}$ values at SR-2, following seepage of water through the wetland to the north of the basin are lower than at SR-1 indicating that much of the SO_4^- at SR-2 was sourced from within the wetlands and mixed with the SO_4^- derived from SR-1. Not all of the sampling periods are represented because SO_4^- concentrations at these sites commonly fell below the levels needed to provide adequate SO_4^- for isotopic measurements.

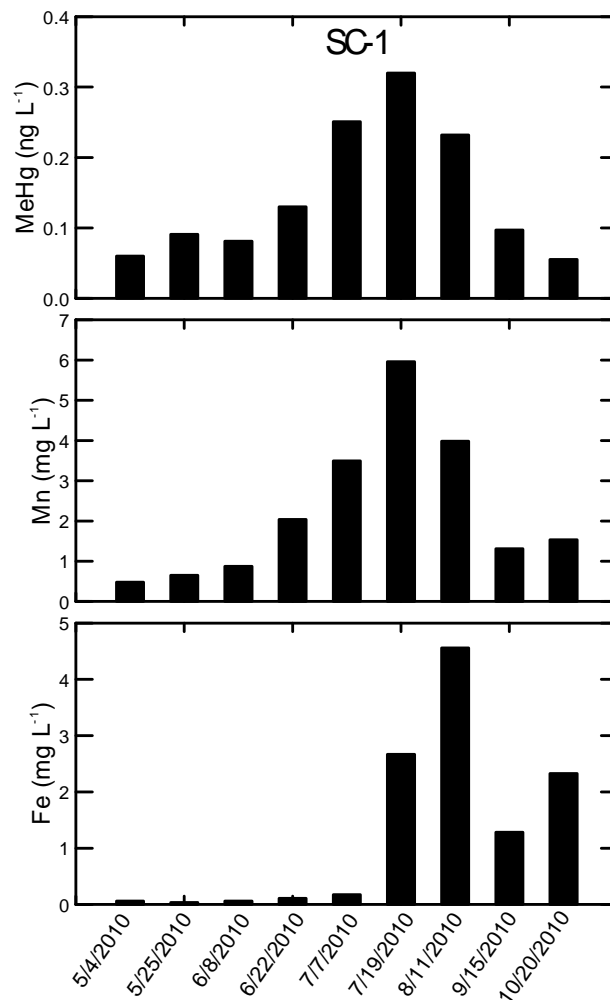


Fig. 11. MeHg, Mn, and Fe concentrations at sampling location *SR-1*. It is proposed in this study that MeHg concentrations began building at the site when SO_4^- reduction produced H_2S and HS^- at rates too fast for Fe^{++} to control it. As summer progressed, the P_{CO_2} increased causing pH to decrease, mobilizing Mn^{++} (thought to be controlled by solubility of MnCO_3) at this site. Modeling results, not shown, reveal that MeHg speciation shifts in response to pH, from a relatively immobile thiol-bound species attached to organic carbon to MeHgHS^0 , a highly mobile form that is inherently unstable in oxidizing environments. The appearance of dissolved Fe^{++} in water towards the end of the season signals the ending of H_2S and HS^- - related formation and transport of MeHgHS^0 . However, dissolved Mn^{++} concentrations also decline indicating a decline in P_{CO_2} with a corresponding increase in pH. MeHgHS^0 becomes an unimportant species again.

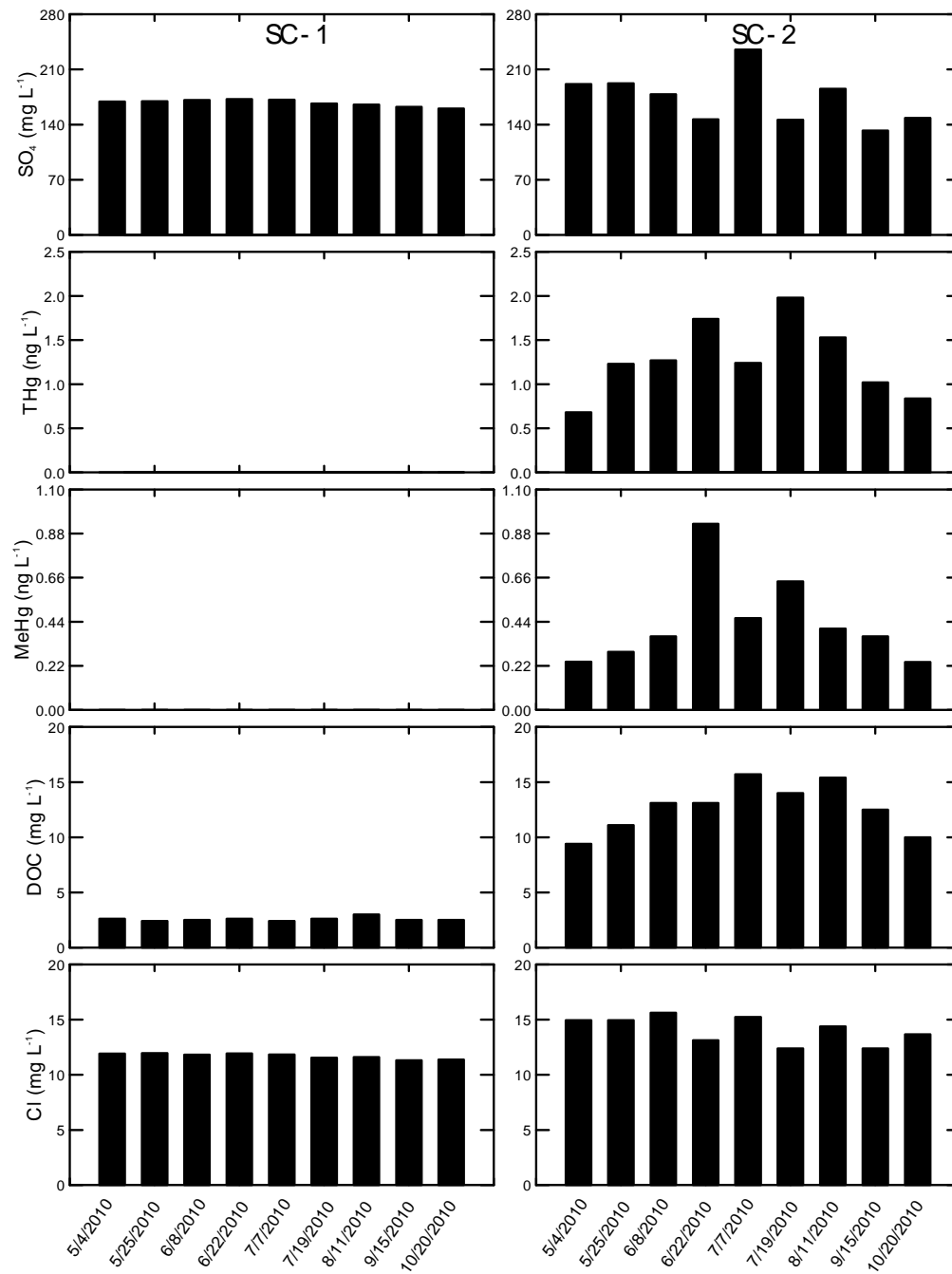


Fig. 12. A comparison of SO₄⁼, THg, MeHg, DOC, and Cl⁻ levels in samples collected from sites SC-1 and SC-2. Site SC-1 is at the toe of the former LTV mining company’s tailings basin. Site SC-2 is located downstream from this and beyond a wetland complex. The higher SO₄⁼ and Cl⁻ levels indicate that other waters from the tailings basin containing elevated SO₄⁼ and Cl⁻ are day-lighting in the wetland.

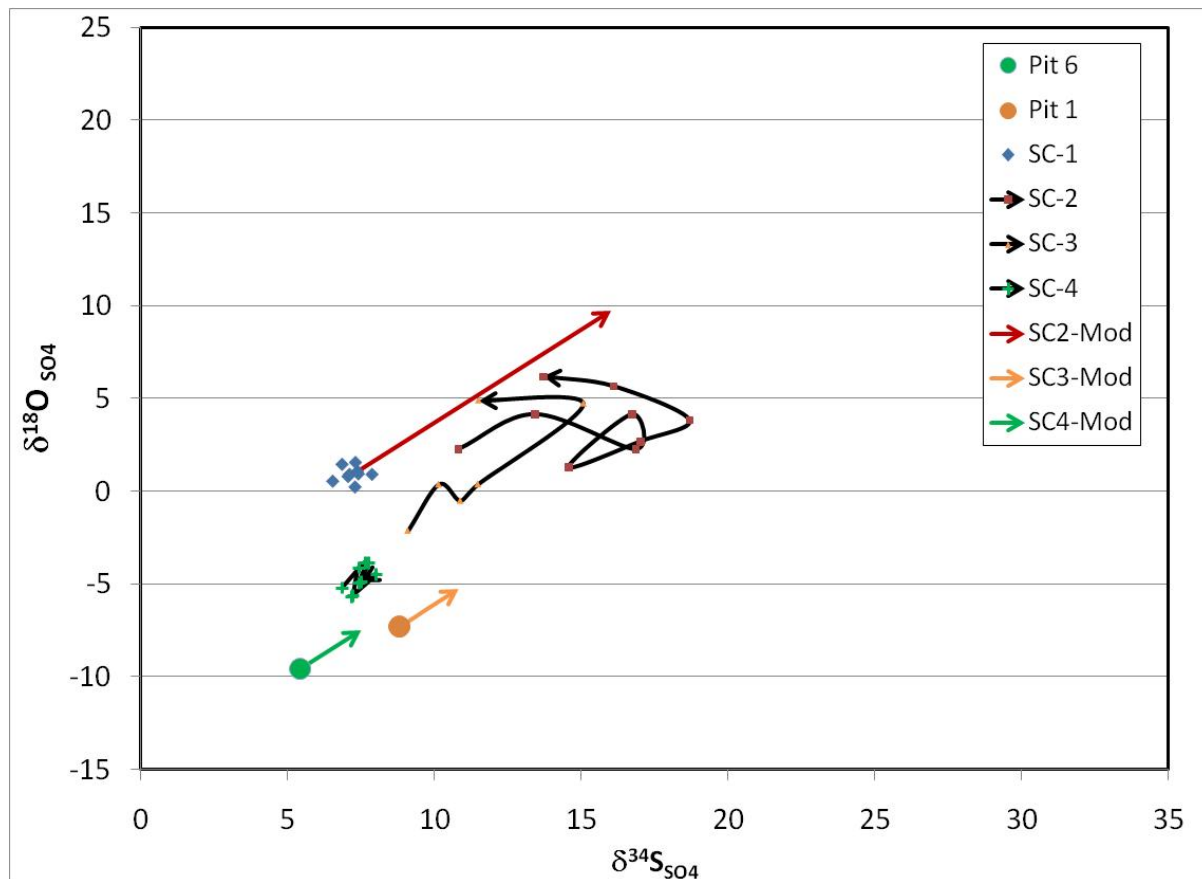


Fig. 13. $\delta^{34}\text{S}$ and $\delta^{18}\text{O}$ values for the dissolved SO_4^- at SC-1, SC-2, SC-3, SC-4, and for the SO_4^- in Pits 1 and 6. The arrows connecting the individual data points for each site show the temporal progression of the samples during the season. SC2-Mod, SC3-Mod, and SC4-Mod are the modeled isotopic pathways for reduction of waters from the LTV tailings basin, Pit-1, and Pit-6, respectively. See text for explanation.

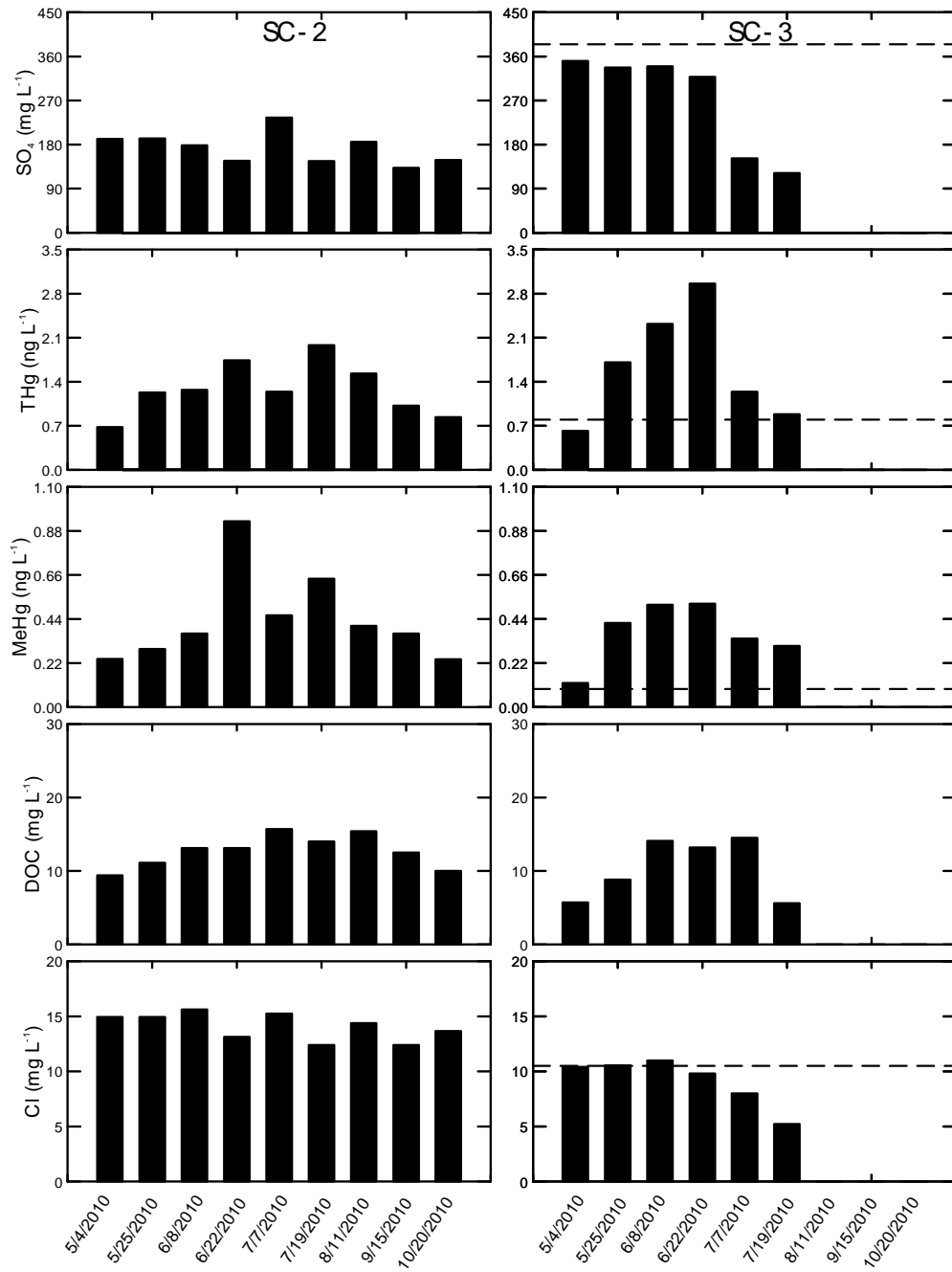


Fig. 14. Comparison of SO_4^{2-} , THg, MeHg, DOC, and Cl^- levels in samples collected from sites SC-2 and SC-3. The dashed line in the SC-3 panels represents the average concentration for the various constituents in Mesabi Nugget Pit 1. Mesabi Nugget was discharging water from Pit 1 into Second Creek until July 1st when pit dewatering was halted. No samples were collected at SC-3 in August, September, or October due to a lack of flow in the creek at that location.

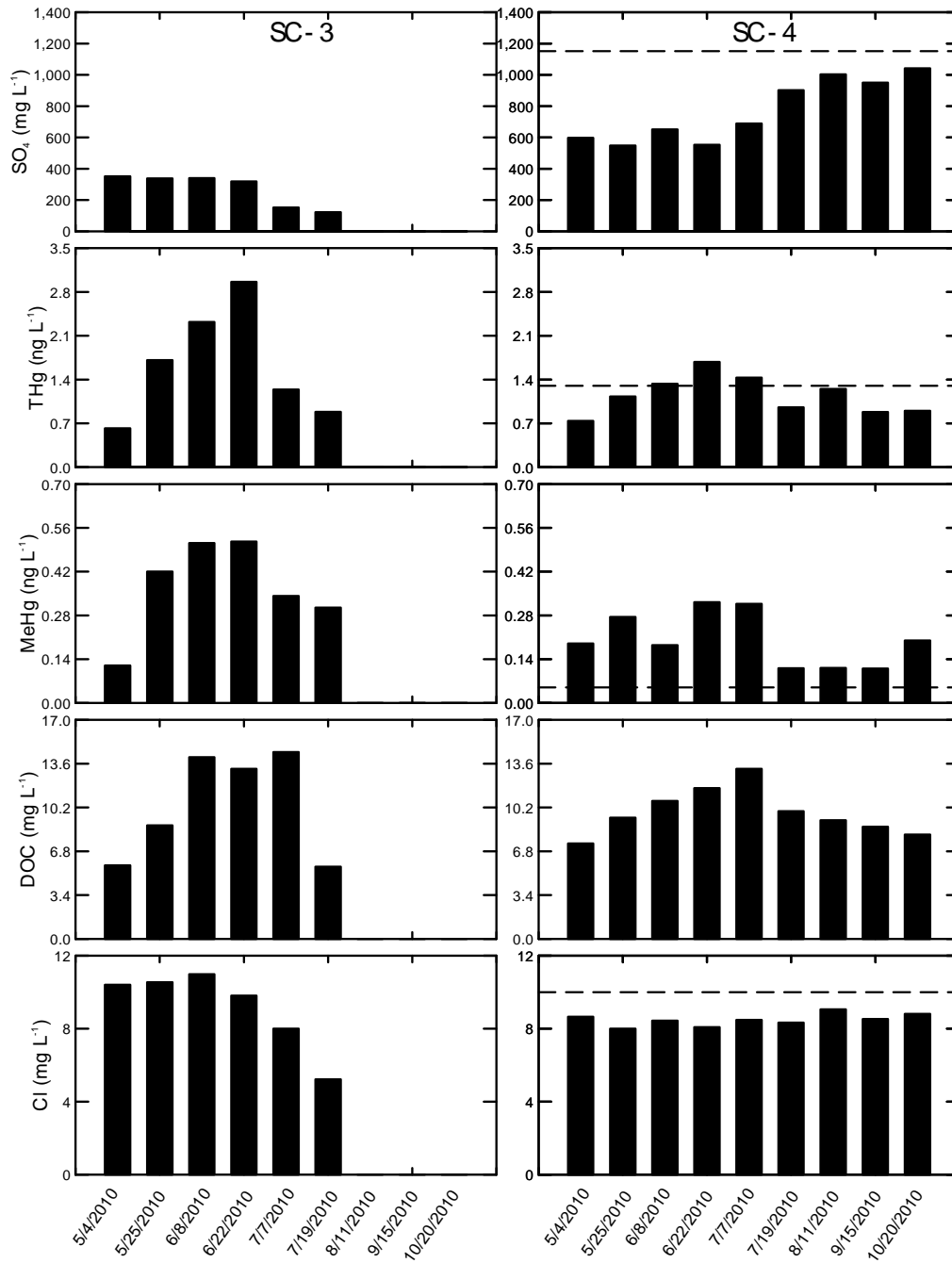


Fig. 15. Comparison of SO_4^- , THg, MeHg, DOC, and Cl^- levels in samples collected from sites SC-3 and SC-4. The dashed line in the SC-4 panels represents the average concentrations for the various constituents in Mesabi Nugget Pit 6. Mesabi Nugget was discharging water from Pit 1 into Second Creek until July 1st when pit dewatering was halted. No samples were collected at SC-3 in August, September, or October due to a lack of flow in the creek at that location.

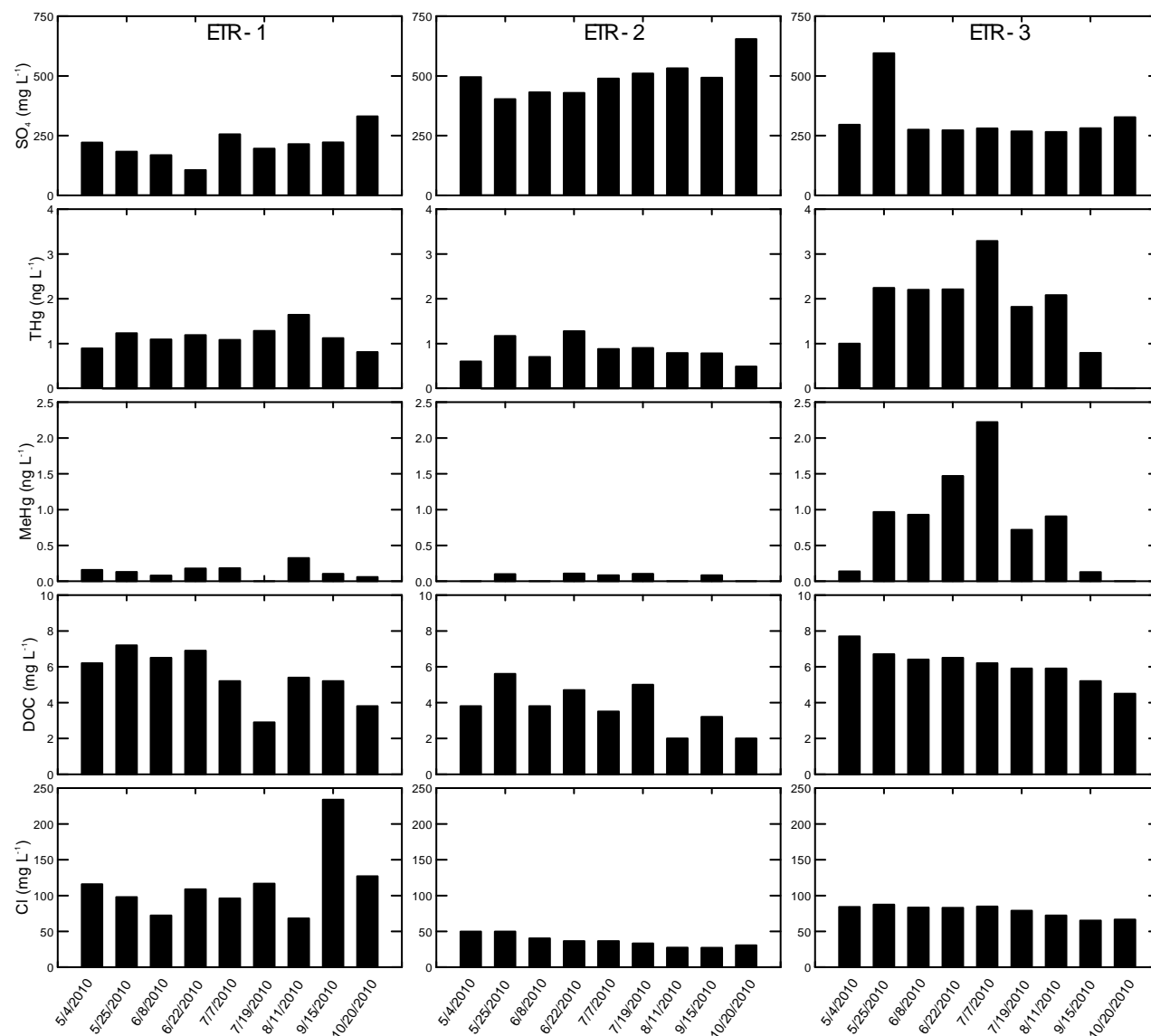


Fig. 16. Comparison of SO_4^{2-} , THg, MeHg, DOC, and Cl^- levels in samples collected from sites *ETR-1*, *ETR-2*, and *ETR-3*. MeHg concentrations were elevated in the lake during the summer with no obvious external source of mercury to methylate. There was no corresponding increase in DOC associated with the increase in MeHg and so it is proposed that the MeHg increase corresponds with formation of MeHgHS^0 in the sediments of this lake during the summer months. This species is believed to be inherently unstable under oxidizing conditions and so concentrations decline rapidly once production stops.

***The precision level for the replicate sulfate analyses for the May 25th ETR-3 sample were very low therefore it should be disregarded.*

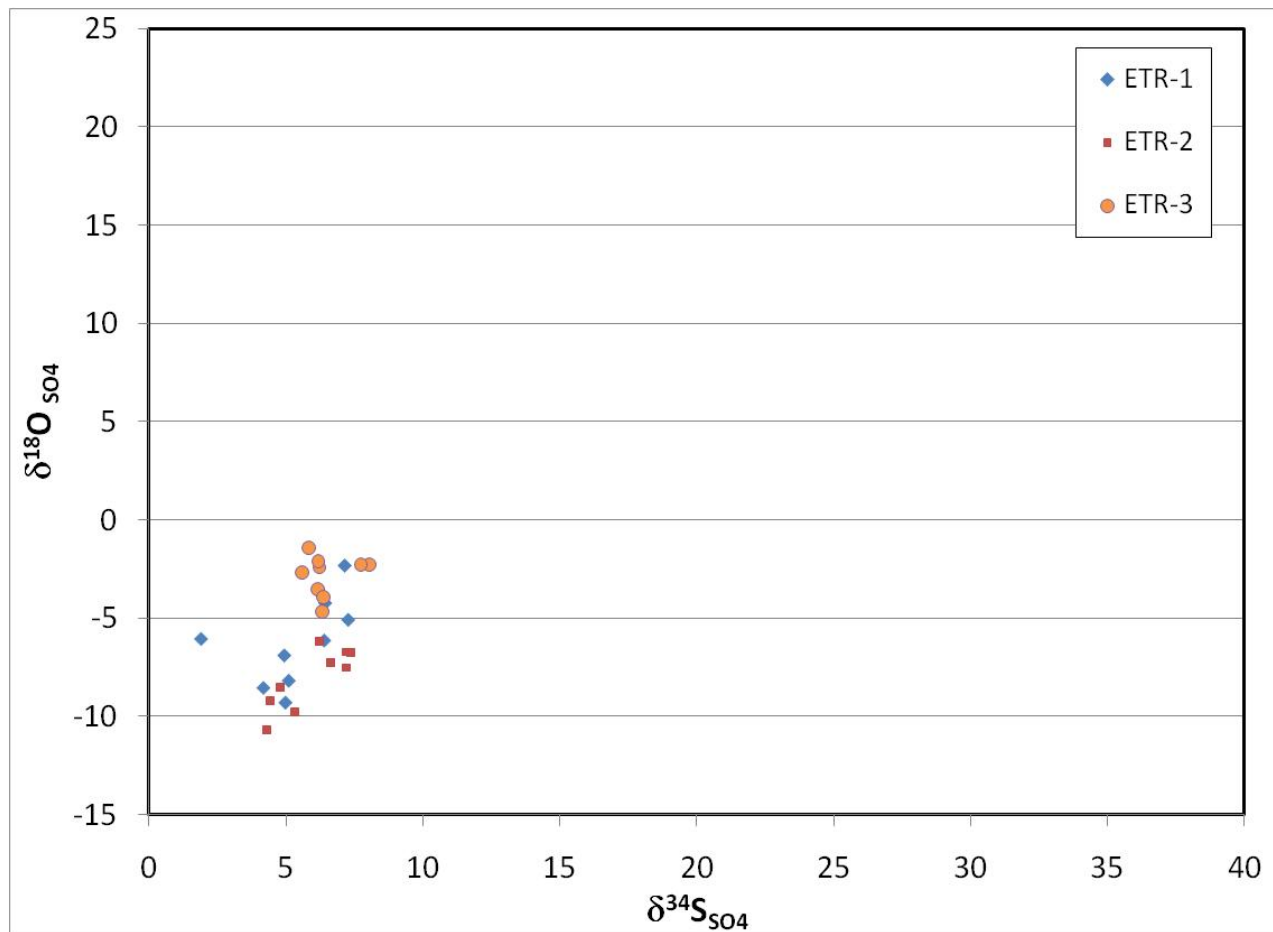


Fig. 17. $\delta^{34}\text{S}_{\text{SO}_4}$ and $\delta^{18}\text{O}_{\text{SO}_4}$ values for the dissolved SO_4^- in samples from at *ETR-1*, *ETR-2*, and *ETR-3*. *ETR-1* and *ETR-2* are inlets to the lake, while *ETR-3* is the lake's outlet. The relatively small change in $\delta^{34}\text{S}_{\text{SO}_4}$ compared to what has been observed at other sites implies that there is relatively little net SO_4^- reduction within the lake. It is proposed that the upward shift in $\delta^{18}\text{O}_{\text{SO}_4}$ without a correspondingly large positive shift in $\delta^{34}\text{S}_{\text{SO}_4}$ implies that SO_4^- reduction and oxidation processes are, however, active within the lake.

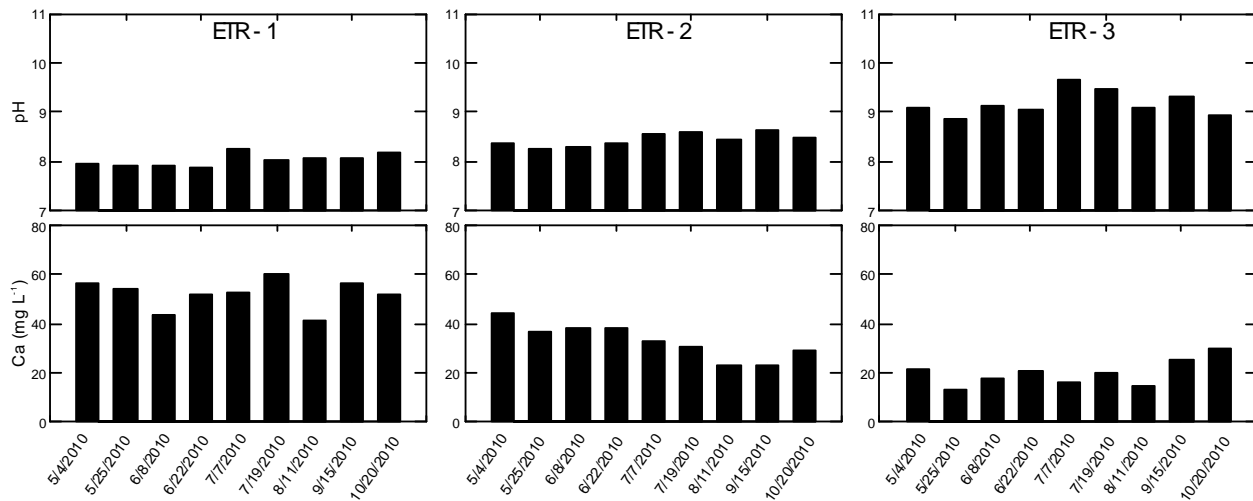


Fig. 18. pH values and Ca concentrations at sampling locations *ETR-1*, *ETR-2*, and *ETR-3*. The large increase in pH and decrease in Ca that occurs in the lake between inlet (*ETR-1*, and *ETR-2*) and outlet (*ETR-3*) sites is indicative of high productivity in the lake, with correspondingly high deposition rates for calcite and organic carbon into the bottom sediments. It is proposed that this high productivity drives SO_4^{2-} reduction and production of HS^- and H_2S in the bottom sediments, especially during the summer months (when pH is highest in the surface waters – indicative of greater productivity in surface waters). The generation of HS^- and H_2S in bottom sediments is believed, in turn, to generate highly mobile MeHgHS^0 .

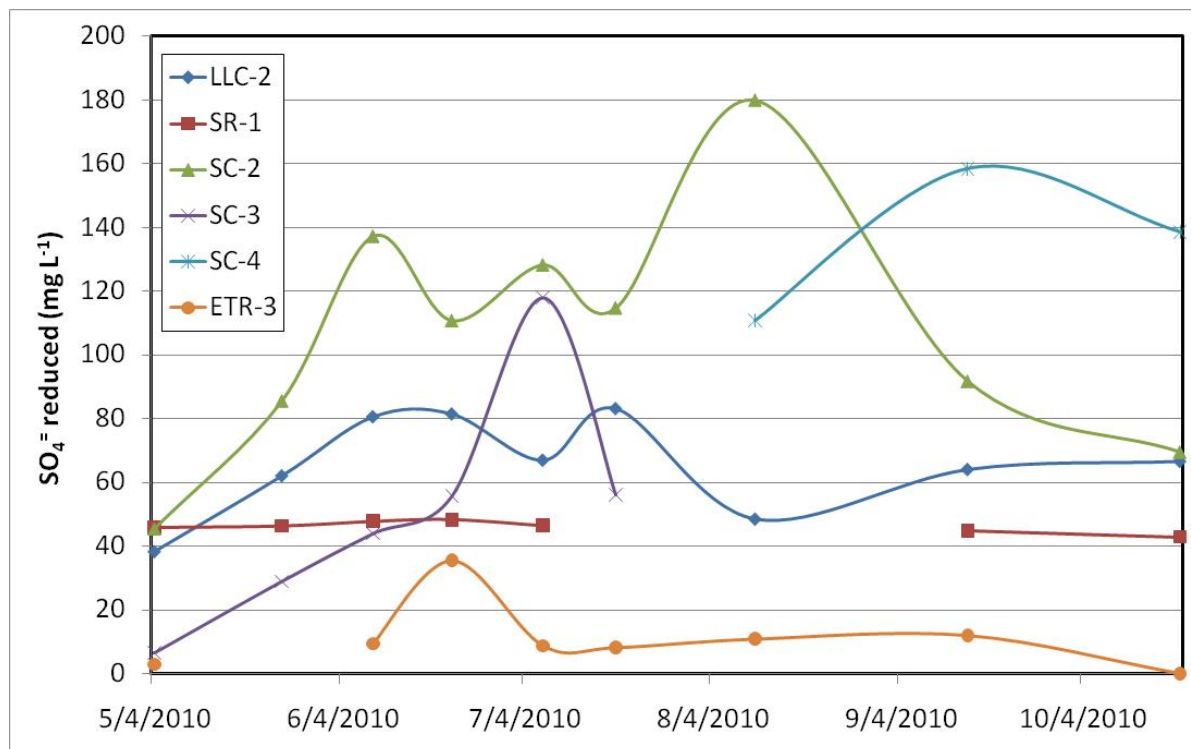


Fig. 19. Sulfur isotope-based estimates of the mass of SO_4^{2-} reduced per liter of water in wetlands and lakes investigated in this study. The plotted values apply to the wetland (LLC-2, SC-3, SC-4), tailings basin (SR-1, SC-2), or lake located immediately upstream from the listed sampling site. The method used to calculate SO_4^{2-} lost relies on the measured changes in $\delta^{34}\text{S}_{\text{SO}_4}$. Estimates for SR-1 were not available in mid-summer because SO_4^{2-} concentrations were below the levels needed to conduct $\delta^{34}\text{S}_{\text{SO}_4}$ analysis. SC-3 estimates are only available before August because flow at the site subsided after July 1 when pumping from Pit 1 was stopped. SC-4 estimates were only available approximately a month after Pit 1 pumping was stopped because the relative inputs from SC-3 and Pit 6 sites to SC-4 were difficult to unravel before the pumping stopped.

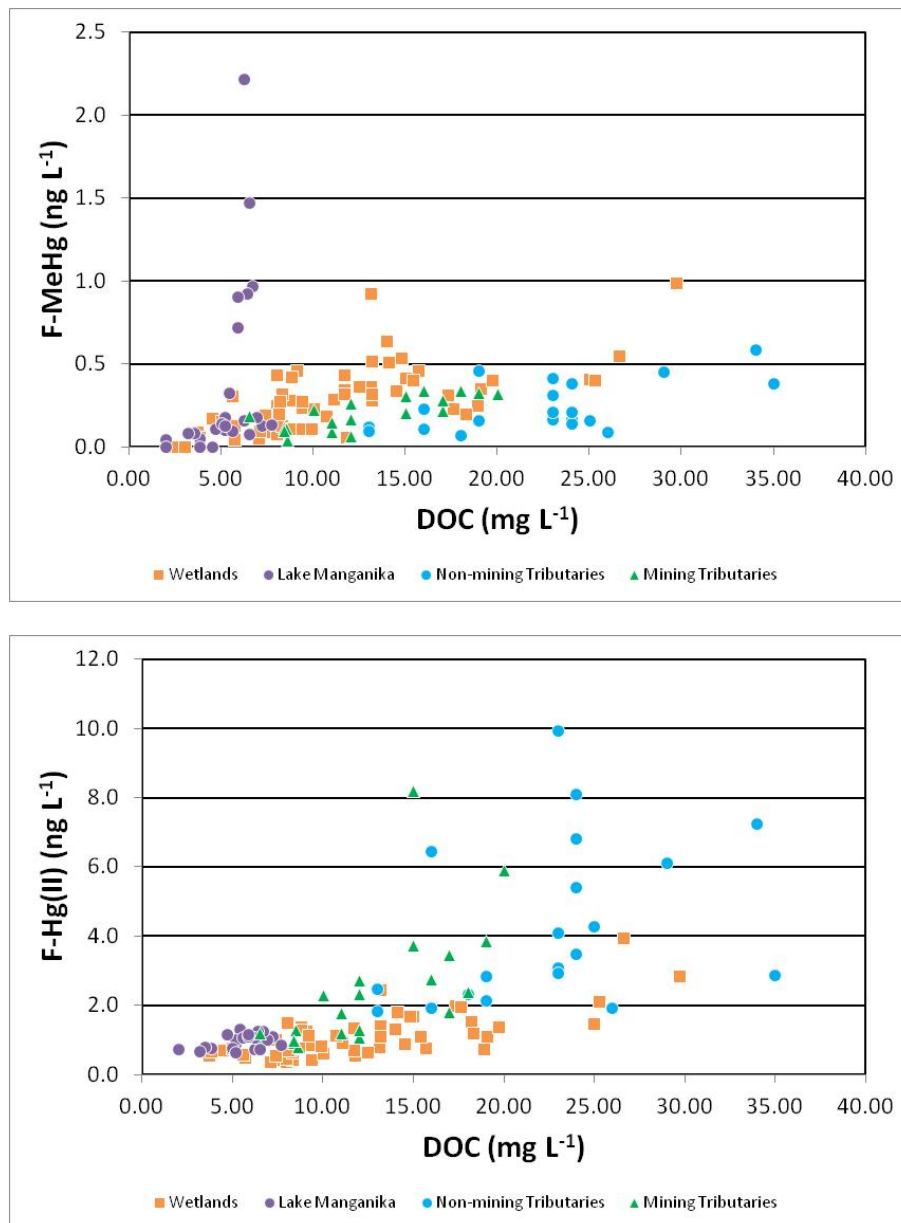


Fig. 20. MeHg (top) and Hg(II) (bottom) in filtered samples from various locations in the St. Louis River watershed. Data labeled Mining and Non-mining Tributaries are from streams sampled near their confluence with the St. Louis River in 2007 to 2009 as reported by Berndt and Bavin (2011a). Wetland and Lake Manganika data are from the present study where sampling was conducted in 2010. It is proposed that MeHgHS^0 released from wetland soils and lake sediments demethylates or decomposes fast compared to MeHg bound to organic carbon, and may account for some of the difference in MeHg/DOC relationships in upstream compared to downstream samples.

Appendices

Appendix 1. Historical sulfate and chloride concentrations in the ArcelorMittal tailings basin and in groundwater wells near the basin.

	*Tailings Basin Reclaim			*Deep Well			*Shallow Well			**Tailings Basin (2001-2009)		
	<i>Min</i>	<i>Max</i>	<i>Mean</i>	<i>Min</i>	<i>Max</i>	<i>Mean</i>	<i>Min</i>	<i>Max</i>	<i>Mean</i>	<i>Min</i>	<i>Max</i>	<i>Mean</i>
Sulfate	28.6	64.1	48.1	12.8	35.0	28.5	12.0	36.0	22.0	23.5	69.4	56.7
Cl	23.1	69.3	51.0	49.1	56.9	52.4	46.8	62.9	51.6	44.3	63.9	53.1

*Values from Berndt et al. (1999)

**Values from ArcelorMittal

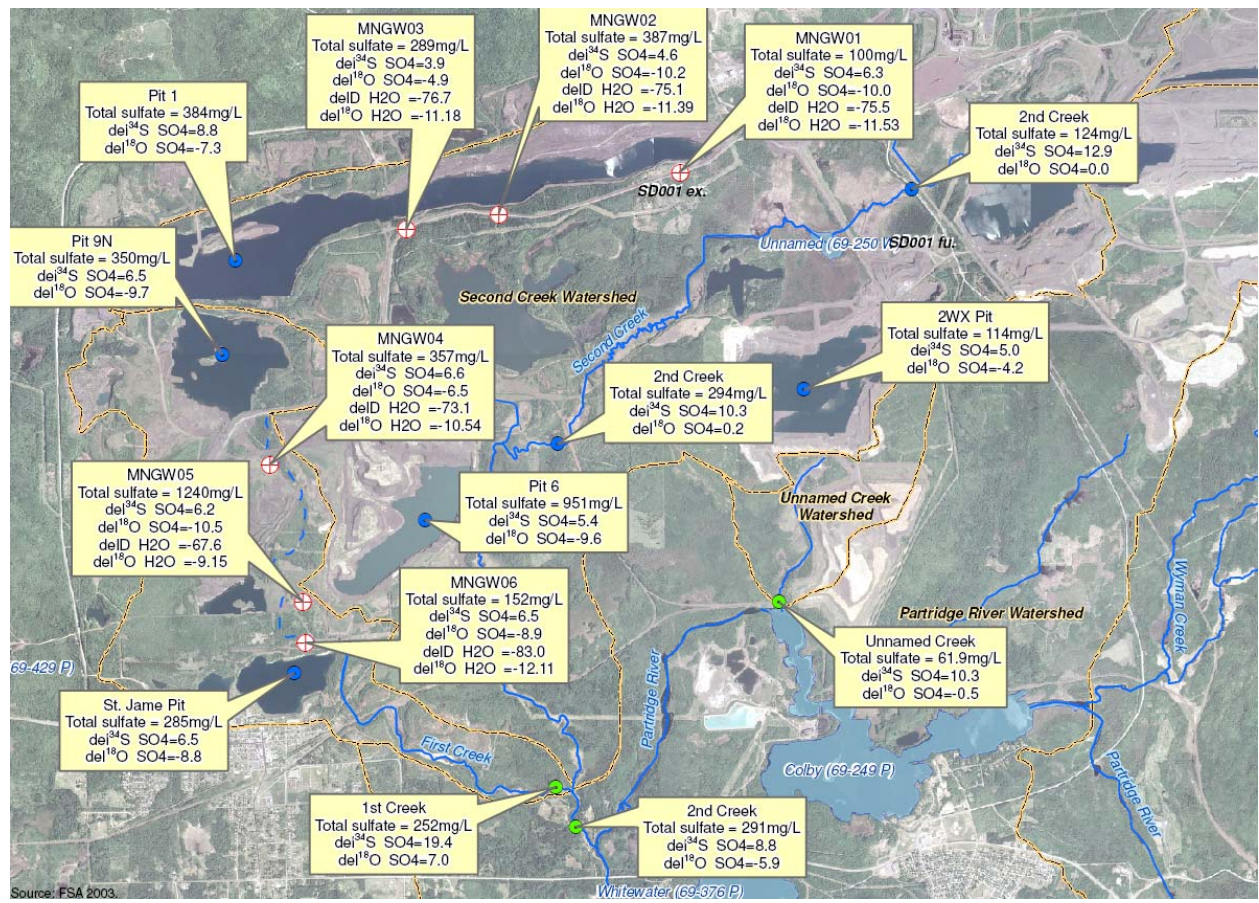
Appendix 2: Average composition of waters in Pit 1 and Pit 6 at Mesabi Nugget. Isotopic data for Pits 1 and 6 were provided by personal communication from Mesabi Nugget. Chemical data were provided by

	Pit 6*	Pit 1**
pH	8.05	8.1
Cond ($\mu\text{S cm}^{-1}$)	2453	1281
Alk, Total	576	364
THg (ng L^{-1})	1.1	0.8
MeHg F (ng L^{-1})	0.1	0.09
Al	0.013	0.013
Ba	0.006	0.004
Ca	52.3	42.7
Fe	0.04	0.03
K	24.3	13.4
Mg	378	163
Mn	2.25	0.86
Na	63.9	15.2
P	0.004	0.003
Si	0.005	0.004
Sr	0.239	0.134
F	0.15	0.1
Cl	10.3	10.5
Br	0.00003	0.00003
Sulfate	1146	386

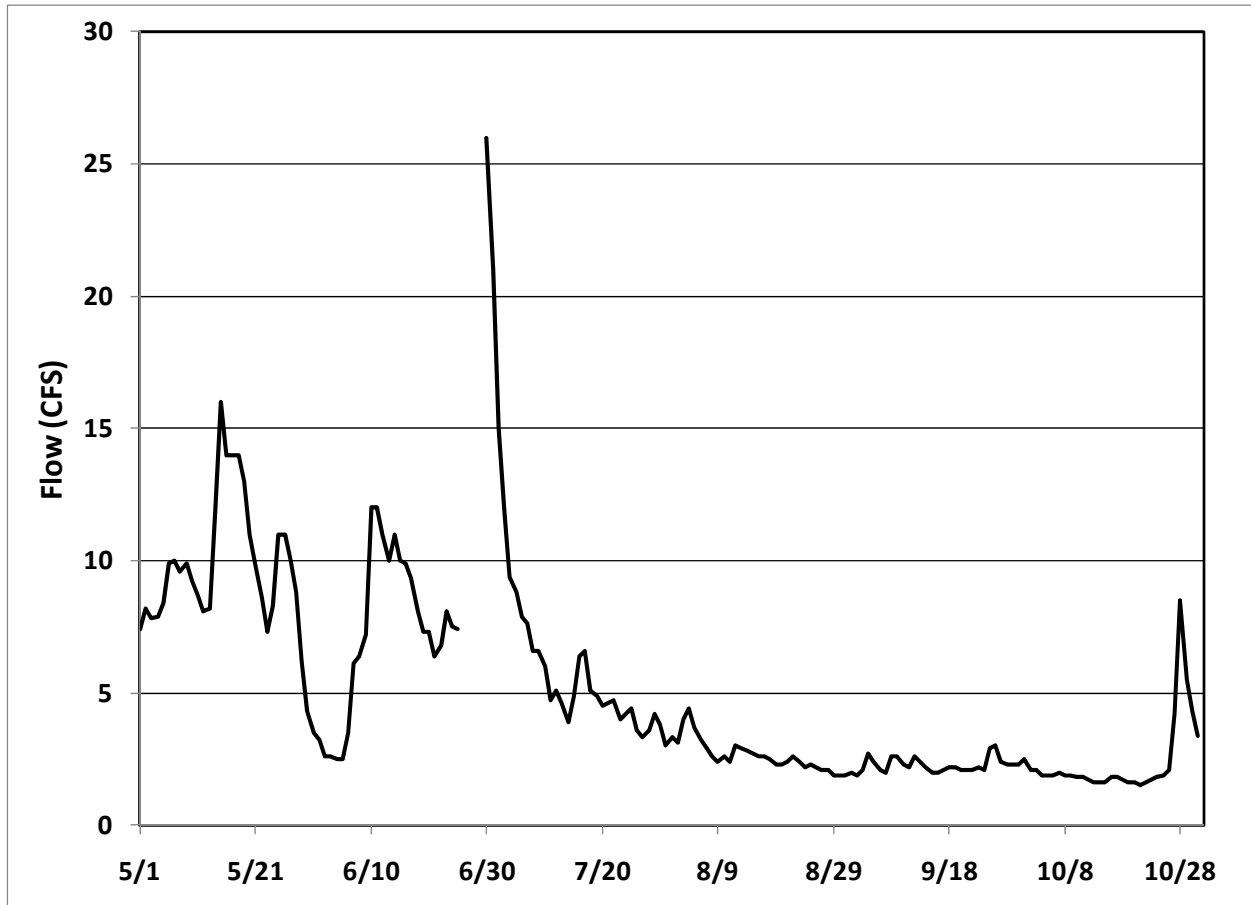
*Barr Engineering. Area 6 Pit Water Treatment Evaluation in Support of the Non-Degradation Analysis: Mesabi Nugget Phase II Project. September 2009.

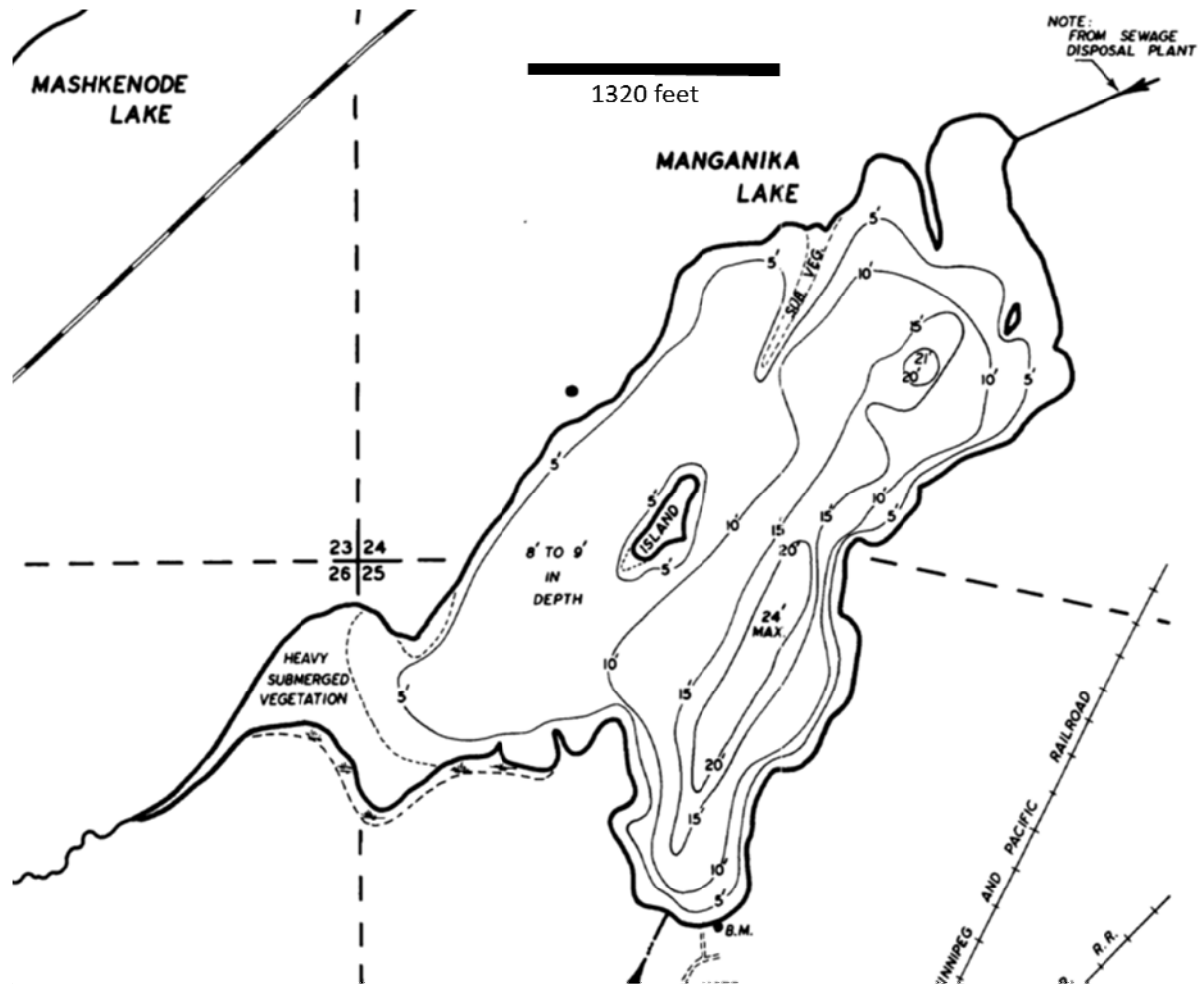
**Barr Engineering. Area 1 Pit Water Treatment Evaluation in Support of the Non-Degradation Analysis: Mesabi Nugget Phase II Project. November 2009.

Appendix 3: Isotopic Composition of waters sampled on the Mesabi Nugget Site provided to the DNR in 2008 (Mesabi Nugget, personal communication).

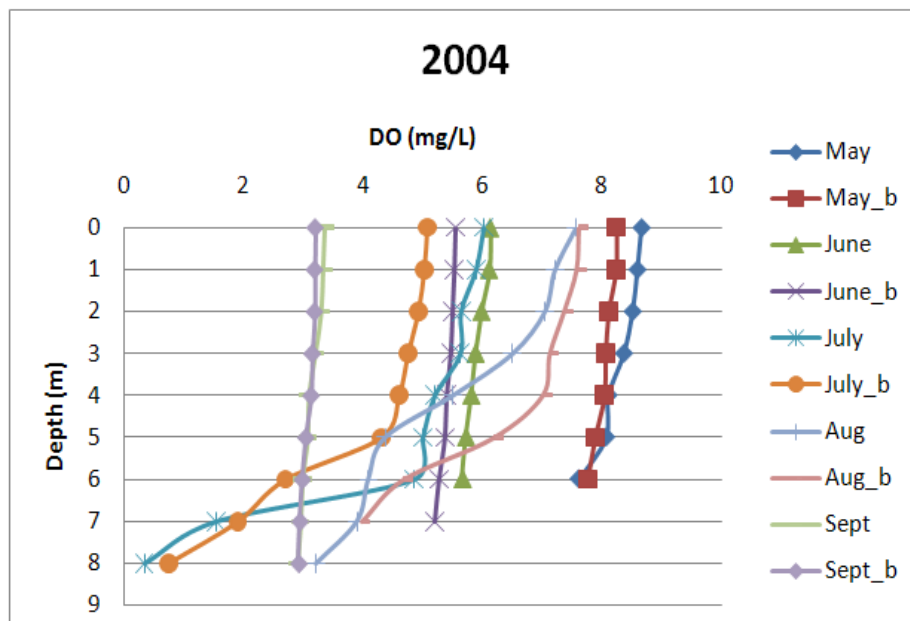
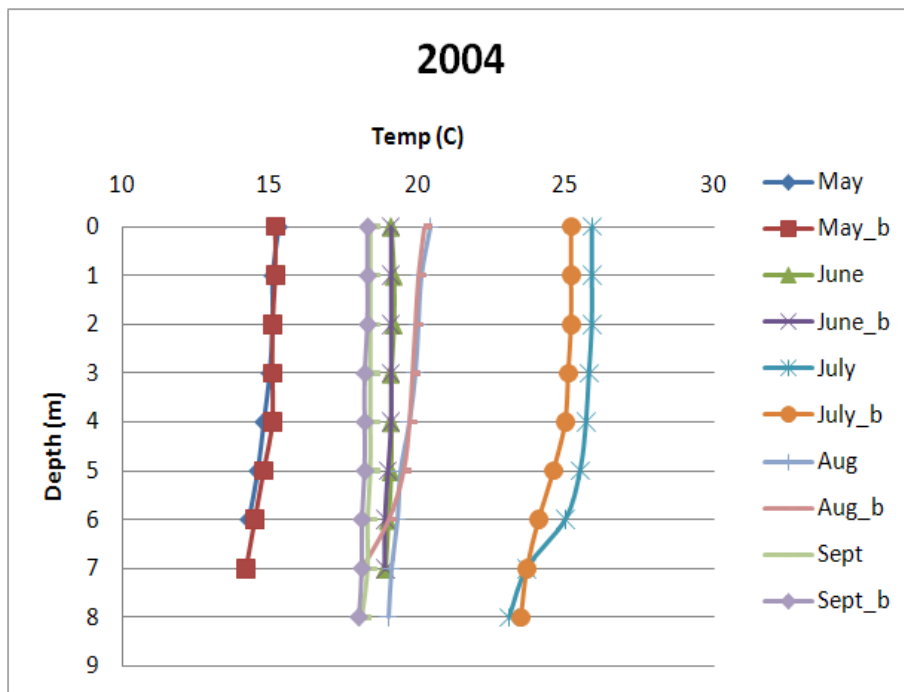


Appendix 4: Flow rates at the DNR gauging station on Second Creek near sampling location SC-4 during the study. Mesabi Nugget stopped pumping Pit 1 to Second Creek on July 1st, 2010. Flow measurements from late June were deemed to be of low quality and were removed from the data set.





Appendix 5: Bathymetric map of Lake Manganika



Appendix 6. Temperature and dissolved oxygen profiles for Lake Manganika In previous summers. Similar data are available for 2005 and 2006. This relatively shallow lake does not typically become thermally stratified, although O₂ levels become depressed at depth in the summer months.

Appendix 7. Field notes.

Site	Date	Comment
LLC-1	5/4/10	Water downstream of culvert approximately one to two inches deep; water clear in color
LLC-1	8/11/10	Water downstream of culvert approximately one to two feet deep and flowing rapidly; water clear in color
LLC-2	5/4/10	Water amber in color; water level very high near culvert; there doesn't appear to be much flow
LLC-2	6/9/10	Road culvert replaced; water still amber in color; water level approximately one foot lower at culvert
LLC-2	6/22/10	Very little flow at culvert; water amber in color
LLC-2	8/11/10	Water level higher at culvert; moderate flow through culvert; water amber in color
SR-1	5/4/10	Water clear; filtered quickly
SR-1	5/25/10	Sediments at bottom of wetland are reddish/brown – almost yellow in color
SR-1	6/8/10	Milky precipitate in water; water whitish / gray colored
SR-1	6/22/10	Turquoise bluish colored water; sediments at bottom of wetland are reddish/yellow in color
SR-1	7/7/10	Water blue/green in color
SR-1	7/19/10	Water brown in color; lots of suspended particulates
SR-1	9/15/10	Water brown in color; few particulates
SR-1	10/20/10	Water olive green/yellow in color; color intensifies with depth
SR-2	5/4/10	Water clear in color; stream a few inches deep by two to three feet wide
SR-2	7/7/10	Water clear in color; water level down from previous sample period
SR-2	7/19/10	Water level appears to be unchanged; water color changed from clear to amber
SR-2	8/11/10	Water level approximately one to one and a half feet deep; water clear in color
SR-2	9/15/10	Water level still high; water clear in color
SR-2	10/20/10	Water level remains high; clear in color; flow downstream impeded by debris
SC-2	5/4/10	Water dark in color and flowing through culvert; remnants of beaver activity near culvert
SC-2	5/25/10	Little water flow; water level appears to be rising; water clear in color
SC-2	6/22/10	Little water flow; water backed up by debris downstream of sample site; water clear in color
SC-2	7/7/10	Water one to two feet lower; water dark in color; lots of particulates
SC-2	7/19/10	Water level and flow still low; water dark in color; water filtered more quickly than during previous sample period
SC-3	5/4/10	Beaver debris in culvert; water flowing
SC-3	5/25/10	Water dammed up on downstream side of culvert but water is still flowing over dam; water light brown in color
SC-3	6/8/10	Water barely flowing; large beaver dam downstream of culvert with

		approximately one to two feet of head behind it
SC-3	6/22/10	Water slightly brown in color; water flowing well through culvert
SC-3	7/7/10	Water level in creek dropped by approximately two feet; lots of particulates; little flow
SC-4	5/4/10	Water cloudy; filtered quickly
SC-4	5/25/10	Water cloudy; water approximately one foot deep at culverts
SC-4	7/7/10	Vegetation flattened near culvert suggesting water levels have declined; water brownish/yellow in color
ETR-3	5/4/10	Water flowing rapidly; full of particulates; musty smell
ETR-3	5/25/10	Water flowing rapidly; full of particulates; chunks of aquatic plants or algae being transported downstream also
ETR-3	6/9/10	Water flowing rapidly; full of large particulates; chunks of aquatic plants or algae being transported downstream
ETR-3	6/22/10	Water flowing rapidly; water green in color; full of large particulates; filtered much slower than previous sample periods
ETR-3	7/7/10	Water very green in stream; lots of visible particulates and floating chunks of aquatic vegetation or algae
ETR-3	7/19/10	Water flowing moderately; water green in color; thick layer of algae coated the filter
ETR-3	8/11/2010	Water level at culvert up from late July; water green in color and full of particulates
ETR-3	9/15/2010	Water very turbid and full of algae and particulates
ETR-3	10/20/2101	Water levels lower than previously; water dull green in color

Appendix 8.**An interpretive framework for $\delta^{34}\text{S}_{\text{SO}_4}$ and $\delta^{18}\text{O}_{\text{SO}_4}$ in water samples from the St. Louis River Basin****Michael E. Berndt****A Minnesota Department of Natural Resources Memo**

June 8, 2011

The Minnesota Department of Natural Resources has recently begun collecting samples and having them analyzed for $\delta^{34}\text{S}_{\text{SO}_4}$ and $\delta^{18}\text{O}_{\text{SO}_4}$ (Berndt and Bavin, 2009, 2011a, 2011b). The detailed changes in $\delta^{34}\text{S}_{\text{SO}_4}$ and $\delta^{18}\text{O}_{\text{SO}_4}$ accompanying sulfur cycling in the watershed are complex and can involve many smaller steps that occur simultaneously and sequentially. The end result is a distribution that spans from 0 to 40 ‰ for $\delta^{34}\text{S}_{\text{SO}_4}$ and from -12 and +18 ‰ for $\delta^{18}\text{O}_{\text{SO}_4}$ (Figure 1). However the distribution is unusually shaped in that samples with 0 to 20 ‰ values for $\delta^{34}\text{S}_{\text{SO}_4}$ all have $\delta^{18}\text{O}_{\text{SO}_4}$ values less than about +8, while all but a single sample with $\delta^{34}\text{S}_{\text{SO}_4}$ greater than 20‰ have $\delta^{18}\text{O}_{\text{SO}_4}$ values greater than +8 ‰. Moreover, the population of samples with $\delta^{34}\text{S}_{\text{SO}_4}$ values less than 20‰ forms a triangular shaped patterning in $\delta^{34}\text{S}_{\text{SO}_4}$ - $\delta^{18}\text{O}_{\text{SO}_4}$ space, revealing a very narrow range of $\delta^{34}\text{S}_{\text{SO}_4}$ for samples with low $\delta^{18}\text{O}_{\text{SO}_4}$ values, and an ever-expanding range of $\delta^{34}\text{S}_{\text{SO}_4}$ as $\delta^{18}\text{O}_{\text{SO}_4}$ reaches a value of approximately +8 ‰. The purpose of this document is to provide an interpretation for this distribution of samples.

The interpretation begins first by considering the $\delta^{34}\text{S}_{\text{SO}_4}$ that might be expected for SO_4^{2-} derived by oxidation of sulfide minerals in the Biwabik Iron Formation. Theriault et al. (2011) summarized and provided new sulfur isotopic data for sulfides in the iron formation. Several populations were identified including primary sulfides deposited at the time that the formation was laid down and various secondary mineral populations that occurred as veins, framboids, and euhedral to subhedral pyrite grains. The primary sulfides had $\delta^{34}\text{S}_{\text{SO}_4}$ for sulfides that ranged narrowly from about +2 to +13 ‰, while the secondary sulfides had $\delta^{34}\text{S}_{\text{SO}_4}$ ranging from -40 to +80, indicating that post-depositional oxidation and re-reduction processes were widely varying in the formation.

Generally, sulfur isotope fractionation associated with simple oxidation of pyrite is minor and we can, thus, make the approximation that $\delta^{34}\text{S}_{\text{SO}_4}$ in water samples found close to the site where oxidation is taking place represents the average $\delta^{34}\text{S}$ of Fe-sulfides (e.g., $\delta^{34}\text{S}_{\text{pyrite}}$) being oxidized at the site. In practice, waters sampled at sites closest to the Iron Range and with the least chance of interacting with organic-rich wetlands have $\delta^{34}\text{S}_{\text{SO}_4}$ values that range typically between about +4 and +9 ‰. This range is consistent with derivation from primary sulfides in the Iron Formation (or of secondary sulfides with average $\delta^{34}\text{S}_{\text{pyrite}}$ that falls within the range of the primary sulfide field). In the framework shown in Figures 1 and 2, we assume that $\delta^{34}\text{S}_{\text{pyrite}} = 5.0$ ‰, although it is recognized that the observed range is between +4 and +9 ‰. If the primary sulfide had a value of +4 or +9 ‰, the entire frame can be shifted horizontally by -1 or right by +4 ‰, respectively, to account for cycling of sulfate derived from lower or higher $\delta^{34}\text{S}_{\text{pyrite}}$, respectively.

In contrast to $\delta^{34}\text{S}_{\text{SO}_4}$, the $\delta^{18}\text{O}_{\text{SO}_4}$ value produced when Fe-sulfides are oxidized does not depend at all on $\delta^{34}\text{S}_{\text{pyrite}}$ but depends, rather, on the mechanism of oxidation and the source of oxygen. Toran and Harris (1989) point out that eight separately electron transfers must occur if sulfur in an oxidation state of -2 is converted SO_4^- where sulfur has a +6 charge. In addition, the central sulfur molecule obtains four oxygen atoms, each with its own separate potential source and fractionation factor that can affect the $\delta^{18}\text{O}_{\text{SO}_4}$ value. In terms of oxygen exchange reactions with water and the atmosphere, there are three broad types of oxidation reactions possible:

Type 1: $\text{S}^- + 2\text{O}_2 = \text{SO}_4^-$ (O_2 is oxidizing agent, and O in SO_4 all comes from O_2)

Type 2: $\text{S}^- + 2\text{O}_2^* + 4\text{H}_2\text{O} = \text{SO}_4^- + 4\text{H}_2\text{O}^*$ (O_2 is oxidizing agent, but O in SO_4 is from H_2O)

Type 3: $\text{S}^- + 8\text{Fe}^{+++} + 4\text{H}_2\text{O} = \text{SO}_4^- + 8\text{H}^+ + 8\text{Fe}^{++}$ (Fe^{+++} is oxidizing agent, and O in SO_4 is all from H_2O)

Although mineral-derived O_2 could potentially be incorporated in the SO_4^- molecule, this type of exchange is almost never observed. Depending on the relative importance of each type of reaction, a different fraction of the oxygen in SO_4^- will be derived from either atmospheric O_2 or H_2O . $\delta^{18}\text{O}_{\text{SO}_4}$ for the wide range of processes can be computed from the following equation:

$$\delta^{18}\text{O}_{\text{SO}_4}(\text{‰}) = f_{\text{H}_2\text{O}} (\delta^{18}\text{O}_{\text{H}_2\text{O}} + E_{\text{H}_2\text{O}}) + f_{\text{O}_2} (\delta^{18}\text{O}_{\text{O}_2} + E_{\text{O}_2})$$

where $f_{\text{H}_2\text{O}}$ and f_{O_2} are the fraction of sulfate oxygen atoms derived from ambient water and atmospheric oxygen, respectively. $E_{\text{H}_2\text{O}}$ and E_{O_2} are the per mil (‰) fractionations for SO_4^- and the subscripted component, ambient water or atmospheric oxygen, respectively. Toran and Harris reviewed two biologic pathways and one abiologic process that resulted in f_{O_2} values of 0, 0.75, and 0.875, respectively. E_{O_2} values ranged from -4.3 to -11.4 ‰ while $E_{\text{H}_2\text{O}}$ values ranged from -6 to 4.1 ‰, depending on the assumptions made in their derivation.

Meteoric water in this region has $\delta^{18}\text{O}_{\text{SO}_4}$ of approximately -10 ‰, which corresponds closely to values for water sampled close to the mining region. This suggests oxidation in the Iron Range is commonly dominated by Type 2 or Type 3 reactions, such that $f_{\text{O}_2}=0$, $f_{\text{H}_2\text{O}} = 1$, and further that $E_{\text{H}_2\text{O}}$ may be close to 0 ‰. This is interpreted in Figure 1, primarily as a Type 3 process, whereby oxidation of pyrite in the Biwabik Iron Formation results in waters containing SO_4^- with $\delta^{18}\text{O}_{\text{SO}_4}$ values close to the meteoric water value of -10 ‰ and $\delta^{34}\text{S}_{\text{SO}_4}$ values set by that of the primary sulfide minerals.

As another possible means to oxidize sulfides in the iron formation, we consider a second Toran and Harris case, where $f_{\text{O}_2}=0.75$, $f_{\text{H}_2\text{O}} = 0.25$, $E_{\text{O}_2}= -4.3$ to -11.4 ‰, and $E_{\text{H}_2\text{O}} = 4.1$ to -6.1 ‰. By this process and using a value of +23.5 ‰ to represent atmospheric O_2 and -10 ‰ for meteoric water, we calculate $\delta^{18}\text{O}_{\text{SO}_4}$ values ranging from 4.6 to 12.7‰. For samples with low $\delta^{34}\text{S}_{\text{SO}_4}$ (indicative that $\delta^{18}\text{O}_{\text{SO}_4}$ was less impacted by sulfate reduction, as discussed below) the maximum $\delta^{18}\text{O}_{\text{SO}_4}$ values found in the DNR studies are in the +6 to +8 ‰ range, consistent with having been derived by an O_2 -mediated process (combined Type 1 and Type 2 processes) with f_{O_2} around 0.75. The final SO_4^- oxidation process discussed by Toran and Harris (1989) (with the fraction of O_2 derived from the atmosphere equal to 0.875) generates $\delta^{18}\text{O}_{\text{SO}_4}$ values ranging from +8 to +16 ‰ using meteoric water and atmospheric

oxygen. This value is above all of the values measured for low- $\delta^{34}\text{S}_{\text{SO}_4}$ that were sampled in the watershed.

In summary, for water samples containing low $\delta^{34}\text{S}_{\text{SO}_4}$, a diverse set of oxidation mechanisms appears to be active in the watershed with f_{O_2} ranging from 0 to 0.75 – and constraining the resulting $\delta^{18}\text{O}_{\text{SO}_4}$ values to fall between -12 and +8 ‰. It is noted, further, that waters sampled close to the Iron Range sites tend to fall closer to the “Fe-mediated oxidation” point and samples collected far downstream in the St. Louis River have $\delta^{18}\text{O}_{\text{SO}_4}$ values that is always ranges from +2 to +6. Though mass balance considerations indicate that most of the SO_4^{2-} in the St. Louis River at Mile 36 is derived from the Iron Range mining district, it is apparent that the $\delta^{18}\text{O}_{\text{SO}_4}$ value shifts considerably as the SO_4^{2-} released from the waste rock piles and pits on the Iron Range migrates through the wetlands, lakes, and streams downstream from the mining region. This process of oxygen isotope re-equilibration for SO_4^{2-} without a corresponding change in sulfur isotopic values is not understood, but similar effects have been previously noted by Caron et al. (2003) in a similar region and by Turchyn and Schrag (2004) on a global scale for seawater. To re-equilibrate the SO_4^{2-} , the central sulfur atoms in the original SO_4^{2-} molecules must be stripped of their original oxygen atoms (e.g., reduced) and have them replaced by a different set of oxygen atoms (e.g., re-oxidation of the sulfide). This behavior has been observed by Berndt and Bavin (2011b) on both the watershed and sub-watershed scales.

The left edge of the frame, extending directly upwards from the Fe-mediated BIF sulfide point, indicates the changes in $\delta^{18}\text{O}_{\text{SO}_4}$ that could be expected for 0 to 100% re-equilibration of the oxygen atoms in the SO_4^{2-} as it travels from the iron formation to Mile 36 in the St. Louis River. The vast majority of samples collected from the watershed have $\delta^{34}\text{S}_{\text{SO}_4}$ as $\delta^{18}\text{O}_{\text{SO}_4}$ that lie distinctly to the right of this, indicative that significant sulfate reduction occurs in the watershed.

Sulfate reduction is a process that affects both $\delta^{34}\text{S}_{\text{SO}_4}$ and $\delta^{18}\text{O}_{\text{SO}_4}$ at the same time, because the bacteria that drive sulfate reduction preferentially use SO_4^{2-} atoms containing the lighter atoms. In Figure 1, the line extending upward and to the right from the Fe-mediated oxidation point is drawn with a slope of 1.0, representative of a sulfate reduction process whereby the isotope fractionation factor is considered to be exactly the same for both O and S (e.g., the fractionation is determined only by the weight of the molecule and not based on the identity of the atom causing the greater molecular weight). The SO_4^{2-} reduction process was, in this case, assigned a fractionation factor ($\Delta^{34}\text{C}_{\text{SO}_4\text{-Sulfide}}$) of +17‰, consistent with data from Berndt and Bavin (2011a) for subsurface bacterial sulfate reduction observed near a tailings basin on the Iron Range. That is, it was assumed that the sulfide that forms is 17‰ lighter than the SO_4^{2-} from which it is derived. Once the sulfide forms, the $\delta^{34}\text{S}_{\text{SO}_4}$ of the residual sulfate becomes elevated. A Rayleigh distillation process is assumed, whereby sulfide formed early in the process becomes instantaneously isolated from the system.

By this process, the $\delta^{34}\text{S}_{\text{SO}_4}$ would shift from +5 to approximately +33 while $\delta^{18}\text{O}_{\text{SO}_4}$ shifted from -10 to 18 if 80% of the sulfate released by oxidation was reduced elsewhere in the environment. Subsequent re-equilibration of the oxygen isotopes in the residual sulfate would cause the $\delta^{18}\text{O}_{\text{SO}_4}$ values to shift downward, approaching a value near 6‰. It is noted that $\delta^{34}\text{S}_{\text{SO}_4}$ as $\delta^{18}\text{O}_{\text{SO}_4}$ distribution in samples collected so far imply that sulfate reduction generally precedes the oxygen isotope equilibration

process. If the reaction sequence occurred in the opposite order, we might expect to find samples in the 5 to 20‰ $\delta^{34}\text{S}_{\text{SO}_4}$ range with $\delta^{18}\text{O}_{\text{SO}_4}$ values between +8 and +18. The distribution also suggests that the majority of the sulfide oxidation in the watershed must occur by an Fe^{+++} mediated process. SO_4^- reduction following an O_2 mediated process would also be expected to produce some samples in the +5 to +20‰ $\delta^{34}\text{S}_{\text{SO}_4}$ range with $\delta^{18}\text{O}_{\text{SO}_4}$ values between +8 and +18 ‰. Extensive sampling in the watersheds has turned up no such samples so far.

Although the framework interpretation displayed in Figure 1 can be used to account for the distribution of isotopic data from samples so-far collected in and near the St. Louis River basin, considerable caution is urged for strict numeric application. In particular, it is possible, if not likely, that more than one type of sulfate-reducing bacterial process is occurring in the watershed. If so, then the sulfur and oxygen fractionation factors could be different from the values used to construct the frame in Figure 1 (see Detmers et al (2001) for list of $\Delta^{34}\text{C}_{\text{SO}_4\text{-Sulfide}}$ values as function of different sulfate reduction processes). The percentages of sulfate removed would be shifted upwards or downwards, depending on the actual fractionation factor used. Moreover, the framework assumed a starting value of +5 for $\delta^{34}\text{S}_{\text{SO}_4}$. The entire frame will shift left or right depending on what the actual starting value is for a particular situation within the watershed.

The interpretation is, however, believed by the author to be representative of the overall processes that dominate SO_4 cycling in the watershed – as illustrated in Figure 2. SO_4^- in the Iron Range is most commonly released from primary sulfides, likely by an Fe^{+++} -mediated oxidation process. This SO_4^- is variably reduced, sometimes by more than 90% (confirmed using alternate method in one case). Once released into the open water flow system, the $\delta^{18}\text{O}_{\text{SO}_4}$ in the SO_4^- that remains following the reduction process is re-equilibrated without much further change in $\delta^{34}\text{S}_{\text{SO}_4}$.

Berndt, M. E. and Bavin, T. K. (2009) Sulfate and Mercury Chemistry of the St. Louis River in Northeastern Minnesota: A Report to the Minerals Coordinating Committee. Minnesota Department of Natural Resources, Division of Lands and Minerals. St. Paul, MN, USA. 83 p.

Berndt, M. E. and Bavin, T. K. (2011a) Sulfate and Mercury Cycling in Five Wetlands and a Lake Receiving Sulfate from Taconite Mines in Northeastern Minnesota: A Report to Iron Ore Cooperative Research Program. Minnesota Department of Natural Resources, Division of Lands and Minerals. St. Paul, MN, USA.

Berndt, M. E. and Bavin, T. K., (2011b) A preliminary assessment of sulfate release and sulfate cycling processes in the St. Louis River watershed. An Environmental and Natural Resources Trust Fund Progress Report. Minnesota Department of Natural Resources Submitted Report.

Caron, F., Tessier, A., Kramer, J. R., Schwarz, H. P., Rees, C. E. (1986) Sulfur and oxygen isotopes of sulfate in precipitation and lakewater, Quebec, Canada. *Applied Geochemistry* 1: 601-606.

Detmers, J., Bruchert, V., Habicht, K. S., and Kuever, J (2001) Diversity of sulfur isotope fractionations by sulfate-reducing prokaryotes. *Appl. Environ. Microbiol.* 67, 888-894.

Therriault, S. A., Miller, J. D., Berndt, M. E., and Ripley, E. M. (2011) The mineralogy, spatial distribution, and isotope geochemistry of sulfide minerals in the Biwabik Iron Formation. *Institute for Lake Superior Geology, Abstract.* 2 pages.

Toran, L. and Harris, R. F. (1989) Interpretation of sulfur and oxygen isotopes in biological and abiological sulfide oxidation. *Geochim. Cosmochim. Acta.* 53, 2341-2348.

Turchyn, A. V. and Schrag, D. P. (2004) Oxygen isotope constraints on the sulfur cycle over the past 10 million years. *Science.* 303, 2004-2007.

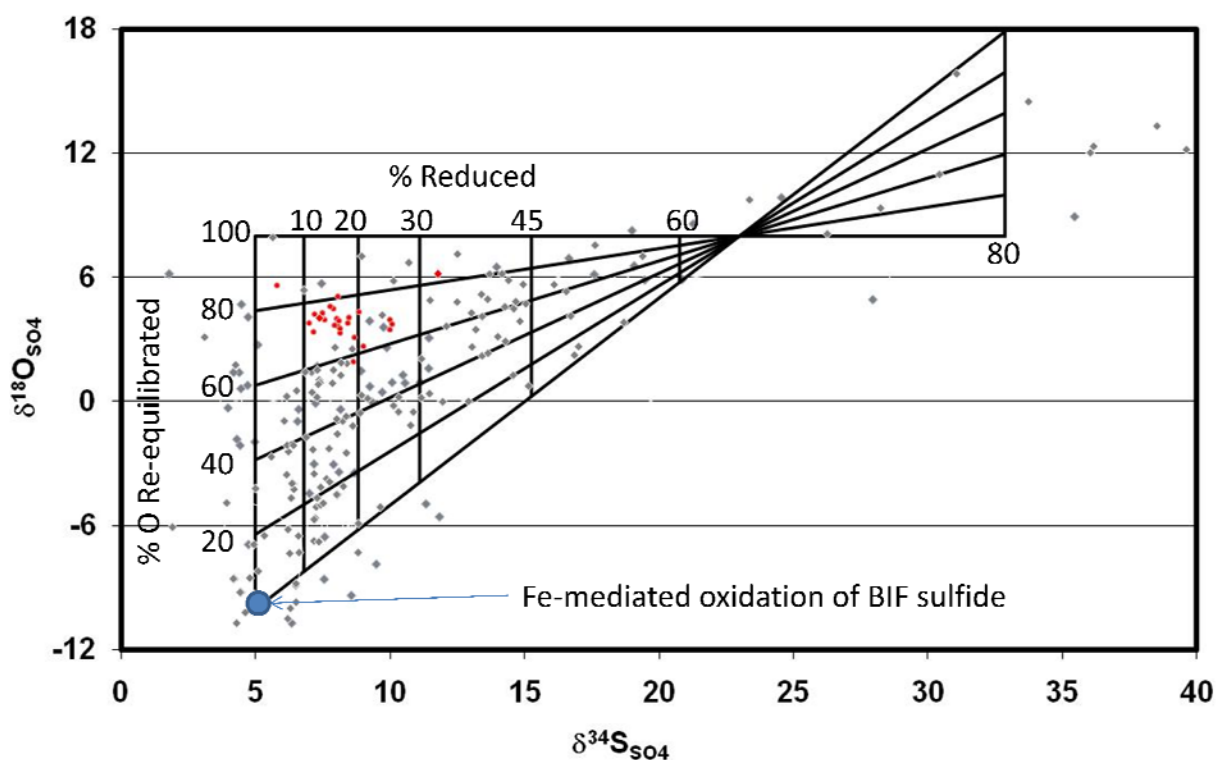


Figure 1. $\delta^{34}\text{S}_{\text{SO}_4}$ and $\delta^{18}\text{O}_{\text{SO}_4}$ data collected through July 2011 by the Minnesota Department of Natural Resources in or near the St. Louis River watershed. Dark gray points are assorted data from lakes, streams, rivers, and wells. Red points are from the St. Louis River at Mile 36. See the text and Figure 2 for a description of the framework model used to interpret the isotopic data from this watershed.

Proposed St. Louis River Sulfur Cycling Model

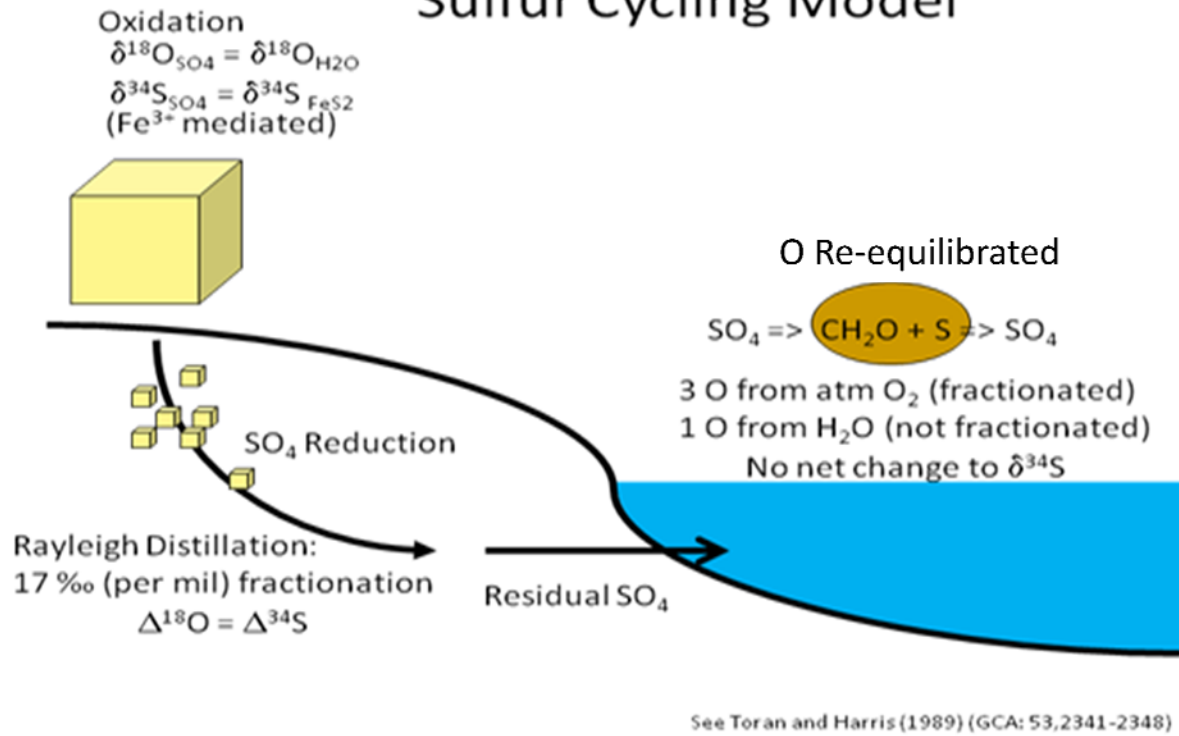


Figure 2. Preliminary sequential model used to account for isotopic data in the St. Louis River watershed. See text.